Sheng, Y. “Wavelet Transform.”
The Transforms and Applications Handbook: Second Edition.
Ed. Alexander D. Poularikas
Boca Raton: CRC Press LLC, 2000

10

Wavelet Transform

Yunlong Sheng
Laval University

ABSTRACT The wavelet transform is a new mathematical tool developed mainly since the middle of the 1980's. It is efficient for local analysis of nonstationary and fast transient wide-band signals. The wavelet transform is a mapping of a time signal to the time-scale joint representation that is similar to the short-time Fourier transform, the Wigner distribution and the ambiguity function. The temporal aspect of the signals is preserved. The wavelet transform provides multiresolution analysis with dilated windows. The high frequency analysis is done using narrow windows and the low frequency analysis is done using wide windows. The wavelet transform is a constant-Q analysis.

The base of the wavelet transform, the wavelets, are generated from a basic wavelet function by dilations and translations. They satisfy an admissible condition so that the original signal can be reconstructed by the inverse wavelet transform. The wavelets also satisfy the regularity condition so that the wavelet coefficients decrease fast with decreases of the scale. The wavelet transform is not only local in time but also in frequency.

To reduce the time bandwidth product of the wavelet transform output, the discrete wavelet transform with discrete dilations and translations of the continuous wavelets can be used. The orthonormal wavelet transform is implemented in the multiresolution signal analysis framework, which is based on the scaling functions. The discrete translates of the scaling functions form an orthonormal basis at each resolution level. The wavelet basis is generated from the scaling function basis. The two bases are mutually orthogonal at each resolution level. The scaling function is an averaging function. The orthogonal projection of a function onto the scaling function basis is an averaged approximation. The orthogonal projection onto the wavelet basis is the difference between two approximations at two adjacent resolution levels. Both the scaling functions and the wavelets satisfy the orthonormality conditions and the regularity conditions.

The discrete orthonormal wavelet series decomposition and reconstruction are computed in the multiresolution analysis framework with recurring two discrete low-pass and high-pass filters, that are, in fact, the 2-band paraunitary perfect reconstruction quadrature mirror filters, developed in the subband coding theory, with the additional regularity. The tree algorithm operating the discrete wavelet transform requires only $O(L)$ operations where L is the length of the data vector. The time bandwidth product of the wavelet transform output is only slightly increased with respect to that of the signal.

The wavelet transform is powerful for multiresolution local spectrum analysis of nonstationary signals, such as the sound, radar, sonar, seismic, electrocardiographic signals, and for image compression, image processing, and pattern recognition.

In this chapter all integrations extend from $-\infty$ to ∞, if not stated otherwise. The formulation of the wavelet transform in this chapter is one-dimensional. The wavelet transform can be easily generalized to any dimensions.

10.1 Introduction

10.1.1 Continuous Wavelet Transform

Definition

Let **L** denote the vector space of measurable, square-integrable functions. The continuous wavelet transform of a function $f(t) \in \mathbf{Z}$ is a decomposition of $f(t)$ into a set of kernel functions $h_{s,\tau}(t)$ called the wavelets:

$$W_f(s,\tau) = \int f(t) h^*_{s,\tau}(t) dt \tag{10.1.1}$$

where * denotes the complex conjugate. However, most wavelets are real valued. The wavelets are generated from a single basic wavelet (mother wavelet) $h(t)$ by scaling and translation:

$$h_{s,\tau}(t) = \frac{1}{\sqrt{s}} h\left(\frac{t-\tau}{s}\right) \tag{10.1.2}$$

where s is the scale factor and τ is the translation factor. We usually consider only positive scale factor $s > 0$. The wavelets are dilated when the scale $s > 1$ and are contracted when $s < 1$. The wavelets $h_{s,\tau}(t)$ generated from the same basic wavelet have different scales s and locations τ, but all have the identical shape.

The constant $s^{-1/2}$ in the expression (10.1.2) of the wavelets is for energy normalization. The wavelets are normalized as

$$\int |h_{s,\tau}(t)|^2 dt = \int |h(t)|^2 dt = 1$$

so that all the wavelets scaled by the factor s have the same energy. The wavelets can also be normalized in terms of the amplitude:

$$\int \left| h_{s,\tau}(t) \right| dt = 1$$

In this case, the normalization constant is s^{-1} instead of $s^{-1/2}$, and the wavelets are generated from the basic wavelet as

$$h_{s,\tau}(t) = \frac{1}{s} h\left(\frac{t-\tau}{s} \right) \tag{10.1.3}$$

In this chapter, we consider mostly the normalization of the wavelet in terms of energy.

On substituting (10.1.2) into (10.1.1) we write the wavelet transform of $f(t)$ as a correlation between the signal and the scaled wavelets $h(t/s)$:

$$W_f(s,\tau) = \frac{1}{\sqrt{s}} \int f(t) h^*\left(\frac{t-\tau}{s} \right) dt \tag{10.1.4}$$

Wavelet Transform in Frequency Domain

The Fourier transform of the wavelet is

$$\begin{aligned} H_{s,\tau}(\omega) &= \int \frac{1}{\sqrt{s}} h\left(\frac{t-\tau}{s} \right) \exp(-j\omega t) dt \\ &= \sqrt{s} H(s\omega) \exp(-j\omega\tau) \end{aligned} \tag{10.1.5}$$

where $H(\omega)$ is the Fourier transform of the basic wavelet $h(t)$. In the frequency domain the wavelet is scaled by 1/s, multiplied by a phase factor $exp(-j\omega\tau)$ and by the normalization factor $s^{1/2}$. The amplitude of the scaled wavelet is proportional to $s^{-1/2}$ in the time domain and is proportional to $s^{1/2}$ in the frequency domain. When the wavelets are normalized in terms of amplitude, the Fourier transforms of the wavelets with different scales will have the same amplitude, that is suitable for implementation of the continuous wavelet transform using the frequency domain filtering.

Equation (10.1.5) shows a well know concept that a dilatation t/s ($s > 1$) of a function in the time domain produces a contraction $s\omega$ of its Fourier transform. The term $1/s$ has a dimension of frequency and is equivalent to the frequency. However, we prefer the term "scale" to the term "frequency" for the wavelet transform. The term "frequency" is reserved for the Fourier transform.

The correlation between the signal and the wavelets, in the time domain can be written as the inverse Fourier transform of the product of the conjugate Fourier transforms of the wavelets and the Fourier transform of the signal:

$$W_f(s,\tau) = \frac{\sqrt{s}}{2\pi} \int F(\omega) H^*(s\omega) \exp(j\omega\tau) d\omega \tag{10.1.6}$$

The Fourier transforms of the wavelets are referred to as the wavelet transform filters. The impulse response of the wavelet transform filter, $\sqrt{s} H(s\omega)$, is the scaled wavelet $s^{-1/2} h(t/s)$. Therefore, the wavelet transform is a bank of wavelet transform filters with different scales, s.

In the definition of the wavelet transform, the kernel function, wavelet, is not specified. This is a difference between the wavelet transform and other transforms such as the Fourier transform. The theory of wavelet transform deals with general properties of the wavelet and the wavelet transform, such as the admissibility, regularity, and orthogonality. The wavelet basis is built to satisfy those basic conditions. The wavelets can be given as analytical or numerical functions. They can be orthonormal or non-orthonormal, continuous or discrete. One can choose or even build himself a proper wavelet basis for a specific application. Therefore, when talking about the wavelet transform one used to specify what wavelet is used in the transform.

The most important properties of the wavelets are the admissibility and regularity. As we shall see below, according to the admissible condition, the wavelet must oscillate to have its mean value equal to zero. According to the regularity condition, the wavelet has exponential decay so that its first low order moments are equal to zero. Therefore, in the time domain the wavelet is just like a small wave that oscillates and vanishes, as that described by the name *wavelet*. The wavelet transform is a local operator in the time domain.

The orthonormality is a property that belongs to the discrete wavelet transform. We discuss the discrete orthonormal and bi-orthonormal wavelet transforms in Sections 10.3 to 10.9.

10.1.2 Time-Frequency Space Analysis

The wavelet transform of a one-dimensional signal is a two-dimensional function of the scale, s, and the time shift, τ, that represents the signal in the time-scale space and is referred to as the time-scale joint representation. The time-scale wavelet representation is equivalent to the time-frequency joint representation, which is familiar in the analysis of nonstationary and fast transient signals.

Nonstationary Signals

The wavelet transform is of particular interest for analysis of nonstationary and fast transient signals. Signals are stationary if their properties do not change during the course of signals. The concept of the stationarity is well defined in the theory of stochastic processes. A stochastic process is called strict-sense stationary if its statistical properties are invariant to a shift of the origin of the time axis. A stochastic process is called wide-sense (or weak) stationary if its second–order statistics is invariant to shift in time and depends only on time difference.

Most signals in nature are nonstationary. Examples of nonstationary signals are speech, radar, sonar, seismic, electrocardiographic signals and music. Two-dimensional images are also nonstationary because the edges, textures, and deterministic objects are distributed at different locations and orientations. The nonstationary signals are in general characterized by their local features rather than by their global features.

Time-Frequency Joint Representation

An example of the nonstationary signal is music. The frequency spectrum of a music signal changes with the time. At a specific time, for instance, a piano key is knocked, which then gives rise to a sound which has a specific frequency spectrum. At another time, another key will be knocked generating another spectrum.

The notation of music score is an example of the time-frequency joint representation. A piece of music can be described accurately by air pressure as a function of time. It can be equally accurately described by the Fourier transform of the pressure function. However, neither of those two signal representations would be useful for a musician, who wants to perform a certain piece. Musicians prefer a two-dimensional plot, with time and logarithmic frequency as axes. The music scores tell them when and what notes should be played.

Fourier Analysis of Nonstationary Signals

The Fourier transform is widely used in signal analysis and processing. When the signal is periodic and sufficiently regular, the Fourier coefficients decay quickly with the increasing of the frequency.

For nonperiodic signals, the Fourier integral gives a continuous spectrum. The Fast Fourier transform (FFT) permits efficient numerical Fourier analysis.

The Fourier transform is not satisfactory for analyzing signals whose spectra vary with time. The Fourier transform is a decomposition of a signal into two series of orthogonal functions $cos\omega t$ and $jsin\omega t$ with $j = (-1)^{1/2}$. The Fourier bases are of infinite duration along the time axis. They are perfectly local in frequency, but are global in time. A signal may be reconstructed from its Fourier components, which are the Fourier base of infinite duration multiplied by the corresponding Fourier coefficients of the signal. Any signal that we are interested in is, however, of finite extent. Outside that finite duration, the Fourier components of the signal, which are nonzero, must be cancelled by their own summation. A short pulse that is local in time is not local in frequency. Its Fourier coefficients decay slowly with frequency. The reconstruction of the pulse from its Fourier components depends heavily on the cancellation of high frequency Fourier components and, therefore, is sensitive to high frequency noise.

The Fourier spectrum analysis is global in time and is basically not suitable to analyze nonstationary and fast varying transient signals. Many temporal aspects of the signal, such as the start and end of a finite signal and the instant of appearance of a singularity in a transient signal, are not preserved in the Fourier spectrum. The Fourier transform does not provide any information regarding the time evolution of spectral characteristics of the signal.

The short-time Fourier transform, or called the Gabor transform, the Wigner distribution, and the ambiguity function are usually used to overcome the drawback of the Fourier analysis for nonstationary and fast transient signals. The Wigner distribution and the ambiguity function are not linear, but are bilinear transforms.

10.1.3 Short-Time Fourier Transform

Definition

An intuitive way to analyze a nonstationary signal is to perform a time-dependent spectral analysis. A nonstationary signal is divided into a sequence of time segments in which the signal may be considered as quasistationary. Then, the Fourier transform is applied to each of the local segments of the signal.

The short-time Fourier transform is associated with a window of fixed width. Gabor in 1946 was the first to introduce the short-time Fourier transform[1] which is known as the sliding window Fourier transform. The transform is defined as

$$S_f(\omega',\tau) = \int f(t)g^*(t-\tau)\exp(-j\omega' t)dt$$

where $g(t)$ is a square integrable short-time window, which has a fixed width and is shifted along the time axis by a factor τ.

Gabor Functions

The Gabor transform may also be regarded as an inner product between the signal and a set of kernel functions, called the Gabor functions: $g(t-\tau)\exp(j\omega' t)$. The Gabor basis is generated from a basic window function $g(t)$ by translations along the time axis by τ. The phase modulations $\exp(j\omega' t)$ correspond to translations of the Gabor function spectrum along the frequency axis by ω'. The Fourier transform of the basic Gabor function $g(t)\exp(j\omega' t)$ is expressed as

$$\int g(t)\exp(j\omega' t)\exp(-j\omega t)dt = G(\omega-\omega')$$

The Fourier transform $G(\omega)$ of the basic window function $g(t)$ is shifted along the frequency axis by ω'. The short-time Fourier transform of a one-dimensional signal is a complex valued function of two real parameters: time τ and frequency ω' in the two-dimensional time-frequency space.

Inverse Short-Time Fourier Transform

When τ and ω′ are continuous variables, the signal *f(t)* may be reconstructed completely by integrating the Gabor functions multiplied by the short-time Fourier transform coefficients:

$$f(t)=\frac{1}{2\pi}\iint S_f(\omega',\tau)g(t-\tau)\exp(j\omega' t)d\omega' d\tau$$

and this holds for any chosen window *g(t)*. The inverse short-time Fourier transform may be proved by the following calculation:

$$\begin{aligned}&\iint S_f(\omega',\tau)g(t-\tau)\exp(j\omega' t)d\omega' d\tau\\&=\iiint f(t')g^*(t'-\tau)\exp(-j\omega' t')g(t-\tau)\exp(j\omega' t)d\omega' d\tau dt'\\&=\iint 2\pi\delta(t'-t)f(t')g^*(t'-\tau)g(t-\tau)d\tau dt'=2\pi f(t)\int|g(t-\tau)|^2 d\tau=2\pi f(t)\end{aligned}$$

provided that the window function is normalized as

$$\int|g(t)|^2 dt=1 \tag{10.1.7}$$

Time and Frequency Resolution

In the short-time Fourier transform, the signal is multiplied by a sliding window that localizes the signal in time domain, but results in a convolution between the signal spectrum and the window spectrum; that is, a blurring of the signal in the frequency domain. The narrower the window, the better we localize the signal and the poorer we localize its spectrum.

The width Δt of the window *g(t)* in time domain and the bandwidth $\Delta\omega$ of the window *G(ω)* in frequency domain are defined respectively as

$$\Delta t^2=\frac{\int t^2|g(t)|^2 dt}{\int|g(t)|^2 dt}\qquad \Delta\omega^2=\frac{\int\omega^2|G(\omega)|^2 d\omega}{\int|G(\omega)|^2 d\omega} \tag{10.1.8}$$

where the denominator is the energy of the window in time and frequency domains.

The two sinusoidal signals can be discriminated only if they are more than $\Delta\omega$ apart. Thus, $\Delta\omega$ is the resolution in the frequency domain of the short-time Fourier transform. Similarly, two pulses in time domain can be discriminated only if they are more than Δt apart. Note that once a window has been chosen for the short-time Fourier transform, the time and frequency resolutions given by (10.1.8) are fixed over the entire time-frequency plane. The short-time Fourier transform is a fixed window Fourier transform.

Uncertainty Principle

The time-frequency joint representation has an intrinsic limitation, the product of the resolutions in time and frequency is limited by the uncertainty principle:

$$\Delta t\Delta\omega\geq 1/2 \tag{10.1.9}$$

This is also referred to as the Heisenberg inequality, familiar in quantum mechanics and important for time-frequency joint representation. A signal can not be represented as a point in the time frequency space. One can only determine its position in the time-frequency space within a rectangle of $\Delta t\Delta\omega$.

Gaussian Window

The time-bandwidth product $\Delta t\Delta\omega$ must obey the uncertainty principle. We can only trade time resolution for frequency resolution or vice versa. Gabor proposed the Gaussian function as the window function. The Gaussian function has the minimum time-bandwidth product determined by the uncertainty principle (10.1.9). The Fourier transform of the Gaussian window is still a Gaussian as

$$g(t) = \frac{1}{\sqrt{2\pi}s}\exp\left(-\frac{t^2}{2s^2}\right) \quad \text{and} \quad G(\omega) = \exp\left(-s^2\omega^2/2\right)$$

which have a minimum spread. A simple calculation shows that

$$\Delta t^2 = \frac{s^2}{2} \quad \text{and} \quad \Delta\omega^2 = \frac{1}{2s^2}$$

which satisfies the uncertainty principle (10.1.9) and achieves the minimum time-bandwidth product $\Delta t\Delta\omega = 1/2$.

The short-time Fourier analysis depends critically on the choice of the window. Its application requires *a priori* information concerning the time evolution of the signal properties in order to make *a priori* choice of the window function. Once a window is chosen, the width of the window along both time and frequency axes are fixed in the entire time-frequency plane.

Discrete Short-Time Fourier Transform

When the translation factors of the Gabor functions along the time and the frequency axes, τ and ω', take discrete values, $\tau = n\tau_0$ and $\omega' = m\omega_0$ with m and $n \in \mathbf{Z}$, the discrete Gabor functions are written as:

$$g_{m,n}(t) = g(t - n\tau_0)\exp(jm\omega_0 t)$$

and their Fourier transforms are

$$G_{m,n}(\omega) = G(\omega - m\omega_0)\exp\left[j(\omega - m\omega_0)n\tau_0\right]$$

The discrete Gabor transform is

$$S_f(m,n) = \int f(t)g^*(t - n\tau_0)\exp(-jm\omega_0 t)dt$$

The signal $f(t)$ can still be recovered from the coefficients $S_f(m,n)$, provided that τ_0 and ω_0 are suitably chosen. Gabor's original choice was $\omega_0\tau_0 = 2\pi$.

Regular Lattice

If the window function is normalized as shown in (10.1.7) and is centered to the origin in the time-frequency space, so that:

$$\int t\left|g(t)\right|^2 dt = 0 \qquad \int \omega\left|G(\omega)\right|^2 d\omega = 0$$

then the locations of the Gabor functions in the time-frequency space are determined by:

$$\int t\left|g_{m,n}(t)\right|^2 dt = \int t\left|g(t - n\tau_0)\right|^2 dt = n\tau_0$$

and

$$\int \omega \left| G_{m,n}(\omega) \right|^2 d\omega = \int \omega \left| G(\omega - m\omega_0) \right|^2 d\omega = m\omega_0$$

The discrete Gabor function set will be represented by a regular lattice with the equal intervals τ_0 and ω_0 in the time-frequency space, as will be shown in Figure 10.2a.

10.1.4 Wigner Distribution and Ambiguity Functions

The Wigner distribution function and the ambiguity function are second-order transform or bilinear transforms that perform the mapping of signals into the time-frequency space.

Wigner Distribution Function

The Wigner distribution function[2] is an alternative to the short-time Fourier transform for nonstationary and transient signal analysis. The Wigner distribution of a function *f(t)* is defined in the time domain as

$$W_f(\tau,\omega) = \int f\left(\tau + \frac{t}{2}\right) f^*\left(\tau - \frac{t}{2}\right) \exp(-j\omega t)\, dt \tag{10.1.10}$$

that is the Fourier transform of the product, $f(\tau + t/2)f^*(\tau - t/2)$, between the dilated function $f(t/2)$ and the dilated and inverted function $f^*(-t/2)$. The product is shifted along the time axis by τ. The Wigner distribution is a complex valued function in the time-frequency space and is a time-frequency joint representation of the signal. In the frequency domain the Wigner distribution function is expressed as

$$W_f(\tau,\omega) = \frac{1}{2\pi} \int F\left(\omega + \frac{\xi}{2}\right) F^*\left(\omega - \frac{\xi}{2}\right) \exp(j\tau\xi)\, d\xi \tag{10.1.11}$$

where $F(\omega)$ is the Fourier transform of $f(t)$.

The inverse relations of the Wigner distribution function can be obtained from the inverse Fourier transforms of (10.1.10) and (10.1.11). With the changes of variables $t_1 = \tau + t/2$ and $t_2 = \tau - t/2$, the inverse Fourier transform of the Wigner distribution of (10.1.10) gives

$$f(t_1) f^*(t_2) = \frac{1}{2\pi} \int W_f\left(\frac{t_1 + t_2}{2}, \omega\right) \exp\left[j(t_1 - t_2)\omega\right] d\omega \tag{10.1.12}$$

Similarly, with the changes of variables $\omega_1 = \omega + (\xi/2)$ and $\omega_2 = \omega - (\xi/2)$ the inverse Fourier transform of (10.1.11) gives

$$F(\omega_1) F^*(\omega_2) = \int W_f\left(\tau, \frac{\omega_1 + \omega_2}{2}\right) \exp\left[-j(\omega_1 - \omega_2)\tau\right] d\tau$$

The signal $f(t)$ can be recovered from the inverse Wigner distribution function. Let $t_1 = t$ and $t_2 = 0$, (10.1.12) becomes

$$f(t) f^*(0) = \frac{1}{2\pi} \int W_f\left(\frac{t}{2}, \omega\right) \exp(j\omega t)\, d\omega$$

where $f^*(0)$ is a constant. Hence, the function $f(t)$ is reconstructed from the inverse Fourier transform of the Wigner distribution function, $W_f(t/2,\omega)$, dilated in the time domain.

For the basic properties of the Wigner distribution function we mention that the projections of $W_f(\tau,\omega)$ along the τ-axis in the time-frequency space gives the square modulus of $F(\omega)$, because according to (10.1.11) the projection along the τ-axis is

$$\int W_f(\tau,\omega)d\tau = \frac{1}{2\pi}\iint F\left(\omega+\frac{\xi}{2}\right)F^*\left(\omega-\frac{\zeta}{2}\right)\exp(j\tau\xi)d\tau d\xi = \left|F(\omega)\right|^2$$

The projection of $W_f(\tau,\omega)$ along the ω-axis gives the square modulus of $f(t)$, because according to (10.1.10) the projection along the ω-axis is

$$\int W_f(\tau,\omega)d\omega = \iint f\left(\tau+\frac{t}{2}\right)f^*\left(\tau-\frac{t}{2}\right)\exp(-j\omega t)dtd\omega = 2\pi\left|f(t)\right|^2$$

Also, there is the conservation of energy of the Wigner distribution in the time-frequency joint representation:

$$\frac{1}{2\pi}\int W_f(\tau,\omega)d\tau d\omega = \frac{1}{2\pi}\int\left|F(\omega)\right|^2 d\omega = \int\left|f(t)\right|^2 dt$$

Ambiguity Function

The ambiguity function is also a mapping of a transient time function $f(t)$ into the time-frequency space. The ambiguity function is defined in the time domain as:[3]

$$A_f(t,\omega) = \int f\left(\tau+\frac{t}{2}\right)f^*\left(\tau-\frac{t}{2}\right)\exp(-j\omega\tau)d\tau \qquad (10.1.13)$$

In the frequency domain, the ambiguity function is expressed as

$$A_f(t,\omega) = \frac{1}{2\pi}\int F\left(\xi+\frac{\omega}{2}\right)F^*\left(\xi-\frac{\omega}{2}\right)\exp(j\tau\xi)d\xi$$

The ambiguity function can be viewed as a time-frequency auto-correlation function of the signal with the time delay t and the Doppler frequency shift, ω. The ambiguity function has found wide applications for radar signal processing.

According to the definitions (10.1.10) and (10.1.13) the double Fourier transform of the product $f(\tau + t/2)f^*(\tau - t/2)$ with respect to both variables t and τ gives the relation between the Wigner distribution function and the ambiguity function:

$$\int A_f(t,\omega)\exp(-j\omega t)dt = \int W_f(\tau,\omega)\exp(-j\omega\tau)d\tau$$

The cross ambiguity function is defined as the Fourier transform of the product, $f(\tau)g^*(\tau)$ of two functions $f(\tau)$ and $g(\tau)$:

$$A(t,\omega) = \int f\left(\tau+\frac{t}{2}\right)g^*\left(\tau-\frac{t}{2}\right)\exp(j\omega\tau)d\tau$$

High values of $A(t,\omega)$ mean that the two functions are ambiguous. The function $g(\tau)$ can also be considered as a window function of fixed width that is shifted along the time axis by t. Hence, the cross

ambiguity function is the fixed-window, short-time Fourier transform. The cross Wigner distribution function is defined as

$$W(\tau,\omega)=\int f\left(\tau+\frac{t}{2}\right)g^{*}\left(\tau-\frac{t}{2}\right)\exp(j\omega t)dt$$

that can be seen as the Fourier transform of the signal $f(t)$ dilated by a factor of two and multiplied with an inverted window $g(-t)$ which is also dilated by a factor of two and shifted by τ.

Both the ambiguity function and the Wigner distribution function are useful for active and passive transient signal analysis. Both transforms are bilinear transform. However, the mapping of a summation of signals $f_1(t) + f_2(t)$ into the time-frequency space with the ambiguity function or with the Wigner distribution function produces cross-product interference terms that might be a nuisance in the projections in the time-frequency space and in the reconstruction of the signal.

10.2 Properties of the Wavelets

In this section we discuss some basic properties of the wavelets. One of them is related to the fact that we must be able to reconstruct the signal from its wavelet transform. This property involves the resolution of identity, the energy conservation in the time-scale space and the wavelet admissible condition. Any square integrable function which has finite energy and satisfies the wavelets admissible condition can be a wavelet. The second basic property is related to the fact that the wavelet transform should be a local operator in both time and frequency domains. Hence, the regularity condition is usually imposed on the wavelets. The third basic property is related to the fact that the wavelet transform is a multiresolution signal analysis.

10.2.1 Admissible Condition

Resolution of Identity

The wavelet transform of a one-dimensional signal is a two-dimensional time-scale joint representation. No information should be lost during the wavelet transform. Hence, the resolution of identity must be satisfied, that is expressed as

$$\int\frac{ds}{s^2}\int d\tau\langle f_1,h_{s,\tau}\rangle\langle h_{s,\tau},f_2\rangle=c_h\langle f_1,f_2\rangle \tag{10.2.1}$$

where $<\ ,\ >$ denotes the inner product and c_h is a constant. In the left-hand side of (10.2.1) the extra factor $1/s^2$ in the integral is the Haar invariant measure, owing to the time-scale space differential elements, $d\tau d(1/s) = d\tau ds/s^2$. We have assumed positive dilation $s > 0$; using (10.1.6) for wavelet transform in the Fourier domain, we have:

$$\begin{aligned}
&\int\frac{ds}{s^2}\int d\tau\langle f_1,h_{s,\tau}\rangle\langle h_{s,\tau},f_2\rangle\\
&=\frac{1}{4\pi^2}\int\frac{ds}{s^2}\int d\tau\iint sF_1(\omega_1)H^{*}(s\omega_1)F_2^{*}(\omega_2)H(s\omega_2)e^{j\tau(\omega_1-\omega_2)}d\omega_1\omega_2\\
&=\frac{1}{2\pi}\iint F_1(\omega_1)F_2^{*}(\omega_1)\left|H(s\omega_1)\right|^2\frac{ds}{s}d\omega_1\\
&=\frac{c_h}{2\pi}\int F_1(\omega_1)F_2^{*}(\omega_1)d\omega_1
\end{aligned}$$

where we used the change of variables $\omega = s\omega_1$ and $ds = d\omega/|\omega_1|$, so that ds and $d\omega$ are of the same sign. Because $s > 0$, we have $ds/s = d\omega/|\omega|$, then we defined the constant:

$$c_h = \int |H(\omega)|^2 \frac{d\omega}{|\omega|}$$

According to the Parseval's equality in the Fourier transform, we have:

$$\frac{1}{2\pi}\int F_1(\omega_1)F_2^*(\omega_1)d\omega_1 = \int f_1(t)f_2^*(t)dt = \langle f_1, f_2 \rangle$$

Hence, the resolution of identity is satisfied on the condition that

$$c_h = \int \frac{|H(\omega)|^2}{|\omega|} d\omega < +\infty \tag{10.2.2}$$

Admissible Condition

The condition (10.2.2) is the admissible condition of the wavelet, which implies that the Fourier transform of the wavelet must be equal to zero at the zero frequency:

$$|H(\omega)|_{\omega=0} = 0 \tag{10.2.3}$$

Equivalently, in the time domain the wavelet must be oscillatory, like a wave, to have a zero-integrated area, or a zero-mean value:

$$\int h(t)dt = 0 \tag{10.2.4}$$

Energy Conservation

When $f_1 = f_2$, the resolution of identity, (10.2.1) becomes:

$$\iint |W_f(s,\tau)|^2 d\tau \frac{ds}{s^2} = c_h \int |f(t)|^2 dt \tag{10.2.5}$$

This is the energy conservation relation of the wavelet transform, equivalent to the Parseval energy relation in the Fourier transform.

Inverse Wavelet Transform

By withdrawing $f_2\rangle$ from the both sides of the resolution of identity (10.2.1), we have directly:

$$f(t) = \frac{1}{c_h}\iint W_f(s,\tau)\frac{1}{\sqrt{s}}h\left(\frac{t-\tau}{s}\right)d\tau\frac{ds}{s^2} \tag{10.2.6}$$

This is the inverse wavelet transform. The function $f(t)$ is recovered from the inverse wavelet transform by the integrating in the time-scale space the wavelets $h_{s,\tau}(t)$ weighted by the wavelet transform coefficients, $W_f(s,\tau)$.

The wavelet transform is a decomposition of a function into a linear combination of the wavelets. The wavelet transform coefficients $W_f(s,\tau)$ are the inner products between the function and the wavelets, which indicate how close the function $f(t)$ is to a particular wavelet $h_{s,\tau}(t)$.

Reproducing Kernel

The inverse wavelet transform shows that the original signal may be synthesized by summing up all the projections of the signal onto the wavelet basis. In this sense, the continuous wavelet transform behaves like an orthogonal transform. We refer to this property of the continuous wavelet transform as the quasi-orthogonality. Obviously, the set of the wavelet kernel functions $h_{s,\tau}(t)$ with continuously varying scaling and shift is not orthogonal, but is heavily redundant.

Applying the wavelet transforms in the two sides of (10.2.6) yields:

$$W_f(s_0,\tau_0) = \iint W_f(s,\tau) K(s_0,s;\tau_0,\tau) d\tau \frac{ds}{s^2}$$

where the reproducing kernel:

$$K(s_0,s;\tau_0,\tau) = \frac{1}{c_h} \frac{1}{\sqrt{s s_0}} \int h^*\left(\frac{t-\tau_0}{s_0}\right) h\left(\frac{t-\tau}{s}\right) dt$$

is not zero with continuously varying factors s_0, s, ω_0, and ω that describes the intrinsic redundancy between the values of the wavelets at (s,τ) and at (s_0,τ_0).

Any square integrable function satisfying the admissible condition may be a wavelet. When the wavelets satisfy the admissible condition, the signal can be recovered by the inverse wavelet transform. No signal information is lost.

10.2.2 Regularity

The wavelets should be local in both time and frequency domains. This is achieved by applying the regularity condition to the wavelet. The regularity is not an obligated condition, but is usually required as an important property of the wavelet.

Regularity of Wavelet

For the sake of simplicity, let the translation of the wavelet $\tau = 0$ and consider the convergence to zero of the wavelet transform coefficients with increasing of $1/s$ and decreasing of s. The signal $f(t)$ is expanded into the Taylor series at $t = 0$ until order n. The wavelet transform coefficients become[4]

$$\begin{aligned} W_f(s,0) &= \frac{1}{\sqrt{s}} \int f(t) h^*\left(\frac{t}{s}\right) dt \\ &= \frac{1}{\sqrt{s}} \left[\sum_{p=0}^{n} f^{(p)}(0) \int \frac{t^p}{p!} h\left(\frac{t}{s}\right) dt + \int R(t) h\left(\frac{t}{s}\right) dt \right] \end{aligned} \tag{10.2.7}$$

where the remainder in the Taylor series is

$$R(t) = \int_0^t \frac{(t-t')^n}{n!} f^{(n+1)}(t') dt'$$

and $f^{(p)}(0)$ denotes the pth derivative. Denoting the moments of the wavelets by M_p:

$$M_P = \int t^P h(t) dt$$

it is easy to show that the last term in the right-hand side of (10.2.7) which is the wavelet transform of the remainder, decreases as s^{n+2}. We then have a finite development as:

$$W_f(s,0) = \frac{1}{\sqrt{s}}\left[f(0)M_0 s + \frac{f'(0)}{1!}M_1 s^2 + \frac{f''(0)}{2!}M_2 s^3 + \ldots + \frac{f^{(n)}(0)}{n!}M_n s^{n+1} + O\left(s^{n+2}\right)\right] \quad (10.2.8)$$

According to the admissible condition of the wavelet, $M_0 = 0$, the first term in the right-hand side of (10.2.8) must be zero. The speed of convergence to zero of the wavelet transform coefficients $W_f(s,\tau)$ with decreasing of the scale s or increasing of $1/s$ is then determined by the first nonzero moment of the basic wavelet $h(t)$. It is in general required that the wavelets have the first $n+1$ moments until order n, equal to zero:

$$M_p = \int t^p h(t)dt = 0 \qquad for \qquad p = 0,1,2,\ldots,n \quad (10.2.9)$$

Then, according to (10.2.8) the wavelet transform coefficient $W_f(s,\tau)$ decays as fast as $s^{n+(1/2)}$ for a smooth signal $f(t)$. The regularity leads to localization of the wavelet transform in the frequency domain.

The wavelet satisfying the condition (10.2.9) is called the wavelet of order n. In frequency domain, this condition is equivalent to the derivatives of the Fourier transform of the wavelet $h(t)$ up to order n to be zero at the zero frequency $\omega = 0$:

$$H^{(p)}(0) = 0 \qquad for \qquad p = 0,1,2,\ldots n. \quad (10.2.10)$$

The Fourier transform of the wavelet has a zero of order $n+1$. The order $(n+1)$ is a measure of the flatness of the wavelet in the frequency domain about $\omega = 0$.

Time Bandwidth Product

While the wavelet transform of a one-dimensional function is two-dimensional, the wavelet transform of a two-dimensional function is four-dimensional. As a consequence, we would have an explosion of the time bandwidth product with the wavelet transform, which is in contradiction with the restrictions of many applications, such as data compression and pattern classification, where the signals need to be characterized efficiently by fewer transform coefficients.

We usually impose the regularity property to the wavelets such that the wavelet transform coefficients decrease fast with decreasing of the scale, s and increasing of $1/s$. For this purpose, the Fourier transform, $H(\omega)$, of the basic wavelet should have some smoothness and concentration in frequency domains, according to the wavelet transform in the frequency domain (10.1.6). The wavelet transform should be a local operator in frequency domain.

10.2.3 Multiresolution Wavelet Analysis

The wavelet transform performs the multiresolution signal analysis with the varying scale factor, s. The purpose of the multiresolution signal analysis is decomposing the signal in multiple frequency bands, in order to process the signal in multiple frequency bands differently and independently. Hence, we need the wavelet to be local in both time and frequency domains. Historically, looking for a kernel function which is local in both time and frequency domains has been a hard research topic and was conducted to invent the wavelet transform.

Example

Figure 10.1 shows a typical wavelet multiresolution analysis for an electrical power system transient signal. The signal is decomposed with different resolutions corresponding to different scale factors of the

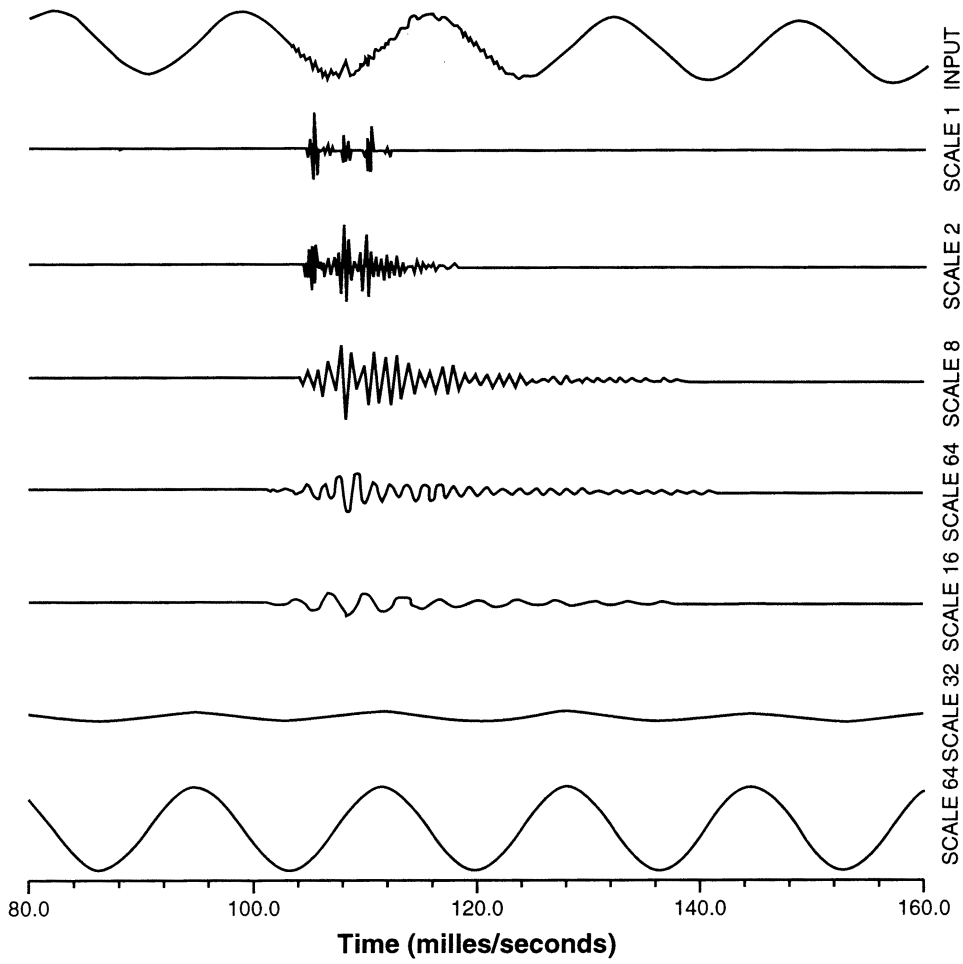

FIGURE 10.1 Multiresolution wavelet analysis of a transient signal in the electrical power system. (From Robertson, D. C. et al., *Proc. SPIE*, 2242, 474, 1994. With permission.)

wavelets. The signal components in multiple frequency bands and the times of occurrence of those components are well presented in the figure. This figure is a time-scale joint representation, with the vertical axis in each discrete scale representing the amplitude of wavelet components. More detailed discussion will be given in Section 10.10.1.

Localization in Time Domain

According to the admissible condition, the wavelet must oscillate to have a zero mean. According to the regularity condition the wavelet of order n has first $n+1$ vanishing moments and decays as fast as t^{-n}. Therefore, in the time domain, the wavelet must be a small wave that oscillates and vanishes, as that described by the name wavelet. The wavelet is localized in the time domain.

Localization in Frequency Domain

According to the regularity condition the wavelet transform with a wavelet of order, n, decays with s, as $s^{n+(1/2)}$, for a smooth signal. According to the frequency domain wavelet transform, (10.1.6) when the scale s decreases the wavelet, $H(s\omega)$ in the frequency domain is dilated to cover a large frequency band of the signal Fourier spectrum. Therefore, the decay with s as $s^{n+(1/2)}$ of the wavelet transform coefficient

implies that the Fourier transform of the wavelet must decay fast with the frequency, ω. The wavelet must be local in frequency domain.

Band-Pass Filters

In the frequency domain, the wavelet is localized according to the regularity condition, and is equal to zero at the zero frequency according to the admissible condition. Therefore, the wavelet is intrinsically a band-pass filter.

Bank of Multiresolution Filters

The wavelet transform is the correlation between the signal and the dilated wavelets. The Fourier transform of the wavelet is a filter in the frequency domain. For a given scale, the wavelet transform is performed with a wavelet transform filter $\sqrt{s}H(s\omega)$ in the frequency domain, whose impulse response is the scaled wavelet, *h(t/s)*. When the scale *s* varies, the wavelet transform performs a multiscale signal analysis.

In the time-scale joint representation, the horizontal stripes of the wavelet transform coefficients are the correlations between the signal and the wavelets *h(t/s)* at given scales. When the scale is small, the wavelet is concentrated in time and the wavelet analysis gives a detailed view of the signal. When the scale increases, the wavelet becomes spread out in time and the wavelet analysis gives a global view and takes into account the long-time behavior of the signal. Hence, the wavelet transform is a bank of multiresolution filters.

The wavelet transform is a bank of multiresolution band-pass filters.

Constant Fidelity Analysis

Scale change of the wavelets permits the wavelet analysis to zoom in on discontinuities, singularities, and edges and to zoom out for a global view. This is a unique property of the wavelet transform, important for nonstationary and fast–transient signal analysis. The fixed window short-time Fourier transform does not have this ability.

With the bank of multiresolution wavelet transform filters, the signal is divided into different frequency subbands. In each subband the signal is analyzed with a resolution matched to the scales of the wavelets. When the scale changes, the bandwidth, $(\Delta\omega)_s$, of the wavelet transform filter becomes, according to the definition of the bandwidth (10.1.8):

$$(\Delta\omega)_s^2 = \frac{\int \omega^2 |H(s\omega)|^2 d\omega}{\int |H(s\omega)|^2 d\omega} = \frac{\int (s\omega)^2 |H(s\omega)|^2 d(s\omega)}{s^2 \int |H(s\omega)|^2 d(s\omega)} = \frac{1}{s^2}(\Delta\omega)^2$$

The fidelity factor, Q, refers to, in general, the central frequency divided by the bandwidth of a filter. By this definition, the fidelity factor, Q, is the inverse of the relative bandwidth. The relative bandwidths of the wavelet transform filters are constant because:

$$\frac{1}{Q} = \frac{(\Delta\omega)_s}{1/s} = (\Delta\omega) \tag{10.2.11}$$

which is independent of the scale, *s*. Hence, the wavelet transform is a constant-*Q* analysis. At low frequency, corresponding to a large scale factor, *s*, the wavelet transform filter has a small bandwidth, which implies a broad time window with a low time resolution. At high frequency, corresponding to a small scale factor, *s*, the wavelet transform filter has a wide bandwidth, which implies a narrow time window with high-time resolution. The time resolution of the wavelet analysis increases with decreases of the window size. This adaptive window property is desirable for time-frequency analysis.

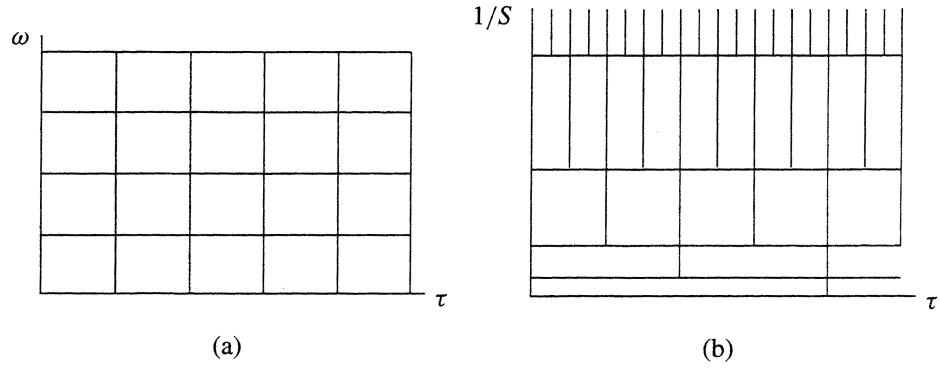

FIGURE 10.2 Coverage of the time-frequency space with (a) the short-time Fourier transform, where $\Delta\omega$ and Δt are fixed in the whole plane; (b) the wavelet transform, where the frequency bandwidth $\Delta\omega$ increases and the time resolution Δt improves with increase of $\Delta(1/s)$.

When the constant-Q relation (10.2.11) is satisfied, the frequency bandwidth $\Delta\omega$ changes with the center frequency, *1/s*, of the wavelet transform filter. The product $\Delta\omega\Delta t$ still satisfies the uncertainty principle (10.1.9). In the wavelet transform, the time window size Δt can be arbitrarily small at small scale and the frequency window size, $\Delta\omega$, can be arbitrarily small at large scale. Figure 10.2 shows the coverage of the time-scale space for the wavelet transform and, as a comparison, that for the short-time Fourier transform.

Scale and Resolution

The scale is related to the window size of the wavelet. A large scale means a global view and a small scale means a detailed view. The resolution is related to the frequency of the wavelet oscillation. For some wavelets, such as the Gabor wavelets, the scale and frequency may be chosen separately. For a given wavelet function, reducing the scale will reduce the window size and increase the resolution in the same time.

Example

Figure 10.3a shows the cos-Gaussian wavelets in comparison with the real part of the Gabor transform basis. Both functions consist of a cosine kernel with a Gaussian window. The cos-Gaussian wavelet is

$$h(t) = \frac{1}{\sqrt{2\pi}} \cos(\omega_0 t) \exp\left(\frac{-t^2}{2}\right)$$

where $\omega_0 = 5$. The wavelets $h_{m,n}(t)$ are generated from $h(t)$ by dilation and translation:

$$h_{s,\tau} = \frac{1}{\sqrt{s}} h\left(\frac{t-\tau}{s}\right)$$

with the discrete scale factor, $s = 2^m$, and the discrete translation factor, $(\tau/s) = n$.

The discrete Gabor function $g_{m,n}(t)$ is defined as:

$$g_{m,n}(t) = g(t - n\tau_0) \exp(jm\omega_0 t)$$

where g(t) is the Gaussian window with a fixed width and $\omega_0 = \pi$.

In Figure 10.3a we see that the wavelets are with the dilated window. All the dilated wavelets contain the same number of oscillations. The wavelet transform performs multiresolution analysis with high–frequency analysis for narrow windowed signals and low–frequency analysis for wide windowed signals. This constant-Q analysis property makes the wavelet transform surpass the fixed-window short-time Fourier transform for analysis of the local property of signals.

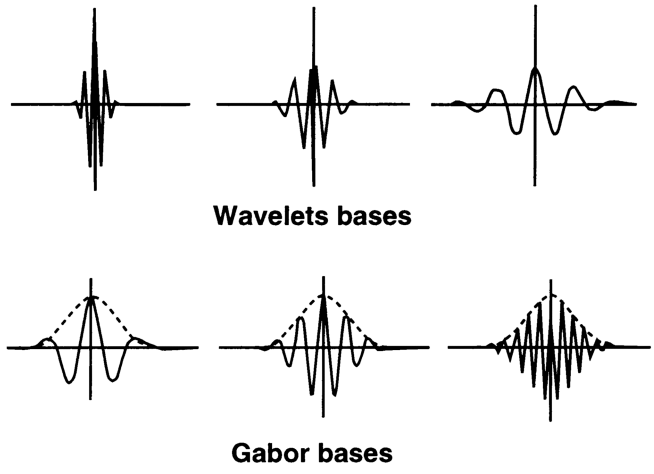

(a)

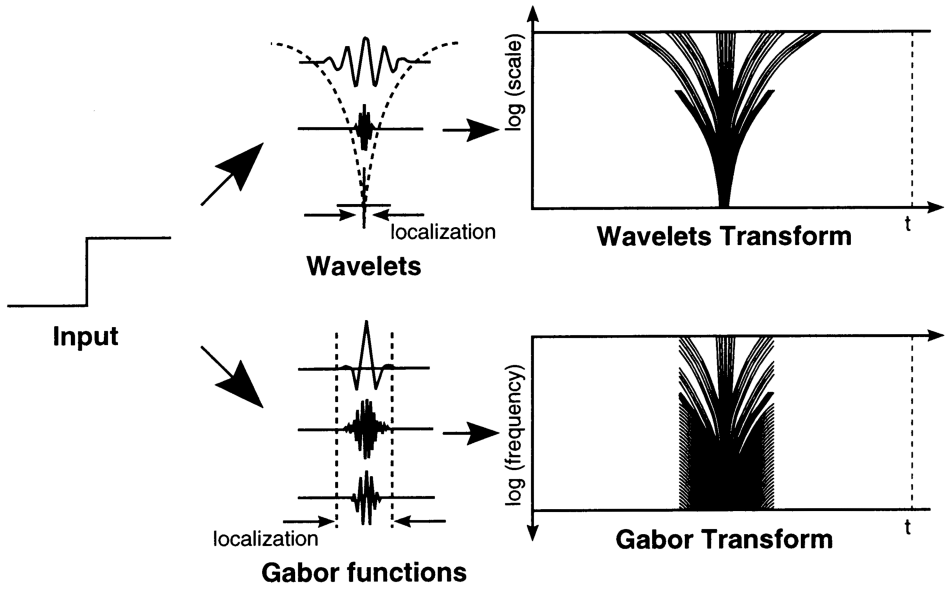

(b)

FIGURE 10.3 (a) The cos-Gaussian wavelets $h_{m,n}(t)$ and the real part of the Gabor functions $g_{m,n}(t)$, with the scale factor $s = 2^m$ and the translation factor $\tau = ns$ for different values of m. The wavelets have a dilated window. The Gabor functions have a window with fixed width. (b) Time-scale joint representation of the wavelet transform and time-frequency joint representation of the Gabor transform for a step function. (From Szu, H. et al. *Appl. Optics*, 31(17), 1992. Freeman, M.O. *Photonics New*, August 1995, 8-14. With permission.)

Figure 10.3b shows a comparison between the wavelet transform and the Gabor transform for a step function input. The wavelets are with the dilated windows. The Gabor functions are with windows of fixed width. The time-scale joint representation, *log s – t*, of the wavelet transform and the time-frequency joint representation, *log* ω *– t*, of the Gabor transform are also shown. The wavelet transform with a very small scale, *s*, and a very narrow window is able to "zoom in" on the discontinuity and to indicate the arrival time of the step signal.

10.2.4 Linear Transform Property

By definition the wavelet transform is a linear operation. Given a function *f(t)*, its wavelet transform $W_f(s,\tau)$, satisfies the following relations:

Linear superposition without the cross terms:

$$W_{f_1+f_2}(s,\tau)=W_{f_1}(s,\tau)+W_{f_2}(s,\tau)$$

Translation:

$$W_{f(t-t_0)}(s,\tau)=W_{f(t)}(s,\tau-t_0)$$

Rescale:

$$W_{\alpha^{1/2}f(\alpha t)}(s,\tau)=W_{f(t)}(\alpha s,\alpha\tau)$$

Different from the standard Fourier transform and other transforms, the wavelet transform is not ready for closed form solution apart from some very simple functions such as:

1. For $f(t) = 1$, from the definition (10.1.4) and the admissible condition of the wavelets, (10.2.4) we have

$$W_f(s,\tau)=0$$

   The wavelet transform of a constant is equal to zero.
2. For a sinusoidal function $f(t) = exp(j\omega_0 t)$, we have directly from the Fourier transform of the wavelets (10.1.6) that

$$W_f(s,\tau)=\sqrt{s}H^*(s\omega_0)\exp(j\omega_0\tau)$$

   The wavelet transform of a sinusoidal function is a sinusoidal function of the time shift, τ. Its modulus $|W_f(s,\tau)|$ depends only on the scale, *s*.
3. For a linear function $f(t) = t$, we have

$$W_f(s,\tau)=\frac{1}{\sqrt{s}}\int th^*\left(\frac{t-\tau}{s}\right)dt$$

$$=s^{3/2}\int th^*(t-\tau')dt=\frac{s^{3/2}}{j}\frac{dH^*(\omega)}{d\omega}\bigg|_{\omega=0}$$

Hence, if the wavelet $h(t)$ is regular and of order $n \geq 1$ so that its derivatives of first–order is equal to zero at $\omega = 0$, the wavelet transform of $f(t) = t$ is equal to zero.

For most functions the wavelet transforms have no closed analytical solutions and can be calculated only by numerical computer or by optical analog computer. The optical continuous wavelet transform is based on the explicit definition of the wavelet transform and implemented using a bank of optical wavelet transform filters in the Fourier plane in an optical correlator.[21]

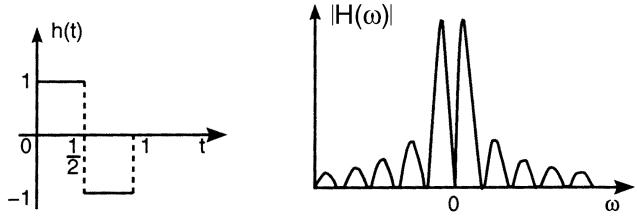

FIGURE 10.4 Haar basic wavelet $h(t)$ and its Fourier transform $H(\omega)$. (From Sheng, Y. et al. *Opt. Eng.*, 31, 1840, 1992. With permission.)

Wavelet Transform of Regular Signals

According to what was discussed above, the wavelet transform of a constant is zero, and the wavelet transform of a linear signal is zero, if the wavelet has the first–order vanishing moment: $M_1 = 0$. The wavelet transform of a quadratic signal could be zero, if the wavelet has the first and second–order vanishing moments: $M_1 = M_2 = 0$. The wavelet transform of a polynomial signal of degree m could be equal to zero, if the wavelet has the vanishing moments up to the order $n \geq m$.

The wavelet transform is efficient for detecting singularities and analyzing nonstationary, transient signals.

10.2.5 Examples of the Wavelets

In this section we give some examples of the wavelets, useful mainly for the continuous wavelet transform. Examples of the wavelets for the discrete orthonormal wavelet transform will be given in Section 10.8.

Haar Wavelet

The Haar wavelet was historically introduced by Haar[5] in 1910. It is a bipolar step function:

$$h(t) = \begin{cases} 1 & \text{when } 0 < t < 1/2 \\ -1 & \text{when } 1/2 < t < 1 \\ 0 & \text{otherwise} \end{cases}$$

The Haar wavelet can be written as a correlation between a dilated rectangle function $rect(2t)$ and two delta functions:

$$h(t) = \text{rect}\left(2\left(t - \frac{1}{4}\right)\right) - \text{rect}\left(2\left(t - \frac{3}{4}\right)\right)$$

$$= \text{rect}(2t) * \left[\delta\left(t - \frac{1}{4}\right) - \delta\left(t - \frac{3}{4}\right)\right]$$

The rectangular function is defined as:

$$\text{rect}(t) = \begin{cases} 1 & \text{when } -1/2 < t < 1/2 \\ 0 & \text{otherwise} \end{cases}$$

The Haar wavelet is real-valued and antisymmetric with respect to $t = 1/2$, as shown in Figure 10.4. The wavelet admissible condition (10.2.4) is satisfied. The Fourier transform of the Haar wavelet is complex valued and is equal to the product of a sine function and a sinc function.

$$\begin{aligned} H(\omega) &= 2j\exp\left(-j\frac{\omega}{2}\right)\sin c\left(\frac{\omega}{4}\right)\sin\left(\frac{\omega}{4}\right) \\ &= 4j\exp\left(-j\frac{\omega}{2}\right)\frac{1-\cos\dfrac{\omega}{2}}{\omega} \end{aligned} \tag{10.2.12}$$

whose amplitude is even and symmetric to $\omega = 0$. That is a band-pass filter, as shown in Figure 10.4. The phase factor $\exp(-j\omega/2)$ is related only to the shift of $h(t)$ to $t = 1/2$, which is necessary for the causal filtering of time signals.

The Haar wavelet transform involves a bank of multiresolution filters that yield the correlations between the signal and the Haar wavelets scaled by factor, s. The Haar wavelet transform is a local operation in the time domain. The time resolution depends on the scale, s. When the signal is constant, the Haar wavelet transform is equal to zero. The amplitude of the Haar wavelet transform has high peak values when there are discontinuities of the signal.

The Haar wavelet is also irregular. It is discontinuous and its first–order moment is not zero. According to (10.2.12), the amplitude of the Fourier spectrum of the Haar wavelet converges to zero very slowly as $1/\omega$. According to (10.2.8), the Haar wavelet transform decays with increasing of $1/s$ as $(1/s)^{-3/2}$.

The set of discrete dilations and translations of the Haar wavelets constitute the simplest discrete orthonormal wavelet basis. We shall use the Haar wavelets as an example of the orthonormal wavelet basis in Sections 10.5 and 10.7. However, the Haar wavelet transform has not found many practical applications because of its poor localization property in the frequency domain.

Gaussian Wavelet

The Gaussian function is perfectly local in both time and frequency domains and is infinitely derivable. In fact, a derivative of any order, n, of the Gaussian function may be a wavelet. The Fourier transform of the nth order derivative of the Gaussian function is

$$H(\omega) = (j\omega)^n \exp\left(-\frac{\omega^2}{2}\right)$$

that is the Gaussian function multiplied by $(j\omega)^n$, so that $H(0) = 0$. The wavelet admissible condition is satisfied. Its derivatives up to nth order $H^{(n-1)}(0) = 0$. The Gaussian wavelet is a regular wavelet of order n. Both $h(t)$ and $H(\omega)$ are infinitely derivable. The wavelet transform coefficients decay with increasing of $1/s$ as fast as $(1/s)^{n-(1/2)}$.

Mexican Hat Wavelet

The Mexican hat-like wavelet was first introduced by Gabor. It is the second–order derivative of the Gaussian function:[7]

$$h(t) = (1-t^2)\exp\left(-\frac{t^2}{2}\right)$$

The Mexican hat wavelet is even and real valued. The wavelet admissible condition is satisfied. The Fourier transform of the Mexican hat wavelet is

$$H(\omega) = -\omega^2 \exp\left(-\frac{\omega^2}{2}\right)$$

that is also even and real valued, as shown in Figure 10.5.

The two-dimensional Mexican hat wavelet is well known as the Laplacian operator, widely used for zero-crossing image edge detection.

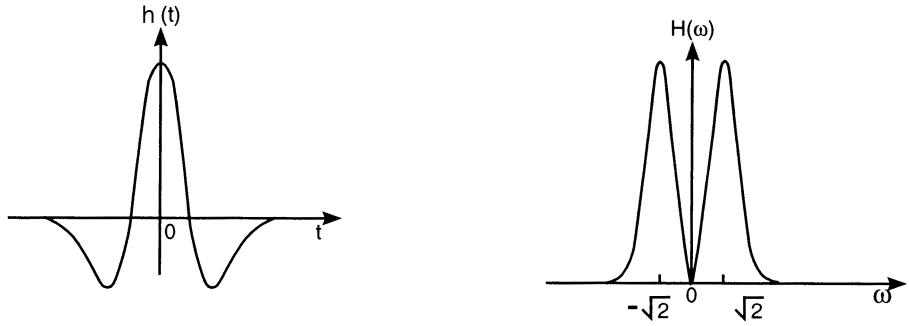

FIGURE 10.5 Mexican hat wavelet $h(t)$ and its Fourier transform $H(\omega)$. (From Sheng, Y. et al. *Opt. Eng.*, 31, 1840, 1992. With permission.)

Gabor Wavelet

The Gabor function in the short time Fourier transform with Gaussian window is

$$h(t) = \exp(j\omega_0 t)\exp\left(-\frac{(t-\tau)^2}{2}\right)$$

Its real part is a cosine-Gaussian and the imaginary part is a sine-Gaussian function. The Gaussian window has a fixed width and is shifted along the time axis by τ. The Fourier transform of the Gabor function is a Gaussian window which is shifted along the frequency axis by ω_0, as discussed in Subsection 10.1.3.

The Gabor function can also have a dilated window as:

$$h(t) = \exp(j\omega_0 t)\exp\left(-\frac{t^2}{2s^2}\right)$$

where s is the scale factor and is the width of the Gaussian window, $\exp(j\omega_0 t)$ introduces a translation of the spectrum of the Gabor function. The Gabor function with the dilation of both window and Fourier kernel is the Gabor wavelet. This wavelet was used by Martinet, Morlet, and Grossmann for analysis of sound patterns. The Morlet's basic wavelet function is a multiplication of the Fourier basis with a Gaussian window. Its real part is the Cosine-Gaussian wavelet, whose Fourier transform consists of two Gaussian functions shifted to ω_0 and $-\omega_0$, respectively:

$$H(\omega)=\sqrt{2\pi}\pi\left[\exp\left(-\frac{(\omega-\omega_0)^2}{2}\right)+\exp\left(-\frac{(\omega+\omega_0)^2}{2}\right)\right]$$

that are real positive-valued, even, and symmetric to the origin $\omega = 0$. The Gaussian window is perfectly local in both time and frequency domains and achieves the minimum time-bandwidth product determined by the uncertainty principle, as shown by (10.1.9). The cosine-Gaussian wavelets are band-pass filters in frequency domain. They converge to zero like the Gaussian function as the frequency increases. Figure 10.6 shows the cosine-Gaussian wavelet and its Fourier spectrum.

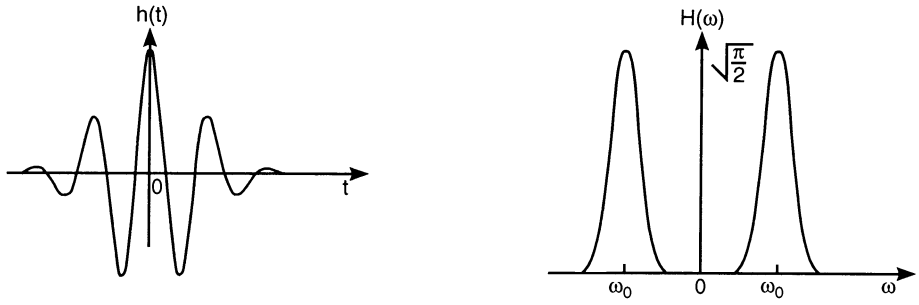

FIGURE 10.6 Cos-Gaussian wavelet $h(t)$ and its Fourier transform $H(\omega)$. (From Sheng, Y. et al. *Opt. Eng.*, 31, 1840, 1992. With permission.)

The Gabor wavelets do not satisfy the wavelet admissible condition, because:

$$H(0)\neq 0$$

that leads to $c_h = +\infty$. But the value of $H(0)$ is very close to zero provided that the ω_0 is sufficiently large. When $\omega_0 = 5$, for example,

$$H(0)=(2\pi)^{3/2}\exp\left(-\frac{25}{2}\right)$$

that is of 10^{-5} order of magnitude and can be practically considered as zero in numerical computations.

10.3 Discrete Wavelet Transform

The continuous wavelet transform maps a one-dimensional time signal to a two–dimensional time-scale joint representation. The time bandwidth product of the continuous wavelet transform output is the square of that of the signal. For most applications, however, the goal of signal processing is to represent the signal efficiently with fewer parameters. The use of the discrete wavelet transform can reduce the time bandwidth product of the wavelet transform output.

By the term discrete wavelet transform, we mean, in fact, the continuous wavelets with the discrete scale and translation factors. The wavelet transform is then evaluated at discrete scales and translations. The discrete scale is expressed as $s = s_0^i$, where i is integer and $s_0 > 1$ is a fixed dilation step. The discrete translation factor is expressed as $\tau = k\tau_0 s_0^i$, where k is an integer. The translation depends on the dilation step, s_0^i. The corresponding discrete wavelets are written as:

$$h_{i,k}(t) = s_0^{-i/2} h\left(s_0^{-i}\left(t - k\tau_0 s_0^i\right)\right)$$
$$= s_0^{-i/2} h\left(s_0^{-i} t - k\tau_0\right) \tag{10.3.1}$$

The discrete wavelet transform with the dyadic scaling factor of $s_0 = 2$, is effective in the computer implementation.

10.3.1 Time-Scale Space Lattices

The discrete wavelet transform is evaluated at discrete times and scales that correspond to a sampling in the time-scale space. The time-scale joint representation of a discrete wavelet transform is a grid along the scale and time axes. To show this, we consider localization points of the discrete wavelets in the time-scale space.

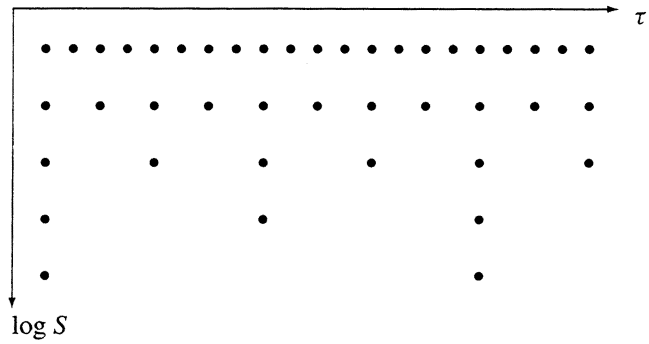

FIGURE 10.7 Localization of the discrete wavelets in the time-scale space.

The sampling along the time axis has the interval, $\tau_0 s_0^i$, that is proportional to the scale, s_0^i. The time sampling step is small for small-scale wavelet analysis and is large for large-scale wavelet analysis. With the varying scale, the wavelet analysis will be able to "zoom in" on singularities of the signal using more concentrated wavelets of very small scale. For this detailed analysis the time sampling step is very small. Because only the signal detail is of interest, only a few small time translation steps would be needed. Therefore, the wavelet analysis provides a more efficient way to represent transient signals.

There is an analogy between the wavelet analysis and the microscope. The scale factor s_0^i corresponds to the magnification or the resolution of a microscope. The translation factor, τ, corresponds to the location where one makes observation with the microscope. If one looks at very small details, the magnification and the resolution must be large and that corresponds to a large and negative *i*. The wavelet is very concentrated. The step of translation is small, that justifies the choice, $\tau = k\tau_0 s_0^i$. For large and positive *i*, the wavelet is spread out, and the large translation steps, $k\tau_0 s_0^i$ are adapted to this wide width of the wavelet analysis function. This is another interpretation of the constant-Q analysis property of the wavelet transform, discussed in Section 10.2.3.

The behavior of the discrete wavelets depends on the steps, s_0 and τ_0. When s_0 is close to 1 and τ_0 is small, the discrete wavelets are close to the continuous wavelets. For a fixed scale step s_0, the localization points of the discrete wavelets along the scale axis are logarithmic as $\log s = i \log s_0$, as shown in Figure 10.7.

The unit of the frequency sampling interval is called an octave in music. One octave is the interval between two frequencies having a ratio of two. One octave frequency band has the bandwidth equal to one octave.

The discrete time step is $\tau_0 s_0^i$. We choose usually $\tau_0 = 1$. Hence, the time sampling step is a function of the scale and is equal to 2^i for the dyadic wavelets. Along the τ-axis, the localization points of the discrete wavelets depends on the scale. The intervals between the localization points at the same scale

are equal and are proportional to the scale s_0^i. The translation steps are small for small positive values of i with the small scale wavelets, and are large for large positive values of i with large scale wavelets. The localization of the discrete wavelets in the time-scale space is shown in Figure 10.7, where the scale axis is logarithmic, $\log s = i \log 2$, and the localization is uniform along the time axis τ with the time steps proportional to the scale factor $s = 2^i$.

10.3.2 Wavelet Frame

With the discrete wavelet basis a continuous function $f(t)$ is decomposed into a sequence of wavelet coefficients:

$$W_f(i,k) = \int f(t) h^*_{i,k}(t) dt = \langle f, h_{i,k} \rangle \tag{10.3.2}$$

A question for the discrete wavelet transform is how well the function $f(t)$ can be reconstructed from the discrete wavelet coefficients:

$$f(t) = A \sum_i \sum_k W_f(i,k) h_{i,k}(t) \tag{10.3.3}$$

where A is a constant that does not depend on $f(t)$. Obviously, if s_0 is close enough to 1 and τ_0 is small enough, the wavelets approach as a continuum. The reconstruction (10.3.3) is then close to the inverse continuous wavelet transform. The signal reconstruction takes place without nonrestrictive conditions other than the admissible condition on the wavelet $h(t)$. On the other hand, if the sampling is sparse, $s_0 = 2$ and $\tau_0 = 1$, the reconstruction (10.3.3) can be achieved only for very special choices of the wavelet $h(t)$.

The theory of wavelet frames provides a general framework that covers the above mentioned two extreme situations. It permits one to balance between the redundancy, i.e., the sampling density in the scale-time space, and the restriction on the wavelet $h(t)$ for the reconstruction scheme (10.3.3) to work. If the redundancy is large with high over-sampling, then only mild restrictions are put on the wavelet basis. If the redundancy is small with critical sampling, then the wavelet base are very constrained.

Daubechies[8] has proven that the necessary and sufficient condition for the stable reconstruction of a function $f(t)$ from its wavelet coefficients, $W_f(i,k)$, is that the energy, which is the sum of square moduli of $W_f(i,k)$, must lie between two positive bounds:

$$A\|f\|^2 \le \sum_{j,k} |\langle f, h_{i,k} \rangle|^2 \le B\|f\|^2 \tag{10.3.4}$$

where $\|f\|^2$ is the energy of $f(t)$, $A > 0$, $B < \infty$ and A, B are independent of $f(t)$. When $A = B$, the energy of the wavelet transform is proportional to the energy of the signal. This is similar to the energy conservation relation (10.2.5) of the continuous wavelet transform. When $A \neq B$, there is still some proportional relation between the two energies.

When (10.3.4) is satisfied, the family of kernel functions $\{h_{i,k}(t)\}$ with $i, k \in \boldsymbol{Z}$ is referred to as a frame and A, B are termed frame bounds. Hence, when proportionality between the energy of the function and the energy of its discrete transform function is bounded between something greater than zero and less than infinity for all possible square integrable functions, then the transform is complete. No information is lost and the signal can be reconstructed from its decomposition.

Daubechies has shown that the accuracy of the reconstruction is governed by the frame bounds A and B. The frame bounds A and B can be computed from s_0, τ_0 and the wavelet basis, $h(t)$. The closer A and B, the more accurate the reconstruction. When $A = B$ the frame is tight and the discrete wavelets behave exactly like an orthonormal basis. When $A = B = 1$, (10.3.4) is simply the energy conservation equivalent

to the Parseval relation of the Fourier transform. It is important to note that the same reconstruction works even when the wavelets are not orthogonal to each other.

When $A \neq B$, the reconstruction can still work exactly for the discrete wavelet transform if for reconstruction we use the synthesis function basis which is different from the decomposition function basis for analysis. The former constitutes the dual frame of the later.

10.4 Multiresolution Signal Analysis

The multiresolution signal analysis is a technique that permits us to analyze signals in multiple frequency bands. Two existing approaches of multiresolution analysis are the Laplacian pyramid and the subband coding, which were developed independently in the late 1970s and early 1980s. Meyer and Mallat[9] found in 1986 that the orthonormal wavelet decomposition and reconstruction can be implemented in the multiresolution signal analysis framework.

10.4.1 Laplacian Pyramid

The multiresolution signal analysis was first proposed by Burt and Adelson in 1983[10] for image decomposition, coding, and reconstruction.

Gaussian Pyramid

The multiresolution signal analysis is based on a weighting function also called a smoothing function. The original data, represented as a sequence of real numbers, $c_0(n)$, $n \in \boldsymbol{Z}$, is averaged in neighboring pixels by the weighting function, which can be a Gaussian function and is a low-pass filter. The correlation of the signal with the weighting function reduces the resolution of the signal. Hence, after the averaging process the data sequence is down-sampled by a factor of two. The resultant data sequence $c_1(n)$ is the averaged approximation of $c_0(n)$.

The averaging and down-sampling process can be iterated and applied to the averaged approximation data $c_1(n)$ with the smoothing function also dilated by a scale factor of two, and so on. In the iteration process, the smoothing function is dilated with dyadic scales 2^i with $i \in \boldsymbol{Z}$ to average the signals at multiple resolutions. Hence, the original data is represented by a set of successive approximations. Each approximation corresponds to a smoothed version of the original data at a given resolution. Given an original data of size 2^N, the smoothed sequence $c_1(n)$ has a reduced size, 2^{N-1}. By iterating the process, the successive averaging and down-sampling result in a set of data sequences of exponentially decreasing size. If we imagine these data sequences stacked on top of one another, then they constitute a hierarchical pyramid structure with $log_2 N$ pyramid levels.

The original data $c_0(n)$ are at the bottom or zero level of the pyramid. At ith pyramid level, the signal sequence is obtained from the data sequence in the $(i-1)$-th level by:

$$c_i(n) = \sum_k p(k-2n)c_{i-1}(k) \tag{10.4.1}$$

where $p(n)$ is the weighting function. The operation described in (10.4.1) is a correlation between $c_{i-1}(k)$ and $p(k)$ followed by a down-sampling by two, because a shift by two in $c_{i-1}(k)$ results in a shift by one in $c_i(n)$. The sampling interval in level i is double that in the previous level $i-1$. The size of the sequence $c_i(n)$ is half as long as its predecessor $c_{i-1}(n)$. When the weighting function is the Gaussian function, the pyramid of the smoothed sequences is referred to as the Gaussian pyramid. Figure 10.8 shows a part of the Gaussian pyramid.

Laplacian Pyramid

By the low-pass filtering with the weighting function $p(n)$, the high frequency detail of the signal is lost. To compute the difference between two successive Gaussian pyramid levels of different size, we have to

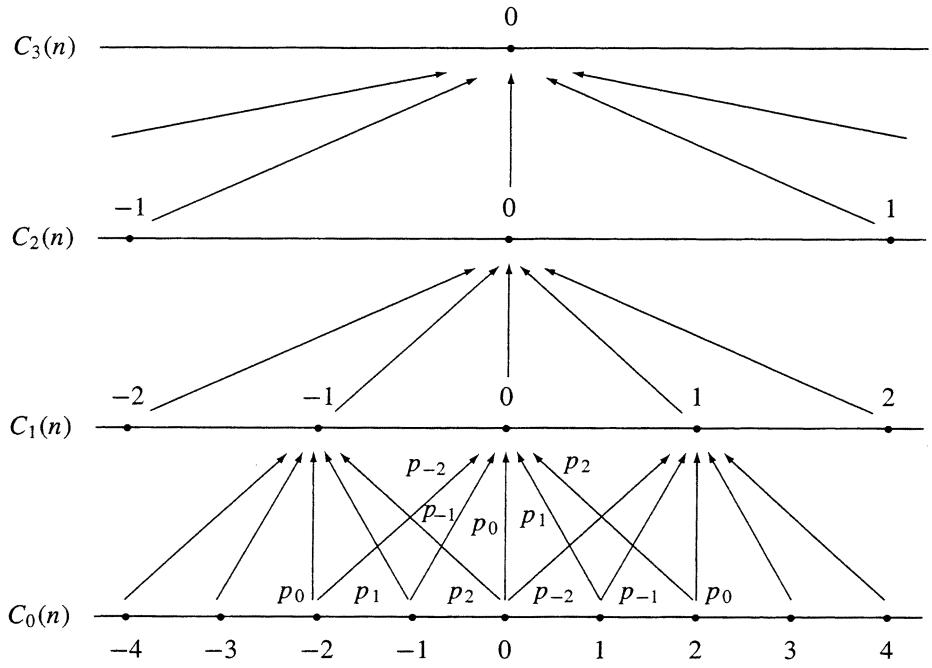

FIGURE 10.8 Multiresolution analysis Gaussian pyramid. The weighting function is $p(n)$ with $n = 0 \pm 1, \pm 2$. The even and odd number nodes in $c_0(n)$ have different connections to the nodes in $c_1(n)$.

first expand the data sequence, $c_i(n)$. The expansion of $c_i(n)$ may be done in two steps: (1) inserting a zero between every samples of $c_i(n)$, that is up-sampling $c_i(n)$ by two; (2) interpolating the sequence with a filter whose impulse response is $p'(n)$. The expand process results in a sequence $c'_{i-1}(n)$ that has the same size as the size of $c_{i-1}(n)$. In general $c'_{i-1}(n) \neq c_{i-1}(n)$. The difference is a sequence $d_{i-1}(n)$

$$d_{i-1}(n) = c_{i-1}(n) - c_{i-1}(n) \tag{10.4.2}$$

that contains the detail information of the signal. All the differences between sequences of successive Gaussian pyramid levels form a set of sequences $d_i(n)$ that constitute another pyramid referred to as the Laplacian pyramid. The original signal can be reconstructed exactly by summing the Laplacian pyramid levels.

The Laplacian pyramid contains the compressed signal data in the sense that the pixel-to-pixel correlation of the signal is removed by the averaging and subtracting process. If the original data is an image that is positively valued, then the values on the Laplacian pyramid nodes are both positive and negative and are shifted toward zero. They can be represented by fewer bits. The multiresolution analysis is useful for image coding and compression.

The Laplacian pyramid signal representation is redundant. One stage of the pyramid decomposition leads to a half size, low resolution signal and a full size, difference signal, resulting in an increase in the number of signal samples by 50%. Figure 10.9 shows the pyramid scheme.

10.4.2 Subband Coding

Subband coding[11] is a multiresolution signal processing approach that is different from the Laplacian pyramid. The basic objective of the subband coding is to divide the signal spectrum into independent subbands in order to treat the signal subbands individually for different purposes. Subband coding is an efficient tool for multiresolution spectral analysis and has been successful in speech signal processing.

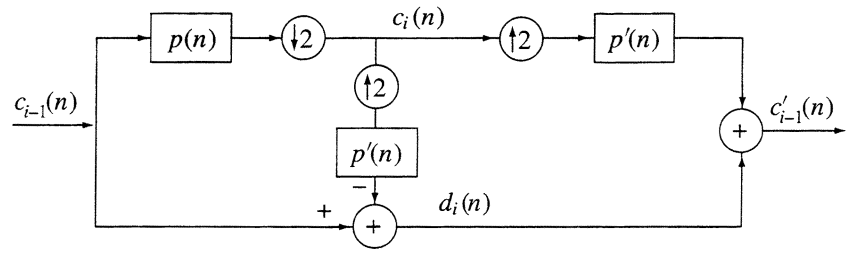

FIGURE 10.9 Schematic pyramid decomposition and reconstruction.

Analysis Filtering

Given an original data sequence $c_0(n)$, $n \in \mathbf{Z}$, the lower resolution approximation of the signal is derived by low-pass filtering with a filter having its impulse response $p(n)$.

$$c_1(n) = \sum_k p(k-2n)c_0(k) \tag{10.4.3}$$

The correlation between $c_0(k)$ and $p(k)$ is down-sampled by a factor of two. The process is exactly the same as the averaging process in the Laplacian pyramid decomposition, as described in Equation (10.4.1). In order to compute the detail information that is lost by the low-pass filtering with $p(n)$, a high-pass filter with the impulse response $q(n)$ is applied to the data sequence $c_0(n)$ as:

$$d_1(n) = \sum_k q(k-2n)c_0(k) \tag{10.4.4}$$

The correlation between $c_0(k)$ and $q(k)$ down-sampled by a factor of two. Hence, the subband decomposition leads to a half–size low resolution signal and a half–size detail signal.

Synthesis Filtering

To recover the signal $c_0(n)$ from the down-sampled approximation $c_1(n)$ and the down-sampled detail $d_1(n)$, both $c_1(n)$ and $d_1(n)$ are up-sampled by a factor of two. The up-sampling is performed by first inserting a zero between each node in $c_1(n)$ and $d_1(n)$ and then interpolating with the filters $p'(n)$ and $q'(n)$ respectively. Finally, adding together the two up-sampled sequences yields $c_0'(n)$. Figure 10.10 shows the scheme of the two-channel subband system.

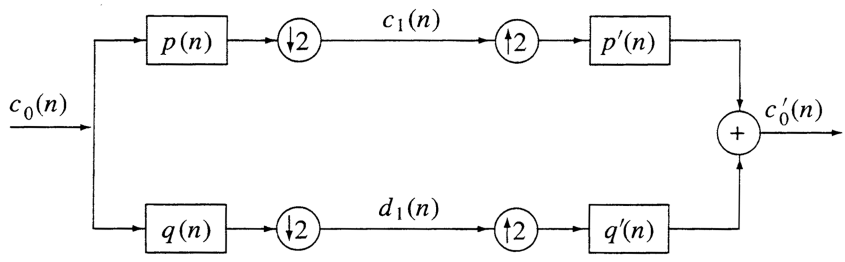

FIGURE 10.10 Schematic two-channel subband coding decomposition and reconstruction.

The reconstructed signal $c_0'(n)$, in general, is not identical to the original $c_0(n)$, unless the filters meet a specific constraint, that the analysis filters $P(n)$, $q(n)$ and the synthesis filters $p'(n)$, $q'(n)$ satisfy the perfect reconstruction condition, discussed in Section 10.6.2.

The scheme shown in Figure 10.10 is a two-channels system with a bank of two-band filters. The two-band filter bank can be extended to M-band filter bank by using a bank of M analysis filters followed by down-sampling and a bank of M up-samplers followed by M synthesis filters.

The two-band filter bank can also be iterated: the filter bank divide the input spectrum into two equal subbands, yielding the low (L) and high (H) bands. The two-band filter bank can be again applied to these (L) and (H) half bands to generate the quarter bands: (LL), (LH), (HL), and (HH). The scheme of this multiresolution analysis has a tree structure.

10.4.3 Scale and Resolution

In the multiresolution signal analysis each layer in the pyramid is generated by a bank of low-pass and high-pass filters of a given scale that corresponds to the scale of that layer.

In general, scale and resolution are different concepts. Scale change of a continuous signal does not alter its resolution. The resolution of a continuous signal is related to its frequency bandwidth. In a map, a large scale means a global view and a small scale means a detailed view. However, if the size of the map is fixed, then enlarging the map scale would require reducing the resolution.

In the multiresolution signal analysis, the term of scale is that of the low-pass and high-pass filters. At each scale, the down-sampling by two, which follows the low-pass filtering, halves the resolution. When a signal is transferred from scale 2^i to scale 2^{i+1}, its resolution is reduced by two. The size of the approximation signal also is reduced by two. Therefore, each scale level corresponds to a specific resolution.

10.5 Orthonormal Wavelet Transform

The first orthonormal wavelet basis was found by Meyer when he looked for the orthonormal wavelets that are localized in both time and frequency domains. The multiresolution Laplacian pyramid ideas of hierarchal averaging and computing the difference triggered Mallat and Meyer to view the orthonormal wavelet bases as a vehicle for multiresolution analysis.[9] The multiresolution analysis is now a standard way to construct orthonormal wavelet bases and to implement the orthonormal wavelets transforms. Most orthonormal wavelet bases are now constructed from the multiresolution analysis framework.

In the multiresolution analysis framework, the dyadic orthonormal wavelet decomposition and reconstruction use the tree algorithm that permits very fast computation of the orthonormal wavelet transform in the computer.

10.5.1 Multiresolution Analysis Bases

Scaling Functions

The multiresolution analysis is based on the scaling function. The scaling function is a continuous, square integrable and, in general, real-valued function. The scaling function does not satisfy the wavelet admission condition: the mean value of the scaling function $\phi(t)$ is not equal to zero, but is usually normalized to unity.

The basic scaling function $\phi(t)$ is dilated by dyadic scale factors. At each scale level the scaling function is shifted by discrete translation factors as:

$$\phi_{i,k}(t) = 2^{-i/2}\phi\left(2^{-i}t - k\right) \tag{10.5.1}$$

where the coefficient $2^{-i/2}$ is a normalization constant. Here, the scaling function basis is normalized in the $L^2(R)$ norm, similar to the normalization of the wavelet described by (10.1.2). We shall restrict

ourselves to the dyadic scaling with $s = 2^i$ for $i \in \mathbf{Z}$. The scaling functions of all scales 2^i with $i \in \mathbf{Z}$ generated from the same $\phi(t)$ are all similar in shape. At each resolution level i, the set of the discrete translations of the scaling functions, $\phi_{i,k}(t)$, forms a function basis that spans a subspace, $\mathbf{V}_i$.

A continuous signal function may be decomposed into the scaling function bases. At each resolution level i, the decomposition is evaluated at discretely translated points. The scaling functions play a role of the average or smoothing function in the multiresolution signal analysis.

At each resolution level, the correlation between the scaling functions and the signal produces the averaged approximation of signal, which is sampled at a set of discrete points. After the averaging by the scaling functions, the signal is down-sampled by a factor of two that halves the resolution. Then, the approximated signal is decomposed into the dilated scaling function basis at the next coarser resolution.

Wavelets

In the multiresolution analysis framework the wavelet bases are generated from the scaling function bases. In order to emphasize the dependence of the wavelets to the scaling functions in the multiresolution analysis framework, from now on we change the notation of the wavelet and use $\psi(t)$ to denote the wavelet in the discrete wavelet transform instead of $h(t)$ in the previous sections for the continuous wavelet transform.

Similar to the scaling function, the wavelet is scaled with dyadic scaling factors and is translated at each resolution level as:

$$\psi_{i,k}(t) = 2^{-i/2}\psi\left(2^{-i}t - k\right) \tag{10.5.2}$$

where the coefficient $2^{-i/2}$ is a normalization constant. The wavelet basis is normalized in the $L^2(R)$ norm for energy normalization, as discussed in Section 10.1. At each resolution level i, the set of the discrete translations of the wavelets, $\psi_{i,k}(t)$, forms a function basis that spans a subspace W_i. A signal function may be decomposed into the wavelet bases. At each resolution level, the decomposition is evaluated at discrete translated points.

In the multiresolution analysis framework, the orthonormal wavelet transform is the decomposition of a signal into approximations at lower and lower resolutions with less and less detail information by the projections of the function onto the orthonormal scaling function bases. The differences between each two successive approximations are computed with the projections of the signal onto the orthonormal wavelet bases, as shown in the next section.

Two-Scale Relation

The two-scale relation is the basic relation in the multiresolution analysis with the dyadic scaling. The scaling functions and the wavelets form two bases at every resolution level by their discrete translates. Let $\phi(t)$ be the basic scaling function that translates with integer step span the subspace V_0. At the next finer resolution the subspace V_{-1} is spanned by the set $\{\phi(2t-k)\}$, that is generated from the scaling function $\phi(t)$ by a contraction with a factor of two and by translations with half-integer steps. The set $\{\phi(2t-k)\}$ can also be considered as a sum of two sets of even and odd translates, $\{\phi(2t-2k)\}$ and $\{\phi[2t-(2k+1)]\}$, all are with integer steps, $k \in \mathbf{Z}$. The scaling function at resolution $i = 0$ may be decomposed as a linear combination of the scaling functions at the higher resolution level $i = 1$, as:

$$\phi(t) = \sum_k p(k)\phi(2t - k) \tag{10.5.3}$$

where the discrete decomposition coefficient sequence $p(k)$ is called the interscale coefficients that will be used in the wavelet decomposition as the discrete low-pass filter and will be discussed in Section 10.5.4. This decomposition may be considered as the projection of the basis function $\phi(t) \in V_0$ onto the finer resolution subspace V_{-1}. The two-scale relation, or called the two-scale difference equation, (10.5.3) is the fundamental equation in the multiresolution analysis. The basic ingredient in the multiresolution

analysis is a scaling function such that the two scale relation holds for some $p(k)$. The sequence $p(k)$ of the interscale coefficients in the two-scale relation governs the structure of the scaling function, $\phi(t)$.

Let $\psi(t) \in V_0$ be the basic wavelet, which can also be expanded onto the scaling function basis $\{\phi(2t–k)\}$ in the finer resolution subspace V_{-1} as:

$$\psi(t) = \sum_k q(k)\phi(2t-k) \tag{10.5.4}$$

where the sequence $q(k)$ is the interscale coefficients that will be used in the wavelet decomposition as the discrete high-pass filter and will be discussed in Section 10.5.4. Equation (10.5.4) is a part of the two-scale relation, and is useful for generating the wavelets from the scaling functions, as shown in the next.

On both sides of the two-scale relations, (10.5.3) and (10.5.4), $\phi(t)$ and $\psi(t)$ are continuous scaling function and wavelet respectively. On the right-hand side of the two-scale relations, the interscale coefficients, $p(k)$ and $q(k)$, are discrete with $k \in \mathbf{Z}$. The two-scale relations express the relations between the continuous scaling function $\phi(t)$ and wavelet $\psi(t)$ and the discrete sequences of the interscale coefficients $p(k)$ and $q(k)$.

10.5.2 Orthonormal Bases

We should show in this subsection first how the discrete translates of the scaling function and of the wavelet form the orthonormal bases at each given resolution, and then how the scaling function generates the multiresolution analysis.

Orthonormal Scaling Function Basis

At a given scale level the discrete translates of a basic scaling function $\phi(t)$ can form an orthonormal basis, if $\phi(t)$ satisfies some orthonormality conditions. The scaling function can be made orthonormal to its own translates. When a basic scaling function $\phi(t)$ has its discrete translates that form an orthonormal set $\{\phi(t–k)\}$, we have:

$$\langle \phi_{i,k}, \phi_{i,k'} \rangle = 2^{-i} \int \phi_i(t-k)\phi_i(t-k')dt = \delta_{k,k'} \tag{10.5.5}$$

Orthonormal Wavelet Basis

Similarly, the discrete translates of a basic wavelet $\psi(t)$ can form an orthonormal basis, if $\psi(t)$ satisfies some orthonormality condition. At the same resolution level, the wavelet can be made orthonormal to its own translates. When a basic wavelet $\psi(t)$ has its discrete translates that form an orthonormal set $\{\psi(t–k)\}$, we have:

$$\langle \psi_{i,k}, \psi_{i,k'} \rangle = 2^{-i} \int \psi_i(t-k)\psi_i(t-k')dt = \delta_{k,k'} \tag{10.5.6}$$

Cross-Orthonormality

The orthonormal wavelet basis is not only orthogonal to their own translates at the same scale level, furthermore, the set of the wavelet translates is orthogonal to the set of the scaling function translates at the same scale level for all k and $n \in \mathbf{Z}$ as shown by:

$$\langle \phi_{i,k}, \psi_{i,n} \rangle = 2^{-i} \int \phi_i(t-k)\psi_i(t-n)dt = 0 \tag{10.5.7}$$

Example: Orthonormal Haar's Bases

A simple example for the orthonormal wavelet basis is the historical Haar wavelet. The Haar scaling function is the simple rectangle function in the interval [0, 1).

$$\phi(t) = \begin{cases} 1 & 0 \le t < 1 \\ 0 & \text{otherwise} \end{cases}$$

Obviously, the translations with integer steps of this rectangular function form an orthonormal set, satisfying (10.5.5) because the translates $\phi(t–k)$ and $\phi(t–k')$ with $k, k' \in \boldsymbol{Z}$ and $k' \neq k$ do not overlap.

The contracted Haar scaling function $\phi(2t)$ is a rectangular function in the interval [0,1/2). Its discrete translates with half integer steps form an orthonormal basis $\{\phi(2t–k)\}$. Automatically, within every fixed scale 2^{-i}, the Haar scaling functions form an orthonormal basis with the translation step of 2^{-i}.

As $\phi(2t–k)$ are of half integer width, the $\phi(t)$ in $\boldsymbol{V}_0$ can be expressed as a linear combination of the even and odd translates of $\phi(2t)$ in $\boldsymbol{V}_{-1}$:

$$\phi(t) = \frac{1}{\sqrt{2}}\left[\phi(2t) + \phi(2t-1)\right]$$

This is the two-scale relation described in (10.5.3) with the interscale coefficients:

$$p(0) = \frac{1}{\sqrt{2}}, \qquad p(1) = \frac{1}{\sqrt{2}},$$

$$p(k) = 0 \qquad \text{for } k \neq 0,1$$

The Haar's basic wavelet has a compact support of $[0, 1)$:

$$\psi(t) = \begin{cases} 1 & \text{when } 0 \le t \le 1/2 \\ -1 & \text{when } 1/2 \le t \le 1 \\ 0 & \text{otherwise} \end{cases}$$

Obviously, the integer translates of $\psi(t)$ constitute an orthonormal basis $\{\psi(t–k)\}$, because the translated wavelets $\psi(t–k)$ and $\psi(t–k')$ do not overlap for k and $k' \in \mathbf{Z}$ and $k \neq k'$. Also, within every fixed scale level i, the discrete translates of the Haar wavelets form an orthonormal basis. The Haar wavelets are orthogonal to the Haar scaling function because:

$$\int \phi(t-k)\psi(t-n)dt = 0$$

The Haar wavelet can be expressed as a linear combination of the Haar scaling functions in a higher resolution level:

$$\psi(t) = \frac{1}{\sqrt{2}}\left[\phi(2t) - \phi(2t-1)\right]$$

This is the two-scale relation described in (10.5.4) with the interscale coefficients:

$$q(0) = \frac{1}{\sqrt{2}}, \qquad q(1) = -\frac{1}{\sqrt{2}}$$

$$q(k) = 0 \qquad for\ k \neq 0,1$$

The Haar wavelets are orthonormal at the same scale and also orthonormal across the scales. One can verify that:

$$\int \psi_{i,k}(t)\psi_{m,n}(t)dt = \delta_{i,m}\delta_{k,n}$$

10.5.3 Orthonormal Subspaces

Assume that the basic scaling function $\phi(t)$ satisfies some orthogonality condition at a given scale level, so that its discrete translates $\{\phi(t–k)\}$ with integer translations $k \in \boldsymbol{Z}$ form an orthonormal set. The projection of a function $f(t) \in \boldsymbol{L}^2(\boldsymbol{R})$ on the orthonormal basis $\{\phi(t–k)\}$ is a correlation between the original function $f(t)$ and the scaling function $\phi(t)$ sampled at integer intervals.

The scaling function plays the role of a smoothing function in the multiresolution analysis. The projection of $f(t)$ on the scaling function basis results in a blurred approximation of $f(t)$. All the approximations of $f(t) \in \boldsymbol{L}^2(\boldsymbol{R})$ form a subspace $\boldsymbol{V}_0 \in \boldsymbol{L}^2(\boldsymbol{R})$. The vector space $\boldsymbol{V}_0$ can be interpreted as the set of all possible approximations of functions in $\boldsymbol{L}^2(\boldsymbol{R})$ generated by the orthonormal set $\{\phi(t–k)\}$. The space $\boldsymbol{V}_0$ is spanned by the basis $\{\phi(t–k)\}$.

Now we consider the dilation of the scaling function. All the scaling functions are generated from the basic scaling function $\phi(t)$ by dyadic dilations and discrete translations. The basic scaling function, $\phi(t)$, generates the orthonormal basis $\{\phi(t–k)\}$ of $\boldsymbol{V}_0$ with integer translation steps. The dilated scaling function $\phi(t/2)$ will generate the orthonormal basis $\{\phi(2^{-1}t–k)\}$ of $\boldsymbol{V}_1$ with a translation step of two, and the dilated scaling function $\phi(t/4)$ will generate the orthonormal basis $\{\phi(2^{-2}t–k)\}$ of $\boldsymbol{V}_2$ with a translation step of four, and so on. There is then a set of orthogonal bases of scaling functions. Each scaling function basis is orthonormal at each resolution level.

The projections of functions in $\boldsymbol{L}^2(\boldsymbol{R})$ on the set of orthonormal scaling function bases form a set of subspaces $\boldsymbol{V}_i$. Each subspace $\boldsymbol{V}_i$ is the set of all possible approximations of functions in $\boldsymbol{L}^2(\boldsymbol{R})$ generated by the orthonormal scaling function basis $\{\phi(2^{-i}t–k)\}$. The subspace $\boldsymbol{V}_i$ is spanned by the orthonormal scaling function basis at the resolution level i. Hence, the scaling function $\phi(t)$ generates the subspaces of the multiresolution analysis.

Similarly, the projection of a signal function $f(t)$ on the orthonormal wavelet bases, at a given resolution level i, is a correlation between $f(t)$ and $\psi_i(t)$ sampled at discrete intervals. The projections of all functions in $\boldsymbol{L}^2(\boldsymbol{R})$ on the orthonormal wavelet basis $\{\psi(2^{-i}t–k)\}$ form a subspace $\boldsymbol{W}_i$. The subspace $\boldsymbol{W}_i$ is spanned by $\{\psi(2^{-i}t–k)\}$.

Because of the cross-orthonormality between the wavelet set and the scaling function set, $\{\phi(2^{-i}t–k)\}$ is orthogonal to $\{\psi(2^{-i}t–k)\}$, the subspace $\boldsymbol{W}_i$ is an orthogonal complement of $\boldsymbol{V}_i$:

$$W_i \perp V_i$$

Both $\boldsymbol{V}_i$ and $\boldsymbol{W}_i$ are the subspaces on $\boldsymbol{V}_{i–1}$: $\boldsymbol{V}_i$, $\boldsymbol{W}_i \in \boldsymbol{V}_{i–1}$. Since $\boldsymbol{W}_i$ is orthogonal to $\boldsymbol{V}_i$, the subspace $\boldsymbol{V}_{i–1}$ is the direct sum of $\boldsymbol{V}_i$ and $\boldsymbol{W}_i$.

$$V_{i-1} = V_i \oplus W_i$$

Properties of the Multiresolution Subspaces

The multiresolution analysis associated with the scaling function has some interesting properties. The approximates of a function *f(t)* at different resolutions must be similar, because they are all generated by the same scaling function only with different scales. The approximation spaces $\boldsymbol{V}_i$ then may be deduced from each other by simple dilation:

$$f(t) \in V_i \Leftrightarrow f(2t) \in V_{i-1}$$

All the information useful to compute the approximate function at the coarser resolution level *i* is contained in the approximate function at the finer resolution level *(i–1)*. The $\boldsymbol{V}_i$ is a subspace in $\boldsymbol{V}_{i-1}$. This is a causality property. We have a fine-to-coarse sequence as:

$$\cdots V_2 \subset V_1 \subset V_0 \subset V_{-1} \subset V_{-2} \cdots \subset L^2(R)$$

where $i \in \boldsymbol{Z}$. When the resolution increases with *i* tending to –∞, the approximated function should converge to the original function. Any function in $\boldsymbol{L}^2(\boldsymbol{R})$ can be approximated as closely as desired by its project in $\boldsymbol{V}_i$ when *i* tends to –∞. This property may be described as:

$$\overline{\bigcup_i V_i} = L^2(R)$$

Conversely, when the resolution decreases to zero with *i* tending to +∞, the approximations contain less and less information and converges to zero:

$$\bigcap_i V_i = \{0\}$$

In summary, the multiresolution analysis is generated by the scaling function $\phi(t)$. The $\phi(t)$ is scaled with the dyadic scaling factor 2^i. The discrete translates $\phi(2^{-i}t-k)$ form an orthonormal basis and span the subspace $\boldsymbol{V}_i$ at the resolution level *i*. All the dilates and translates of the scaling function bases and the wavelet bases are generated from a single basic scaling function and are not linearly independent.

10.5.4 Wavelet Series Decomposition

In this subsection we show how the wavelet series decomposition and reconstruction can be implemented by iterating the discrete filter bank. A function $f(t) \in \boldsymbol{V}_0$ can be represented as a linear superposition of the translated scaling functions $\phi(t-k)$, in $\boldsymbol{V}_0$:

$$f(t) = \sum_k c_0(k)\phi(t-k) \tag{10.5.8}$$

where the coefficients in the combination can be obtained using the orthonormality of the scaling function set as:

$$c_0(k) = \int f(t)\phi(t-k)dt = \langle f, \phi_{0,k} \rangle \tag{10.5.9}$$

We now apply the entire multiresolution analysis to the function *f(t)*.

Orthonormal Projections on the Subspaces

The function to be analyzed is in V_0. At the next coarser resolution $i = 1$, there are two mutually orthogonal subspaces V_1 and W_1, spanned by the orthonormal bases, $\{\phi_{1,k}(t)\}$ and $\{\psi_{1,k}(t)\}$, respectively. The subspace W_1 is the orthogonal complement of V_1. Because V_0 is the direct sum of V_1 and W_1; $V_0 = V_1 \oplus W_1$, there is one and only one way to express a function $f(t) \in V_0$ as the sum of two functions in V_1 and W_1, respectively:

$$f = P_1 f + Q_1 f \tag{10.5.10}$$

where the two components are the orthonormal projections of $f(t)$ on V_1 and W_1, and P_1 and Q_1 denote the orthonormal projection operators on the subspaces V_1 and W_1, respectively.

$$\begin{aligned} P_1 f &= \sum_n c_1(k)\phi_{1,k} \\ Q_1 f &= \sum_n d_1(k)\psi_{1,k} \end{aligned} \tag{10.5.11}$$

where the explicit time dependence in f, $\phi_{i,k}$ *and* $\psi_{i,k}$ is not shown for ease of notation.

Because the scaling function set $\{\phi_{1,k}\}$ is orthonormal in $\boldsymbol{V}_1$ and the wavelet set $\{\psi_{1,k}\}$ is orthonormal in $\boldsymbol{W}_1$ and they are mutually orthogonal, multiplying the scaling function $\phi_{1,k}$ with both sides of the expansions (10.5.10) and computing the inner products yields:

$$\begin{aligned} \langle \phi_{1,k}, f \rangle &= \langle \phi_{1,k}, P_1 f \rangle \\ \langle \psi_{1,k}, f \rangle &= \langle \psi_{1,k}, \phi_1 f \rangle \end{aligned} \tag{10.5.12}$$

Multiplying $\phi_{1,k}$ with both sides of (10.5.11), computing the inner products and using (10.5.12) yields:

$$c_1(k) = \langle \phi_{1,k}, P_1 f \rangle = \langle \phi_{1,k}, f \rangle \tag{10.5.13}$$

$$d_1(k) = \langle \psi_{1,k}, Q_1 f \rangle = \langle \psi_{1,k}, f \rangle \tag{10.5.14}$$

The discrete sequences, $c_1(k)$ and $d_1(k)$, are the coefficients in the decomposition of a continuous function $f(t)$ onto the bases $\{\phi_{1,k}\}$ in V_1 and $\{\psi_{1,k}\}$ in W_1, respectively, where both scaling functions and wavelets are continuous. The sequence c_1 is the averaged approximation of $f(t)$ and referred to as the discrete approximation of $f(t)$. The sequence d_1 represents the difference between the original $f(t)$ and the approximation $P_1 f$ and is referred to as the discrete wavelet transform coefficients of $f(t)$ at the coarse resolution level $i = 1$.

Low-Pass and High-Pass Filters

The discrete expansion coefficient sequence, $c_1(k)$ and $d_1(k)$, may be calculated by:

$$c_1(k) = 2^{-1/2} \sum_n p(n-2k) c_0(n) \tag{10.5.15}$$

$$d_1(k) = 2^{-1/2} \sum_n q(n-2k) c_0(n) \tag{10.5.16}$$

These are the correlations between the signal data c_0 and $p(n)$ and $q(n)$, respectively. The correlation results are down-sampled by a factor of two, because of the double-shift of $p(n)$ and $q(n)$ in the

correlations. The discrete interscale coefficients $p(n)$ and $q(n)$ are called the discrete low-pass and high-pass filters, respectively.

The Equations (10.5.15) and (10.5.16) may be proved as follows: substituting (10.5.8) into (10.5.13), (10.5.14) yields:

$$\begin{aligned} c_1(k) &= \sum_n \langle \phi_{1,k}, \phi_{0,n} \rangle c_0(n) \\ d_1(k) &= \sum_n \langle \psi_{1,k}, \phi_{0,n} \rangle c_0(n) \end{aligned} \tag{10.5.17}$$

The inner product between the scaling function and the wavelet sets, $\{\phi_{1,k}\}$ and $\{\psi_{1,k}\}$, at the scale $i = 1$ and the scaling function set, $\{\phi_{0,n}\}$, at the next higher resolution level $i = 0$ can be computed as:

$$\langle \phi_{1,k}, \phi_{0,n} \rangle = 2^{-1/2} \int \phi\left(\frac{t}{2} - k\right) \phi(t-n)\,dt = 2^{1/2} \int \phi(t) \phi\left[2t - (n-2k)\right] dt \tag{10.5.18}$$

$$\langle \psi_{1,k}, \phi_{0,n} \rangle = 2^{-1/2} \int \psi(t) \phi\left[2t - (n-2k)\right] dt \tag{10.5.19}$$

Substituting the two scale relation:

$$\begin{aligned} \phi(t) &= \sum_n p(n) \phi(2t-n) \\ \psi(t) &= \sum_n q(n) \phi(2tn) \end{aligned}$$

into (10.5.18) and (10.5.19) and using the orthonormality of the set $\{\phi(2t)\}$, we obtain:

$$\langle \phi_{1,k}, \phi_{0,n} \rangle = 2^{-1/2} p(n-2k) \tag{10.5.20}$$

$$\langle \psi_{1,k}, \phi_{0,n} \rangle = 2^{-1/2} q(n-2k) \tag{10.5.21}$$

Substituting (10.5.20) and (10.5.21) into (10.5.17) results in (10.5.15) and (10.5.16).

Recursive Projections

The projection procedure can be iterated. The orthonormal projections at one resolution level can continue to the next coarser resolution. At the next coarser resolution, the subspace $\boldsymbol{V}_2$ and $\boldsymbol{W}_2$ are orthogonal complement, $\boldsymbol{V}_1 = \boldsymbol{V}_2 \oplus \boldsymbol{W}_2$, and $\boldsymbol{V}_1$ is the direct sum of $\boldsymbol{V}_2$ and $\boldsymbol{W}_2$. We can decompose $P_1 f\, 0\, \boldsymbol{V}_1$ into two components along $\mathbf{V}_2$ and $\mathbf{W}_2$

$$P_1 f = p_2 f + Q_2 f \tag{10.5.22}$$

with

$$P_2 f = \sum_n c_2(n) \phi_{2,n} \tag{10.5.23}$$

$$Q_2 f = \sum_n d_2(n)\psi_{2,n} \tag{10.5.24}$$

Multiplying by $\phi_{2,k}$ on both sides of expansions (10.5.22) and (10.5.23) and using the orthonormality of the set $\{\phi_{2,n}\}$ and the mutual orthonormality between $\phi_{2,n}$ and $\psi_{2,k}$, we obtain the discrete approximation $c_2(k)$ as:

$$\begin{aligned} c_2(k) &= \langle \phi_{2,k}, P_2 f \rangle = \langle \phi_{2,k}, P_1 f \rangle \\ &= \sum_n \langle \phi_{2,k}, \phi_{1,n} \rangle c_1(n) \end{aligned}$$

Similarly, multiplying $\psi_{2,k}$ with both sides of expansions (10.5.22) and (10.5.24) and using the orthonormality of $\{\phi_{2,n}\}$, the mutual orthogonality between $\phi_{2,k}$ and $\psi_{2,n}$ within the same scale, we obtain the discrete wavelet coefficients $d_2(k)$ as:

$$\begin{aligned} d_2(k) &= \langle \psi_{2,k}, Q_2 f \rangle = \langle \psi_{2,k}, P_1 f \rangle = \\ &= \sum_n \langle \psi_{2,k}, \phi_{1,n} \rangle c_1(n) \end{aligned}$$

The decomposition into smoothed approximations and details at coarser resolutions can be continued as far as wanted. The procedure can be iterated as many times as wanted. The successive projections $P_i f$ correspond to a more and more blurred version of $f(t)$. The successive projections $Q_i f$ correspond to the differences between the two approximations of $f(t)$ at two successive resolution levels. At every step i, one has the orthonormal projection of $P_{i-1} f$ along the subspaces $\boldsymbol{V}_i$ and $\boldsymbol{W}_i$

$$\begin{aligned} P_{i-1} f &= P_i f + Q_i f \\ &= \sum_k c_i(k)\phi_{i,k} + \sum_k d_i(k)\psi_{i,k} \end{aligned} \tag{10.5.25}$$

It is easy to verify that similarly to (10.5.20) and (10.5.21) and independently of the resolution level, i, we have for scale level i:

$$\begin{aligned} \langle \phi_{i,k}, \phi_{i-1,n} \rangle &= 2^{1/2} p(n-2k) \\ \langle \psi_{i,k}, \phi_{i-1,n} \rangle &= 2^{1/2} q(n-2k) \end{aligned} \tag{10.5.26}$$

It follows that

$$\begin{aligned} c_i(k) &= 2^{-1/2} \sum_n p(n-2k) c_{i-1}(n) \\ d_i(k) &= 2^{-1/2} \sum_n q(n-2k) c_{i-1}(n) \end{aligned} \tag{10.5.27}$$

We define the low-pass and high-pass filtering operators L and H, respectively, such that the operations on a sequence $\alpha(n)$ are

$$(L\alpha)(k) = 2^{-1/2}\sum_n p(n-2k)\alpha(n)$$

$$(H\alpha)(k) = 2^{-1/2}\sum_n q(n-2k)\alpha(n)$$

Equations (10.5.27) can be shortened to

$$c_i = Lc_{i-1}$$

$$d_i = Hc_{i-1}$$

Wavelet Series Decomposition

The approximation $c_{i-1}(n)$ is recursively decomposed into the sequences $c_i(n)$ and $d_i(n)$ by iterating the low-pass and high-pass filters, according to (10.5.27). The successive discrete approximation sequences $c_i(n)$ are lower and lower resolution versions of the original data $c_0(n)$, each sampled twice as sparsely as their predecessor. The successive wavelet coefficient sequence $d_i(n)$ represents the difference between the two approximations at resolutions levels i and $i–1$.

Continuing up to resolution M we can represent the original function $f(t)$ by a series of detail functions plus one smoothed approximation:

$$f(t) = P_M L + Q_M f + Q_{M-1} f + \cdots + Q_1 f$$

and

$$f(t) = \sum_{k\varepsilon Z} 2^{-M/2} c_M(k)\phi\left(2^{-M}t - k\right) + \sum_{i=1}^{M}\sum_{k\varepsilon Z} 2^{-i/2} d_i(k)\psi\left(2^{-i}t - k\right) \qquad (10.5.28)$$

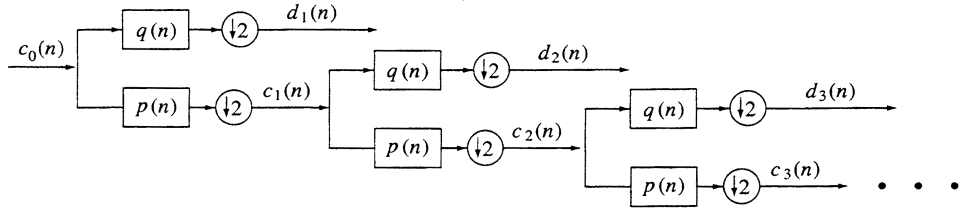

FIGURE 10.11 Schematic wavelet series decomposition in the tree algorithm.

Equation (10.5.28) is referred to as the wavelet series decomposition. The function $f(t)$ is represented as an approximation at resolution $i = M$ plus the sum of M detail components at dyadic scales. The first term in the right-hand side of (10.5.28) is the smoothed approximation of $f(t)$ at very low resolution $i = M$. When M approaches to infinity, the projection of $f(t)$ on the scaling functions of very large scale would smooth out any signal detail and converges to a constant. The function $f(t)$ is then represented as a series of its orthonormal projections on the wavelet bases.

The wavelet series decomposition is a practical representation of the wavelet expansion and points out the complementary role of the scaling function in the wavelet decomposition. Note that in the wavelet series decomposition the function $f(t)$, the scaling function bases and the wavelet bases are all continuous. The approximation coefficients $c_M(k)$ and the wavelet coefficients $d_i(k)$ with $i = 1, 2, \ldots, M$ are discrete. In this sense, the wavelet series decomposition is similar to the Fourier series decomposition.

The discrete approximations $c_i(n)$ and the discrete wavelet coefficients $d_i(n)$ can be computed with an iterative algorithm, described by (10.5.27). This is essentially a discrete algorithm implemented by recursive applications of the discrete low-pass and high-pass filter bank to the discrete approximations, $c_i(n)$. The algorithm is called the tree algorithm. The first two stages of the tree algorithm for computing the wavelet decomposition is shown in Figure 10.11. The decomposition into coarser smoothed approximations and details can be continued as far as one wants.

Example: Decomposition with Haar Wavelets

A simple example for orthonormal wavelet decomposition is that with the Haar's orthonormal bases. Let subspace $\boldsymbol{V}_0$ be spanned by the Haar scaling function basis, $\{\phi(t-k)\}$, defined as a rectangular function of unit width [0, 1). The projection of a function $f(t)$ on $\boldsymbol{V}_0$ is an approximation of $f(t)$ that is piecewise constant over the integer interval. The projection of $f(t)$ on $\boldsymbol{V}_{-1}$ with the orthonormal basis $\{\phi(2t-k)\}$ of the next finer resolution is piecewise constant over the half integer interval. Since $\mathbf{V}_{-1} = \mathbf{V}_0 + \mathbf{W}_0$, and

$$P_{-1}f = P_0 f + Q_0 f$$

The projection $Q_0 f$ represents the difference between the approximation in $\boldsymbol{V}_0$ and the approximation in $\boldsymbol{V}_{-1}$. The approximations $P_0 f$ in $\boldsymbol{V}_0$ and $P_{-1} f$ in $\boldsymbol{V}_{-1}$ and the detail $Q_0 f$ are shown in Figure 10.12. In the figure, the projection $Q_0 f$ is constant over half integer intervals, which can be added to the approximation $P_0 f$ to provide the next finer approximation $P_{-1} f$.

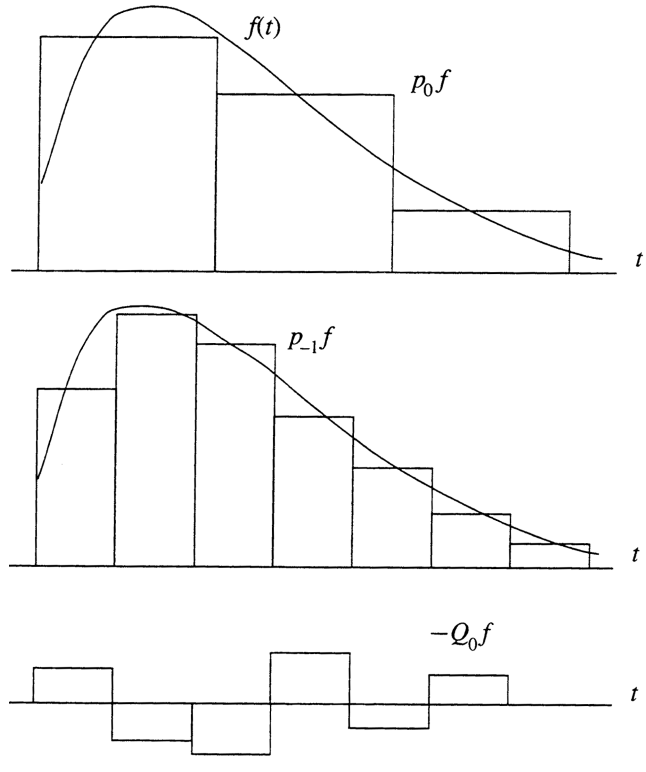

FIGURE 10.12 Orthogonal projections $P_0 f$ and $Q_0 f$ onto the Haar scaling function and wavelet bases. The projection at the next finer resolutions, $P_{-1} f = P_0 f + Q_0 f$. (From Akansu, A. N. and Haddad, R. A. *Multiresolution Signal Decomposition*, Academic Press, Boston, 1992. With permission.)

When the scale level, *i*, approaches minus infinity with finer and finer resolution, the approximations $P_{-i}f$ will converge to the original function *f(t)* as closely as desired. The projection of *f(t)* onto the subspace $\boldsymbol{V}_i$ spanned by the Haar scaling function basis at the resolution level *i* is

$$P_i f = \sum_k c_i(k)\phi_{i,k}$$

with the discrete approximation coefficients:

$$c_i(k) = \langle f, \phi_{i,k} \rangle = 2^{-i/2} \int_{2^i k}^{2^i(k+1)} f(t)dt$$

Because $\phi_{i+1,k}$ is a rectangular function with width of 2^{i+1} and $\phi_{i,k}$ is with width of 2^i it is easy to verify that:

$$\begin{aligned} \phi_{i+1,k} &= 2^{-1/2}\left(\phi_{i,2k} + \phi_{i,2k+1}\right) \\ \psi_{i+1,k} &= 2^{-1/2}\left(\phi_{i,2k} - \phi_{i,2k+1}\right) \end{aligned} \tag{10.5.29}$$

The discrete approximation $c_{i+1}(k)$ can be obtained directly by the orthonormal projection of *f(t)* onto $\mathbf{V}_{i+1}$

$$c_{i+1}(k) = \langle f, \phi_{i+1,k} \rangle = 2^{-1/2}\left(c_i(2k) + c_i(2k+1)\right) \tag{10.5.30}$$

The difference between the two successive approximations is obtained using (10.5.29) and

$$\begin{aligned} P_i f - P_{i+1} f &= \sum_k \left[c_i(k)\phi_{i,k} - c_{i+1}(k)\phi_{i+1,k}\right] \\ &= \sum_k \left[\left(c_i(2k)\phi_{i,2k} + c_i(2k+1)\phi_{i,2k+1}\right)\right. \\ &\quad \left. -2^{-1/2}\left(c_i(2k) + c_i(2k+1)\right)2^{-1/2}\left(\phi_{i,2k} + \phi_{i,2k+1}\right)\right] \\ &= \frac{1}{2}\sum_k \left(c_i(2k) - c_i(2k+1)\phi_{i,2k} - \phi_{i,2k+1}\right) \\ &= \frac{1}{2}\sum_k \left(c_i(2k) - c_i(2k+1)\right)\psi_{i+1,k} \end{aligned}$$

Hence, the projection of *f(t)* onto the subspace $\boldsymbol{W}_{i+1}$ is the difference between $P_i f$ and $P_{i+1} f$

$$Q_{i+1,k} = \sum_k d_{i+1}(k)\psi_{i+1,k} = P_i f - P_{i+1} f$$

provided that:

$$d_{i+1}(k) = 2^{-1/2}\left(c_i(k) - c_i(2k+1)\right) \tag{10.5.31}$$

The interscale coefficients that are the discrete low-pass and high-pass filers, $p(n)$ and $q(n)$, are given for the Haar's bases and have been given in Section 10.5.2. Hence, the iterated filtering by the low-pass and high-pass filters becomes:

$$c_{i+1}(k) = \frac{1}{\sqrt{2}} \sum_n p(n-2k) c_i(n) = \frac{1}{\sqrt{2}} \left(c_i(2k) + c_i(2k+1) \right)$$

$$d_{i+1}(k) = \frac{1}{\sqrt{2}} \sum_n q(n-2k) c_i(n) = \frac{1}{\sqrt{2}} \left(c_i(2k) - c_i(2k+1) \right)$$

which are agree with (10.5.30) and (10.5.31).

10.5.5 Reconstruction

Recursive Reconstruction

The original signal sequence $c_0(n)$ can be reconstructed from the sequences of the approximation coefficients $c_i(n)$ and of the wavelet coefficients $d_i(n)$ with $0 < i \le M$, where $i = M$ is the lowest resolution in the decomposition. At each resolution level i we have the wavelet decomposition described by (10.5.25) and (10.5.27). On multiplying both sides of (10.5.25) by $\phi_{i-1,n}$ and integrating both sides we obtain:

$$\begin{aligned} c_{i-1}(n) &= \left\langle P_{i-1} f, \phi_{i-1,n} \right\rangle \\ &= \sum_k c_i(k) \left\langle \phi_{i,k}, \phi_{i-1,n} \right\rangle + \sum_k d_i(k) \left\langle \psi_{i,k}, \phi_{i-1,n} \right\rangle \\ &= 2^{-1/2} \sum_k c_i(k) p(n-2k) + 2^{-1/2} \sum_k d_i(k) q(n-2k) \end{aligned} \tag{10.5.32}$$

where the inner products, $\langle \phi_{i,k}, \phi_{i-1,n} \rangle$ and $\langle \psi_{i,k}, \psi_{i-1,n} \rangle$ are obtained in (10.5.26) as the interscale coefficients $p(n-2k)$ and $q(n-2k)$. Hence, the discrete approximation $c_{i-1}(n)$ at the next finer resolution can be obtained as the sum of two convolutions between the discrete approximation $c_i(n)$ and the low-pass synthesis filter $p(n)$, and between the wavelet coefficients $d_i(n)$ and the high-pass synthesis filter $q(n)$.

The synthesis filters are identical to the analysis filters. But the filtering operations become the convolutions for synthesis instead of the correlations for analysis. To compute the convolution with the synthesis filters in (10.5.32) one must first put zeros between each sample of the sequences $c_i(k)$ and $d_i(k)$ before convolving the resulting sequences with the synthesis low-pass and high-pass filters, $p(n)$ and $q(n)$. The process is quite similar to the expand operation in the reconstruction algorithm of the multiresolution Laplacian pyramid and the subband coding. The reconstruction process can be repeated by iteration. We define the synthesis filtering operators L_0 and H_0 as:

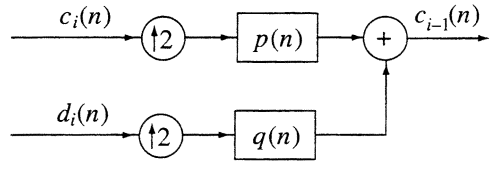

FIGURE 10.13 Schematic wavelet reconstruction.

$$(L_0\alpha)(n) = \frac{1}{\sqrt{2}} \sum_k p(n-2k)\alpha(k)$$

$$(H_0\alpha)(n) = \frac{1}{\sqrt{2}} \sum_k q(n-2k)\alpha(k)$$

and rewrite (10.5.32) in a shorter form:

$$c_{i-1} = L_0 c_i + H_0 d_i$$

The block diagram shown in Figure 10.13 illustrates the reconstruction algorithm, where the up-sampling by two means putting zeros between the sample of the sequences.

To reconstruct the original data $c_0(n)$, we start from the lowest resolution approximation c_M. According to (10.5.32), we have

$$\begin{aligned} c_{M-1} &= H_0 d_M + L_0 c_M \\ c_{M-2} &= H_0 d_{M-1} + L_0 (H_0 d_M + L_0 c_M) \\ &= H_0 d_{M-1} + L_0 H_0 d_M + (L_0)^2 c_M \end{aligned}$$

When the discrete approximation c_{i-1} is obtained from $c_i(n)$ and $d_i(n)$, the next finer approximation $c_{i-2}(n)$ can be obtained from the approximation $c_{i-1}(n)$ and the wavelet coefficients $d_{i-1}(n)$. The process can continue until the original sequence $c_0(n)$ is reconstructed. The reconstruction formula for the original sequence is

$$c_0 = \sum_{i=1}^{M} (L_0)^{i-1} H_0 d_i + (L_0)^M c_M \tag{10.5.33}$$

In this reconstruction procedure it is the low-pass filtering operator, L_0, that is iteratively applied to generate the finer resolution discrete approximations.

Discussion

In summary, in this section we have introduced the orthonormal wavelet series decomposition and reconstruction. In the multiresolution analysis framework, the basic function of the orthonormal wavelet transform is the scaling function $\phi(t)$ that satisfies the two-scale relation. The discrete translates of the scaling functions form the orthonormal bases within each resolution level. The discrete translates of the wavelets also form the orthonormal bases within each resolution level. The scaling and the wavelet function bases are mutually orthogonal within the same resolution level. The recursive orthonormal projections on the multiresolution subspaces yield the wavelet series decomposition.

The wavelet series decomposition and reconstruction are computed by iterating the discrete low-pass filters, $p(n)$, and the discrete high-pass filters $q(n)$, in the tree algorithms, in order to compute a set of discrete wavelet transform coefficients, $d_i(n)$ and a set of discrete approximation coefficients $c_i(n)$.

The scaling function and wavelet bases are orthonormal only with discrete translations and dilations. The decomposition of a continuous function onto the orthonormal scaling and wavelet function bases yields discrete sequences of expansion coefficients. Hence, there is an analogy of the orthonormal wavelet transform with the Fourier series decomposition.

10.5.6 Biorthogonal Wavelet Bases

The biorthogonal wavelet bases give more flexibility to the filter design. We define in the multiresolution framework two hierarchies of approximation subspaces:

$$\cdots V_2 \subset V_1 \subset V_0 \subset V_{-1} \subset V_{-2} \subset \cdots$$
$$\cdots \overline{V}_2 \subset \overline{V}_1 \subset \overline{V}_0 \subset \overline{V}_{-1} \subset \overline{V}_{-2} \subset \cdots$$

where the subspaces $\boldsymbol{V}_i$ are spanned by the translates of the scaling function $\phi(t)$, and $\overline{\boldsymbol{V}}_i$ are spanned by the translates of the dual scaling function $\phi(t)$. The wavelet subspace $\boldsymbol{W}_i$ is complementary to $\boldsymbol{V}_i$ in the finer resolution subspace $\boldsymbol{V}_{i-1}$, but is not orthogonal complement. Instead, $\mathbf{W}_i$ is the orthogonal complement to $\overline{\mathbf{V}}_i$. Similarly, the dual wavelet subspace $\overline{\mathbf{W}}_i$ is the orthogonal complement to $\boldsymbol{V}_i$. Thus,

$$W_i \perp \overline{V}_i \quad \text{and} \quad \overline{W}_i \perp V_i$$
$$\overline{V}_{i-1} = \overline{V}_i \oplus W_i \quad \text{and} \quad V_{i-1} = V_i \oplus \overline{W}_i$$

The orthogonality between the wavelet and the dual scaling function and between the scaling function and the dual wavelet can also be expressed as:

$$\left\langle \overline{\phi}(t-k), \psi(t-n) \right\rangle = 0$$
$$\left\langle \overline{\psi}(t-k), \phi(t-n) \right\rangle = 0$$

for any $n, k \in \boldsymbol{Z}$. We expect also the orthogonality between the scaling function and the wavelet and its dual:

$$\left\langle \overline{\phi}(t-k), \phi(t-n) \right\rangle = \delta_{k,n}$$
$$\left\langle \overline{\psi}(t-k), \psi(t-n) \right\rangle = \delta_{k,n}$$

The orthogonality expressed in the four preceding equations is referred to as biorthogonality. Indeed, the biorthogonal scaling functions and wavelets can be found with the polynomial B-splines scaling functions and wavelets. The cross scale orthogonality of the wavelet and its dual can also be obtained:

$$\left\langle \psi_{i,k}, \overline{\psi}_{m,n} \right\rangle = \delta_{i,m}\delta_{k,n}$$

Any function $f \in L^2(\boldsymbol{R})$ can be expanded onto the biorthogonal scaling function and the wavelet bases as:

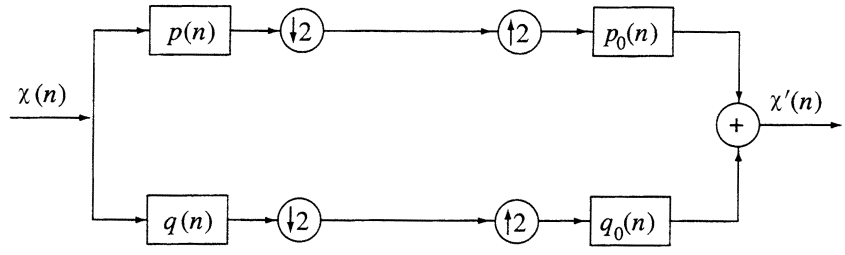

FIGURE 10.14 Schematic wavelet decomposition and reconstruction with the biorthogonal scaling function and wavelet bases.

$$f(t) = \sum_i \sum_k \langle f, \overline{\psi}_{i,k} \rangle \psi_{i,k}(t)$$
$$= \sum_i \sum_k \langle f, \psi_{i,k} \rangle \overline{\psi}_{i,k}(t)$$

and also

$$f(t) = \sum_i \sum_k \langle f, \overline{\phi}_{i,k} \rangle \phi_{i,k}(t)$$
$$= \sum_i \sum_k \langle f, \phi_{i,k} \rangle \overline{\phi}_{i,k}(t)$$

The implementation of the wavelet transform on the biorthogonal bases is also with the discrete low-pass and high-pass filters, $p(n)$ and $q(n)$, in the multiresolution framework. In the reconstruction from the biorthogonal wavelet transform, however, the discrete synthesis filters $p_0(n)$ and $q_0(n)$ are not identical to the analysis filters $p(n)$ and $q(n)$. They can have no equal length. We shall discuss the low-pass and high-pass filters for the biorthogonal wavelet transform in detail in Section 10.6.4. in the framework of the subband coding theory. The discrete iterated filters are introduced with the two-scale relations as:

$$\phi(t) = \sum_n p(n) \phi(2t - n)$$
$$\overline{\phi}(t) = \sum_n p_0(-n) \overline{\phi}(2t - n)$$

and

$$\psi(t) = \sum_n q(n) \phi(2t - n)$$
$$\overline{\psi}(t) = \sum q_0(-n) \overline{\phi}(2t - n)$$

One stage of the wavelet decomposition and reconstruction with the biorthogonal filter bank is shown in Figure 10.14.

Biorthogonal Wavelet Decomposition

Similar to the orthogonal decomposition in (10.5.27), the decomposition with the biorthogonal wavelets is implemented with the biorthogonal analysis filters $p(n)$ and $q(n)$ as:

$$c_i(k) = 2^{-l/2} \sum_n p(n - 2k) c_{i-1}(n)$$

and

$$d_i(k) = 2^{-l/2} \sum_n q(n - 2k) c_{i-1}(n)$$

Biorthogonal Wavelet Reconstruction

Similar to the reconstruction with the orthonormal wavelet transform (10.5.32), the signal is reconstructed with the biorthogonal synthesis filters $p_0(n)$ and $q_0(n)$ as:

$$c_{i-1}(n) = 2^{-1/2}\sum_k c_i(k)p_0(n-2k) + 2^{-1/2}\sum_k d_i(k)q_0(n-2k)$$

We shall discuss the biorthogonal analysis and synthesis filters in Section 10.6.

10.6 Filter Bank

The discrete and dyadic wavelet transform is computed in the multiresolution signal analysis framework with the recurring low-pass and high-pass filters that can be designed in the multiresolution signal analysis framework with the subband coding theory. The properties of the filters may be studied equivalently in the time domain and in the frequency or the z-transform domain.

10.6.1 FIR Filter Bank

Two Channel Filter Bank

The two-channel filter bank, shown in the Figure 10.14, is a building block of the discrete wavelet transform and subband coding. An input signal $x(k)$ is filtered in the two channels by the low-pass filter, $p(k)$ and high-pass filter, $q(k)$, which are the analysis filters for decomposing the signal. The analysis filtering is followed by a down-sampling by two. The filters, $p_0(k)$ and $q_0(k)$, are the synthesis filters for reconstructing the signal. There is up-sampling before the synthesis filters.

The low-pass and high-pass filters, $p(k)$ and $q(k)$, are discrete and usually real-valued sequences with $k \in \boldsymbol{Z}$. For the sake of consistency with the wavelet decomposition described in Section 10.5, we define that the analysis filtering is a correlation operation, and the synthesis filtering is a convolution operation.

Finite Impulse Response (FIR) Filters

Digital filters can be classified into two groups. In the first group, the filter is a finite-extent sequence, called the finite impulse response (FIR) filter. In the second group, the filter is of infinite extent, called the infinite impulse response (IIR) filters. The FIR filters have compact supports. Only a finite number of $p(k)$ and $q(k)$ are not zero: $p(k) \neq 0$ and $q(k) \neq 0$, for $0 \leq k \leq N-1$. However, in the biorthonormal filter banks the low-pass and high-pass filters can have different lengths.

The Fourier transforms of the FIR filters, $p(k)$ and $q(k)$, with compact support would have no fast decay. There is a trade-off between the compactness and the regularity of the FIR filter.

Transfer Functions

Both filters $p(k)$ and $q(k)$ for $k \in \boldsymbol{Z}$ have limited lengths (FIR filters). The filter length is N. Their Fourier transforms exist as:

$$\begin{aligned} P(\omega) &= \sum_k p(k)\exp(-jk\omega) \\ Q(\omega) &= \sum_k q(k)\exp(-jk\omega) \end{aligned} \tag{10.6.1}$$

where $k = 0, 1, 2, \ldots N-1$ and the Fourier transforms of the filters, i.e., the transfer functions, $P(\omega)$ and $Q(\omega)$, are complex-valued continuous functions. Note that (10.6.1) may be considered as the Fourier series expansions of $P(\omega)$ and $Q(\omega)$, therefore, both $P(\omega)$ and $Q(\omega)$ are periodic functions of period $\omega = 2\pi$.

The Fourier series expansions (10.6.1) are equivalent to the *Z*-transform of the sequences *p(k)* and *q(k)*. With the definition of *z* as $z = exp(j\omega)$, (10.6.1) can be rewritten as the Laurent polynomial :

$$P(z) = \sum_k p(k) z^{-k}$$
$$Q(z) = \sum_k q(k) z^{-k} \tag{10.6.2}$$

where $k = 0, 1, 2, \ldots N-1$ and both *P(z)* and *Q(z)* are complex-valued continuous functions of the complex variable, *z*.

The degree of the Laurent polynomial *P(z)* is then equal to *N–1*, i.e., the length of the FIR filter *p(k)* minus one.

The analysis filtering is a correlation operation. In the frequency domain, the filtering of the signal *x(k)* by the low-pass and high-pass filters, *p(k)* and *q(k)*, is equivalent to multiplying the Fourier transform of *x(k)*, *X(z)*, by the transfer functions. That yields $X(z)P(z^{-1})$ and $X(z)Q(z^{-1})$, respectively, where $P(z^{-1})$ and $Q(z^{-1})$ are complex conjugated *P(z)* and *Q(z)* used in the correlation operations. Note that the coefficients *p(k)* and *q(k)* are real-valued in the Laurent polynomial (10.6.2).

Delay and Causality

If the signal *x(n)* is a time sequence, then the filtering convolution operation with a filter *g(k)* is written as:

$$\sum_k g(k) x(n-k) = g(0) x(n) + g(1) x(n-1) + \ldots$$

where *x(n)* is the current input, *x(n–1)* is the input earlier by one time step, etc. The output has a time delay with respect to the input. The filter g*(k)* is a causal filter and g*(–k)* must be zero because the output cannot be a function of the later input. For instance, if $g(-1) \neq 0$, then the filtering output would contain a term of $g(-1)x(n+1)$, where *x(n+1)* is the input of one time step later. The filtering output cannot be a function of *x(n+1)* so that g*(–1)* must be zero.

Linear-Phase Filters

The low-pass FIR filters *p(k)* are usually real-valued and symmetric. In this case, the transfer function $P(\omega)$ as the Fourier transform of *p(k)* is itself a real valued and even function, with zero phase. Because *p(k)* is causal, *p(–k)* is not allowed. Therefore, the filter *p(k)* must be shifted in time domain and centered at *N/2*, which corresponds to a time delay. Hence, the symmetric and antisymmetric filters should be

$$\begin{aligned} &\text{Symmetric} && p(k) = p(N-k) \\ &\text{Antisymmetric} && p(k) = -p(N-k) \end{aligned} \tag{10.6.3}$$

Their transfer function $P(\omega)$ would have a linear phase, and becomes $P(\omega)exp(-jm\omega)$, or $P(z)z^{-m}$. Its modulus $|P(\omega)|$ would be even.

In some wavelet bases, such as the Daubechies bases, the low-pass filters are not symmetric. A non-symmetric filter would introduce a nonlinear phase to the transfer function that can distort the proper registration of different frequency components. For instance, in image processing applications the use of nonsymmetrical filters will introduce important image distortions.

Binary Coefficient Filters

A binary coefficient or dyadic coefficient is an integer divided by a power of 2. In the computer, multiplication by a binary number can be executed entirely by shifts and adds without round-off error.

Also, in some architectures, the filters need less time and less space. We are, therefore, highly interested in binary coefficient filters.

10.6.2 Perfect Reconstruction

Down-Sampling

The down-sampling by a factor of two is a decimation operation that is performed to save the even-numbered components of a data sequence. Down-sampling by two can be considered as being achieved in two steps. First, the signal, $x(n)$, is sampled with the double sampling interval:

$$x'(n) = \begin{cases} x(n) & \text{for n} = 0, \pm 2, \pm 4, \ldots \\ 0 & \text{otherwise} \end{cases}$$

The intermediate signal, $x'(n)$, has the same time clock rate as that of $x(n)$. Then, the time clock rate is reduced by two to obtain the down-sampled signal, $y(n)$ as:

$$y(n) = x'(2n) \qquad \text{for} \quad n = 0, \pm 1, \pm 2, \ldots.$$

In the Fourier domain the spectrum $Y(\omega)$ is two times larger than $X(\omega)$ because $Y(\omega) = X'(\omega/2)$.

Discarding the odd-numbered components leads to a loss of information. This loss of information is definitive. In the frequency domain this is an aliasing error. The down-sampling process is not invertible.

Down-sampling is not shift-invariant. Down-sampling by two for the convolution output of a filter is equivalent to the convolution with the filter that is shifted only by even numbers, i.e. double shift convolution. Therefore, when the input signal is shifted by an odd number, the results of the double shift convolution can change dramatically. The Laplacian pyramid, discrete and dyadic wavelet transform, subband coding, and all other multiresolution analysis using down-sampling are highly dependent on the relative alignment of the input signal with the sub-sampling lattices and are not shift-invariant.

Up-Sampling

The up-sampling by a factor of two is an expansion operation, and involves inserting zeros as the odd-numbered components into the data sequence. The up-sampling is also implemented in two steps. First, insert zeros between nodes of the down-sampled signal, $y(n)$, and then increase the timeclock rate by two and let:

$$y'(n) = \begin{cases} y(n/2) & \text{for n} = 0, \pm 2, \pm 4, \ldots \\ 0 & \text{otherwise} \end{cases}$$

In the Fourier domain, the spectrum of the up-sampled data, $Y'(\omega)$, is compressed by two with respect to the original $Y(\omega)$ because $Y'(\omega) = Y(2\omega)$. Thus, a low-pass filter should be used for smoothing the up-sampled signal. The up-sampling processes are also not shift-invariant. When the input signal is shifted by an odd number, the results of the up-sampling can change dramatically.

Aliasing Cancellation

Aliasing error is introduced by down-sampling. The signal, $x(k)$, is filtered in the two channels by the low-pass and high-pass filters. The filtered signals are described in the frequency domain as $X(z)P(z^{-1})$ and $X(z)Q(z^{-1})$ before the down-sampling. The combination process of the down-sampling followed by the up-sampling would put all the odd-numbered components of the filtered signals equal to zero. This

corresponds in the z-domain to keep only the even powers of z in $X(z)P(z^{-1})$ and $X(z)Q(Z^{-1})$ that can be represented as:

$$\begin{aligned} &\text{Low-pass channel output} && \frac{1}{2}\left[X(z)P(z^{-1})+X(-z)P(-z^{-1})\right] \\ &\text{High-pass channel output} && \frac{1}{2}\left[X(z)Q(z^{-1})+X(-z)Q(-z^{-1})\right] \end{aligned} \tag{10.6.4}$$

or equivalently in the frequency domain:

$$\begin{aligned} &\frac{1}{2}\left[X(\omega)P^{*}(\omega)+X(\omega+\pi)P^{*}(\omega+\pi)\right] \\ &\frac{1}{2}\left[X(\omega)Q^{*}(\omega)+X(\omega+\pi)Q^{*}(\omega+\pi)\right] \end{aligned} \tag{10.6.5}$$

The terms $X(-z)P(-z^{-1})$ and $X(-z)Q(-z^{-1})$ are aliasing errors introduced by the down-sampling, which are not cancelled by the up-sampling.

In the two channel filter bank, the alias terms $X(-z)P(-z^{-1})$ and $X(-z)Q(-z^{-1})$ can be cancelled by the synthesis filters $P_0(z)$ and $Q_0(z)$. At the synthesis step the aliasing term, $X(-z)P(-z^{-1})$, in the low-pass channel is multiplied by $P_0(z)$ and the aliasing term, $X(-z)Q(-z^{-1})$, in the high-pass channel is multiplied by $Q_0(z)$. Hence, the aliasing terms are cancelled, if the condition:

$$P_0(z)P(-z^{-1})+Q_0(z)Q(-z^{-1})=0 \tag{10.6.6}$$

is satisfied.

Perfect Reconstruction Condition

The perfect reconstruction requires $x'(n) = cx(n)z^{-m}$, i.e., the output is equal to the input in the building block shown in Figure 10.14 with an extra constant, c. When the input, $x(n)$, passes the two channels without being divided by two, but the data from the two channels are added up in the end for the output, we have $c = 2$. If the analysis and synthesis filters are normalized to remove the constant c, we have $c = 1$. The extra phase shift z^{-m} with $m \in \boldsymbol{Z}$ corresponds to a possible time delay between the output and the input data sequences. The filter bank can be causal.

The signal passes both the low-pass filter and high-pass filter channels. Each is followed by down-sampling and up-sampling, respectively, as expressed in (10.6.4). We then multiply each by the synthesis filters, $P_0(z)$ and $Q_0(z)$, respectively, and sum them up. When the anti-aliasing condition (10.6.6) is satisfied and the two aliasing terms $X(-z)P(-z^{-1})$ and $X(-z)Q(-z^{-1})$ in (10.6.4) are cancelled, the output could be identical to the input, and the building block could behave like an identity operation if

$$P_0(z)P(z^{-1})+Q_0(z)Q(z^{-1})=cz^{-m} \tag{10.6.7}$$

The ensemble of (10.6.7) for perfect reconstruction and (10.6.6) for aliasing error cancellation is referred to as the perfect reconstruction condition.

Modulation Matrix

Two 2 × 2 modulation matrices are defined as:

$$M(z)=\begin{bmatrix} P(z) & P(-z) \\ Q(z) & Q(-z) \end{bmatrix} \quad \text{and} \quad M_0(z)=\begin{bmatrix} P_0(z) & P_0(-z) \\ Q_0(z) & Q_0(-z) \end{bmatrix} \tag{10.6.8}$$

where $M(z)$ is the analysis modulation matrix and $M_0(z)$ is the synthesis modulation matrix.

The perfect reconstruction conditions (10.6.7) and (10.6.6) may be summarized to

$$\begin{bmatrix} P_0(z) & Q_0(z) \end{bmatrix} M\left(z^{-1}\right) = c\begin{bmatrix} 1 & 0 \end{bmatrix} \tag{10.6.9}$$

where the constant extra time delay z^{-m} is removed for the sake of simplicity. If we want the synthesis filters, $P_0(-z)$ and $Q_0(-z)$, to play the same role as $P_0(z)$ and $Q_0(z)$, then the aliasing cancellation equation (10.6.6) becomes:

$$P_0(-z)P\left(-z^{-1}\right)+Q_0(-z)Q\left(-z^{-1}\right)=0$$

and the perfect reconstruction condition (10.6.7) becomes:

$$P_0(-z)P\left(z^{-1}\right)+Q_0(-z)Q\left(z^{-1}\right)=cz^{-m}$$

then combining with (10.6.9), we have

$$M_0(z)^t M\left(z^{-1}\right)=cI \tag{10.6.10}$$

where I is the identity matrix. Note that in the time domain, the filters with the transfer function, $P_0(-z)$ and $Q_0(-z)$, are only shifted by one with respect to that with the transfer function $P_0(z)$ and $Q_0(z)$. Moreover, if we need the two modulation matrices to be even reversible, then we also need the perfect reconstruction condition as:

$$M\left(z^{-1}\right)M_0(z)^t=cI \tag{10.6.11}$$

that will introduce the cross-filter relation as shown in the next subsections.

10.6.3 Orthonormal Filter Bank

Paraunitary Matrix

The orthogonal filter bank is the perfect reconstruction filter bank with the synthesis filters equal to the analysis filters, $P_0(z) = P(z)$ and $Q_0(z) = Q(z)$, in the building block shown in Figure 10.14. Therefore, for the orthogonal filter bank we have from (10.6.10) and (10.6.11):

$$M(z)^t M\left(z^{-1}\right)=cI \quad \text{and} \quad M\left(z^{-1}\right)M(z)^t=cI \tag{10.6.12}$$

The modulation matrix $M(z)$ is a paraunitary matrix if the constant factor c in the right-hand side of (10.6.12) is not considered. Hence, the low-pass and high-pass filters for the discrete wavelet transform are the two-channel paraunitary filter bank.

Orthonormality Condition

From the paraunitary filter bank condition (10.6.12) it follows that:

$$\begin{aligned} \left|P(z)\right|^2 + \left|P(-z)\right|^2 = c \qquad &\text{and} \qquad \left|P(\omega)\right|^2 + \left|P(\omega+\pi)\right|^2 = c \\ \left|Q(z)\right|^2 + \left|Q(-z)\right|^2 = c \qquad &\text{and} \qquad \left|Q(\omega)\right|^2 + \left|Q(\omega+\pi)\right|^2 = c \end{aligned} \tag{10.6.13}$$

We call both $|P(z)|^2$ and $|Q(z)|^2$ half-band filters and shall discuss their properties later in this subsection. The relation (10.6.13) can also be obtained from the orthonormality condition of the scaling function and wavelet bases in the frequency domain, as will be shown in Section 10.7.

Cross-Filter Orthonormality

From the paraunitary filter bank condition (10.6.12) it also follows that:

$$\begin{aligned} P(z^{-1})Q(z) + P(-z^{-1})Q(-z) = 0 \\ Q(z^{-1})P(z) + Q(-z^{-1})P(-z) = 0 \end{aligned} \tag{10.6.14}$$

The relation (10.6.14) can also be obtained from the cross-orthonormality condition of the scaling function and wavelet bases in the frequency domain, as will be shown in Section 10.7.

In this subsection we introduced the paraunitary filter bank, which leads to the orthonormality and cross-filter normality conditions. The paraunitary filter bank is a solution of the aliasing error cancellation and perfect reconstruction conditions (10.6.9) which becomes the modulation matrix Equations (10.6.10) and (10.6.11) with the additional constraints. In Section 10.7 we shall demonstrate the orthonormality and cross-filter normality conditions on the low-pass and high-pass filters, and then use the orthonormality and cross-filter normality conditions to demonstrate the paraunitary filter bank condition.

Alternating Flip

It is easy to verify that the solution:

$$Q(z) = (-z)^{-(N-1)} P(-z^{-1}) \tag{10.6.15}$$

satisfies the cross-filter orthonormality condition (10.6.14), with an arbitrary even number N, which is the length of the filter in the time domain.

The inverse z-transform of the solution (10.6.15) gives the relation between the low-pass filters, $p(n)$, and high-pass filters, $q(n)$, in the time domain. In multiresolution signal analysis, the wavelet bases are generated by the basic scaling functions. Similarly, the high-pass filters in the filter bank are generated from the low-pass filter by the alternating flip relation. In the orthonormal wavelet transform, the high-pass filters, $q(n)$, are obtained from the low-pass filters, $p(n)$, by the inverse z-transform of (10.6.15):

$$q(n) = (-1)^n p(N-1-n) \qquad \text{for} \quad n = 0,1,2,\ldots,N-1 \tag{10.6.16}$$

for an even N, such that the low-pass and high-pass filters, $p(n)$ and $q(n)$, satisfy the cross-filter orthogonality, where N is the length of the FIR filters, or can be any even number. Note that an arbitrary even number can be added to N, resulting in an even number shift of $p(N–1–n)$.

Quadrature Mirror Filters (QMF)

The alternating flip filters are a solution of the cross-filter orthonormality condition (10.6.14). For the alternating flip filter bank, the low-pass and high-pass filters satisfy:

$$\left|Q(z)\right|^2 = \left|P(-z^{-1})\right|^2 \qquad \text{or equivalently} \qquad \left|Q(\omega)\right|^2 = \left|P(\omega+\pi)\right|^2 \tag{10.6.17}$$

and are referred to as a pair of quadrature mirror filters. If the high-pass filter, $Q(\omega)$, is such that $Q(\omega)|_{\omega=0} = 0$, then from the quadrature mirror property (10.6.17) we have $P(\omega)|_{\omega=\pi} = 0$. If the low-pass filter $P(\omega)$ is normalized such that $P(\omega)|_{\omega=0} = 1$, then from the quadrature mirror property (10.6.17) the high-pass filter would be such that $Q(\omega)|_{\omega=\pi} = 1$.

Mirror Filters

A pair of FIR filters $L(\omega)$ and $H(\omega)$ are referred to as mirror filters, if

$$L(z) = H(-z) \qquad \text{or equivalently} \qquad L(\omega) = H(\omega + \pi) \tag{10.6.18}$$

In the time domain, the two FIR mirror filters with real-valued coefficients satisfy the relation

$$l(k) = (-1)^k h(k) \tag{10.6.19}$$

that is the inverse z-transform of (10.6.18).

The filter pair $L(\omega)$ and $H(\omega)$ are mirror filters because on substituting for ω by $\omega - \pi/2$ in (10.6.18) and noting that the low-pass filter, $L(n)$ is real valued, and $|L(\omega)|$ is an even function of ω, we obtain:

$$\left|H\left(\frac{\pi}{2} + \omega\right)\right| = \left|L\left(\frac{\pi}{2} - \omega\right)\right| \tag{10.6.20}$$

This is the mirror image property of $|L(\omega)|$ and $|H(\omega)|$ about $\omega = \pi/2$.

Ideal Half-Band Filters

Intuitively, if a low-pass filter is an ideal low-pass filter: $L(\omega) = 1$ for $-\pi/2 \le \omega \le \pi/2$, and $L(\omega) = 0$ elsewhere, then its mirror filter $H(\omega)$ is the ideal half-band high-pass filter : $H(\omega) = 0$ for $-\pi/2 \le \omega \le \pi/2$, and equal to 1 elsewhere. They are both brick-wall filters and are rectangular functions. Hence, the input spectrum in the full band, $-\pi \le \omega \le \pi$, is divided into two equal subbands by the analysis mirror filters $L(\omega)$ and $H(\omega)$.

Half-Band Filters

The ideal half-band filters are orthonormal. In practice of multiresolution signal analysis, it is not necessary to use the ideal low-pass and high-pass filters. A filter $G(z)$ is a half-band filter if

$$G(z) + G(-z) = 2 \qquad \text{or equivalently} \qquad G(\omega) + G(\omega + \pi) = 2 \tag{10.6.21}$$

The filter $G(\omega)$ is half-band because on substituting for ω by $\omega - \pi/2$ in (10.6.21), and noting that the low-pass filter, $g(n)$, is real valued, and $|G(\omega)|$ is an even function of ω, we obtain:

$$\left|G\left(\frac{\pi}{2} - \omega\right)\right| = \left|G\left(\frac{\pi}{2} + \omega\right)\right| \tag{10.6.22}$$

There is the mirror image property of $|G(\omega)|$ about $\omega = \pi/2$, which is referred to as the half-band frequency.

In the Laurent polynomial (10.6.2) of the half-band filters, $G(z)$, all the even powers of z must be zero, and all the odd powers of z must be cancelled by each other, except the zero power term $G(0) = 1$.

Note that the low-pass and high-pass filters, $P(z)$ and $Q(z)$, in the multiresolution signal analysis are not themselves half-band, but their square modulus are half-band filters according to (10.6.13), and are the quadrature mirror filters according to (10.6.17).

Power Complementary Filters

The filter pair $\{L(\omega), H(\omega)\}$ are referred to as the power complementary filters if

$$\left|L(\omega)\right|^2 + \left|H(\omega)\right|^2 = c \tag{10.6.23}$$

where the constant $c = 1$ or 2. This relation shows the energy complementary property of the low-pass and high-pass filters. From the orthonormality condition (10.6.13) and quadrature mirror condition (10.6.17) it follows that $P(\omega)$ and $Q(\omega)$ are complementary because:

$$\begin{aligned} \left|P(z)\right|^2 + \left|Q(z)\right|^2 = c \qquad &\text{or} \qquad \left|P(\omega)\right|^2 + \left|Q(\omega)\right|^2 = c \\ \left|P(-z)\right|^2 + \left|Q(-z)\right|^2 = c \qquad &\text{or} \qquad \left|P(\omega+\pi)\right|^2 + \left|Q(\omega+\pi)\right|^2 = c \end{aligned} \tag{10.6.24}$$

10.6.4 Orthonormal Filters in Time Domain

From the orthonormal filter condition (10.6.13) both $|P(z)|^2$ and $|Q(z)|^2$ are half-band filters so that in their Laurent polynomials all the even powers of z must be zero. Note that $P(z)$ and $Q(z)$ are the Fourier transforms of the time domain filters, $p(k)$ and $q(k)$, respectively. The inverse Fourier transform of the square modulus $|P(z)|^2$ is the auto-correlation of $p(k)$. Let a product filter $Pr(z) = |P(z)|^2$. In the Laurent polynomial of $Pr(z)$, the coefficients $p_r(2n) = 0$ for $n \neq 0$ and $p_r(0) = 1$. Hence, the time domain low-pass filter has the double-shift orthogonality as:

$$\sum_k p(k)p(k-2n) = \delta(n)$$

and similarly for the high-pass filter:

$$\sum_k q(k)q(k-2n) = \delta(n)$$

From the cross-filter orthonormality (10.6.14) and using the similar process, we can have the cross-filter orthonormallity in the time domain as:

$$\sum_k p(k)q(k-2n) = 0$$

All the filters are shifted in the time domain by even integers in the correlations. Therefore, at the same resolution level, the low-pass filter $p(n)$ is orthonormal to its own translates by two or by any even numbers. The high-pass filter, $q(n)$, also is orthonormal to its own translates by two or by any even numbers. Also, the low-pass and high-pass filters translated by two, or any even numbers, are mutually orthogonal. This is the double-shift orthonormality of the low-pass and high-pass filters in the time domain.

In the multiresolution signal analysis, the double-shift of the low-pass and high-pass filters in the time domain correspond to the filtering followed by down-sampling by a factor of two.

The double-shift orthonormality implies that the orthonormal wavelet transform filters, $p(n)$ and $q(n)$, must have even lengths.

10.6.5 Biorthogonal Filter Bank

In the two-channel filter bank, shown in Figure 10.14, the synthesis filters may be different from the analysis filters that bring more freedom in the filter design. The perfect reconstruction conditions should still be satisfied. The filter bank in this case is biorthogonal.

The choice for the synthesis filters $P_0(z)$ and $Q_0(z)$ as:

$$\begin{aligned} P_0(z) &= Q(-z^{-1}) \\ Q_0(z) &= -P(-z^{-1}) \end{aligned} \tag{10.6.25}$$

satisfies the alias cancellation equation:

$$P_0(z)P(-z^{-1}) + Q_0(z)Q(-z^{-1}) = 0$$

Thus, the synthesis filters are associated to the analysis filters. The low-pass synthesis filter is equal to the high-pass analysis filter. They have the same length. The high-pass synthesis filter is equal to the low-pass analysis filter. They have the same length. The synthesis filters cancel the alias errors, caused by the analysis filters, and the down- and up-sampling.

Product Filters

With the choice of (10.6.25) for the synthesis filters, the perfect reconstruction Equation (10.6.7):

$$P_0(z)P(z^{-1}) + Q_0(z)Q(z^{-1}) = 2z^{-m}$$

becomes

$$P_0(z)P(z^{-1}) - P_0(-z)P(-z^{-1}) = 2z^{-m} \tag{10.6.26}$$

The left-hand side of (10.6.26) is an odd function of z. Therefore, in the right-hand side of (10.6.26) the power $-m$ of z, must be odd. We define the product filter $Pr(z)$ as:

$$Pr(z) = P_0(z)P(z^{-1}) \tag{10.6.27}$$

and the normalized product filter as:

$$\tilde{P}r(z) = P_0(z)P(z^{-1})z^m$$

where m is an odd number. Then, the perfect reconstruction condition (10.6.26) becomes:

$$\tilde{P}r(z) + \tilde{P}r(-z) = 2 \tag{10.6.28}$$

The normalized product filter $\tilde{P}r\ (z)$ has to be a half-band filter. Hence, all the even powers of z in $\tilde{P}r\ (z)$ must be zero, except for zero power term $\tilde{P}r\ (0) = 2$. There are only the odd powers of z in the polynomial $\tilde{P}r\ (z)$ and all the odd powers must be cancelled by each others.

Degrees and Symmetries

Because the normalized product filter is half-band, and m is an odd number, the product filter $Pr(z) = P_0(z)P(z^{-1})$ must be a polynomial in z of even degrees. Its two factors, the low-pass analysis and synthesis filters, $P(z^{-1})$ and $P_0(z)$, must both have even degrees or both have odd degrees. In the time domain, the low-pass analysis and synthesis filters must be both of odd lengths or both of even length.

The symmetric or antisymmetric filters are linear-phase filters. The product filter can be symmetric, but cannot be antisymmetric, because the half-band filter $\tilde{P}r(0) \neq 0$; also the low-pass filter cannot have a zero mean: $\sum p(k) \neq 0$. Hence, the low-pass analysis and synthesis filters, $P(z^{-1})$ and $P_0(z)$, can both only be symmetric. In this case, the low-pass analysis and synthesis filters in the time domain are both symmetric and have either both odd lengths or both even lengths.

The synthesis filters are obtained from the analysis filters as shown in (10.6.25):

$$P_0(z) = Q(-z^{-1})$$

$$Q_0(z) = -P(-z^{-1})$$

by changing $-z$ to z that alters the signs of all the coefficients of the high-pass filters in the time domain, $q(k)$ and $q_0(k)$. When $P(z^{-1})$ and $P_0(z)$ are symmetric and of odd lengths, changing $-z$ to z does not change the symmetry of the high-pass filters. Then, the high-pass filters are also both symmetric and of odd lengths. When $P(z^{-1})$ and $P_0(z)$ are symmetric and of even lengths, changing $-z$ to z and changing the signs of the $p_0(k)$ and $q_0(k)$ of odd k do change the symmetry to antisymmetry, so that the high-pass filters of even lengths are both anti-symmetric.

Design Biorthonormal Filters

The biorthonormal filter bank is designed to satisfy the perfect reconstruction condition (10.6.26). First, one chooses the product filter $\tilde{P}r(z)$ satisfying the half-band condition (10.6.28). If the analysis and synthesis filters in the time domain have the lengths N and N_0, respectively, the degrees of the polynomials $P(z^{-1})$ and $P_0(z)$ would be $N-1$ and $N_0 - 1$, respectively. Then, the degree of the polynomial $\tilde{P}r(z)$ will be $N + N_0 - 2$, which is usually determined at the beginning. Then, one factorizes the product filter $Pr(z)$ into the low-pass analysis and synthesis filters $P(z^{-1})$ and $P_0(z)$. The high-pass filters can be finally determined according to the alternating flip relation (10.6.25). Splitting $Pr(z)$ into $P(z^{-1})$ and $P_0(z)$ can have some degrees of freedom which can be used for providing some useful properties, such as the linear phase filters (symmetry or antisymmetry).

In one of the design methods, the product filter, $Pr(z)$, takes the form of

$$\mathrm{Pr}(z) = \left(\frac{1+z^{-1}}{2}\right)^M F(z) \tag{10.6.29}$$

where the first term is the Fourier spectrum of a low-pass filter whose corresponding scaling function is a spline function, as will be discussed in Section 10.8.1. Note that $z = e^{j\omega}$ and $|(1+e^{-j\omega})/2| = |\cos\omega|$. Hence, this term ensures $|Pr(\omega)|$to have a zero of order M at $z = -1$ and at $\omega = \pi$, and to have M vanishing derivatives at $\omega = 0$. The second term $F(z)$ ensures the $Pr(z)$ to satisfy the perfect reconstruction condition and being a half-band filter.

The biorthonormal wavelet transform filter banks can be designed with the lifting steps and the polyphase representation. Readers interested in the polyphase, lifting and spectral factorization are referred to other reference books.[24] The lifting steps can be considered as a balancing operation between the smoothness of the analysis and synthesis filters,[24] that is moving the factor $(1 + z^{-1})/2$ from the synthesis filter $P_0(z)$ to the analysis filter $P(z^{-1})$ where $P_0(z)$ and $P(z^{-1})$ are two factors in the same product filter $Pr(z) = P_0(z)P(z^{-1})$. Multiplying $(1 + z^{-1})/2$ to $P(z^{-1})$ corresponds to:

$$p^{new}(k) = \frac{1}{2}\left[p^{old}(k) + p^{old}(k-1)\right]$$

in the time domain.

The synthesis filter $P_0(z)$ is divided by $(1 + z^{-1})/2$ then:

$$P_0^{new}(z) = P_0^{old}(z)\left(\frac{1+z^{-1}}{2}\right)^{-1} \quad \text{and} \quad P_0^{new}(z) = 2P_0^{old}(z) - z^{-1}P_0^{new}(z)$$

Hence, the synthesis filter in the time domain is changed as:

$$p_0^{new}(k) = \left[2p_0^{old}(k) - p_0^{new}(k-1)\right]$$

The biorthonormality is preserved because

$$P^{new}(z^{-1})P_0^{new}(z) = P^{old}(z^{-1})P_0^{old}(z)$$

This process also maintains the binary coefficients of the filters.[24]

Example

The pair of low-pass analysis and synthesis filters:

$$p1 = \left[1\right] \quad \text{and} \quad p_07 = \left[-1 \quad 0 \quad 9 \quad 16 \quad 9 \quad 0 \quad -1\right]/16$$

are symmetric and binary coefficient filters. Balancing will produce 2/6 and 3/5 filters as:

$$p2 = \left[1 \quad 1\right]/2 \quad \text{and} \quad p_06 = \left[-1 \quad 1 \quad 8 \quad 8 \quad 1 \quad -1\right]/8$$

$$p3 = \left[1 \quad 2 \quad 1\right]/4 \quad \text{and} \quad p_05 = \left[-1 \quad 2 \quad 6 \quad 2 \quad -1\right]/4$$

These filters are biorthonormal and of binary coefficients.

10.7 Wavelet Theory

The dyadic discrete wavelet decomposition and reconstruction are computed by iterating the discrete low-pass and high-pass filters in the tree algorithm in the multiresolution signal analysis framework. The low-pass and high-pass filters for the orthonormal wavelet transform are the paraunitary two-band perfect reconstruction (PR) quadrature mirror filter (QMF) bank, which can be designed using the subband coding theory.

When computing the discrete wavelet transform one is given by a bank of low-pass and high-pass filters to iterate. The wavelet and scaling function are not explicitly present during the wavelet transform computation. They even have no closed forms for many wavelets. However, in the wavelet theory an extra regularity condition is imposed on the scaling function and the wavelets. The orthonormal wavelet transform can be applied to continuous functions and therefore serves as a transform tool for analytic signals. The multiresolution Laplacian pyramid and the subband coding are discrete. The multiresolution wavelet transform algorithm is also essentially discrete. But the algorithm leads to a wavelet series expansion that decomposes a continuous function into a series of continuous wavelet functions.

The novelties in the wavelet theory with respect to that developed in the subband theory are the wavelet decomposition of continuous signal functions into the continuous scaling function and wavelet bases; the regularity of the scaling function and wavelet as well as the quadrature mirror filters; the localization of the scaling function and wavelet in both time and frequency domains; the zero-mean condition on the high-pass filter and the generation of the continuous scaling function and wavelet by iterating the low-pass and high-pass filters.

The basic properties of the orthonormal scaling functions and wavelets are the orthonormality and regularity, which are applied to the discrete low-pass and high-pass filters as well. Most analysis on the filter properties will be done in the Fourier domain. The knowledge on these properties is useful for designing the wavelet bases.

10.7.1 Orthonormality

The scaling function and the wavelets can be orthonormal to their own discrete translates at each resolution level, constructing orthonormal bases, in the condition that the scaling function and wavelet satisfy the orthonormality conditions. The orthonormality conditions can be expressed in the frequency domain.

Orthonormality Conditions

Consider a generic basic scaling function $\phi(t)$ that is, in most cases, real valued. At a given scale, its discrete translations form an orthonormal set $\{\phi(t-k)\}$, such that:

$$\int \phi(t-k)\phi(t-k')dt = \delta_{k,k'} \qquad k,k' \in Z$$

The orthonormality of the discrete translations of $\phi(t)$ is equivalent to the fact that the autocorrelation of $\phi(t)$ evaluated at discrete time steps $(k-k')$ must be zero everywhere except at the origin, $k = k'$. The Fourier transform of the autocorrelation of a function is equal to the squared modulus of the Fourier transform of that function. Hence, the orthonormality in the Fourier domain may be written as:

$$\int \left|\Phi(\omega)\right|^2 \exp(-jn\omega)d\omega = 2\pi\delta_{n,0} \tag{10.7.1}$$

where $n = k - k'$ with $n \in Z$, and $\Phi(\omega)$ is the Fourier transform of $\phi(t)$. Hence, the Fourier transform of the scaling function, $|\Phi(\omega)|^2$, evaluated at discrete frequency steps n must be equal to zero except at the origin $n = 0$. We shall prove that the orthonormality condition (10.7.1) for the basic scaling function may be expressed as:

$$\sum_n \left|\Phi(\omega + 2n\pi)\right|^2 = 1 \tag{10.7.2}$$

The sum of the series of its Fourier spectrum intensity $|\Phi(\omega)|^2$ discretely translated by $2n\pi$ must be equal to one.

Similarly, the orthogonality condition for a basic wavelet is that its Fourier spectrum satisfies:

$$\sum_n \left|\Psi(\omega + 2n\pi)\right|^2 = 1 \tag{10.7.3}$$

Poisson Summation Formula

To prove the orthonormality condition (10.7.2) and (10.7.3), we need to use the Poisson summation formula

$$\sum_n f(x + 2\pi n) = \frac{1}{2\pi}\sum_n F(n)\exp(jnx) \tag{10.7.4}$$

If $f(x)$ is a delta function, then (10.7.4) is the well known Fourier transform of a comb function. If $f(x)$ is continuous and has a compact support smaller than 2π, then the left-hand side of (10.7.4) is a periodic function, and the right-hand side of (10.7.4) is the Fourier series expansion of that periodic function, where $F(n)$ is the Fourier transform $f(x)$. The Poisson summation formula then corresponds to the simple Fourier series decomposition of the periodic function, $\sum f(x + 2n\pi)$. However, the

Poisson summation formula is valid when *f(x)* satisfies some regularity conditions and has a compact support such that the series $\sum f(x+2n\pi)$ converges to a periodic function of period 2π.

Assume that the Fourier spectrum $|\Phi(\omega)|^2$ of the basic scaling function $\phi(t)$ is regular, and has a compact support. Let $|\Phi(\omega)|^2$ be the *f(x)* in the Poisson summation formula (10.7.4), we obtain:

$$\sum_n \left|\Phi(\omega+2n\pi)\right|^2 = \frac{1}{2\pi}\sum_n R(n)\exp(jn\omega)$$

where *R(n)* is the Fourier transform of $|\Phi(\omega)|^2$. If $\Phi(\omega)$ satisfy the orthonormality condition (10.7.1) *R(n)* would be equal to zero for $n \neq 0$ and equal to 2π for $n = 0$, that proves the orthonormality condition (10.7.2), and similarly we have (10.7.3).

Discussion

To gain an insight of the orthonormality condition (10.7.2), we expand a function *g(t)* onto the orthonormal basis of the translates $\{\phi(t-k)\}$ with $k \in \mathbf{Z}$; that is

$$g(t) = \sum_k c(k)\phi(t-k) = \phi(t) * \sum_k c(k)\delta(t-k)$$

where $*$ denotes the convolution and *c(k)* are the coefficients of expansion. In the Fourier domain this expansion becomes:

$$G(\omega) = \Phi(\omega)\sum_k c(k)\exp(-jk\omega) = \Phi(\omega)M(\omega)$$

where $M(\omega)$ is defined as:

$$M(\omega) = \sum_k c(k)\exp(-jk\omega)$$

which is a periodic with period 2π: $M(\omega) = M(\omega+2n\pi)$. According to the Parseval's relation of the Fourier transform:

$$\frac{1}{2\pi}\int_0^{2\pi} \left|M(\omega)\right|^2 d\omega = \sum_n \left|c(n)\right|^2$$

We can compute the energy of *g(t)* by:

$$\begin{aligned}
\int_{-\infty}^{\infty} \left|g(t)\right|^2 dt &= \frac{1}{2\pi}\int_{-\infty}^{\infty} \left|\Phi(\omega)\right|^2 \left|M(\omega)\right|^2 d\omega \\
&= \frac{1}{2\pi}\sum_{n=-\infty}^{\infty} \int_{2\pi n}^{2\pi(n+1)} \left|\Phi(\omega)\right|^2 \left|M(\omega)\right|^2 d\omega \\
&= \frac{1}{2\pi}\sum_{n=-\infty}^{\infty} \int_0^{2\pi} \left|\Phi(\omega+2n\pi)\right|^2 \left|M(\omega+2n\pi)\right|^2 d\omega \\
&= \frac{1}{2\pi}\int_0^{2\pi} \left|M(\omega)\right|^2 \sum_{n=-\infty}^{\infty} \left|\Phi(\omega+2n\pi)\right|^2 d\omega
\end{aligned}$$

where we used the property that $M(\omega + 2n\pi)$ is periodic of period 2π. From the orthogonality condition (10.7.2) we can write:

$$\int |g(t)|^2 dt = \sum_n |c(n)|^2 \tag{10.7.5}$$

This is the energy conservation relation for the expansion onto the orthonormal scaling function and wavelet bases, and is similar to the energy conservation relation (10.2.5) for the continuous wavelet transform in Section 10.2.1. According to the wavelet frame theory in Section 10.3.3, (10.7.5) means the frame is tight, the discrete scaling function basis behaves like an orthonormal basis.

10.7.2 Two-Scale Relations in Frequency Domain

The two-scale relations in the multiresolution analysis are the basic relations between the continuous scaling function $\phi(t)$, wavelet $\psi(t)$ and the discrete low-pass and high-pass filters, $p(n)$ and $q(n)$:

$$\phi(t) = \sum_k p(k)\phi(2t-k)$$
$$\psi(t) = \sum_k q(k)\phi(2t-k)$$

In the multiresolution wavelet decomposition, the low-pass filter $p(n)$ plays the role of the weighting function and the high-pass filter $q(n)$ is used to compute the detail information. The Fourier transform of the two-scale relations gives:

$$\begin{aligned}\Phi(\omega) &= \sum_k p(k)\int \phi(2t-k)\exp(-j\omega t)dt \\ &= \frac{1}{2}\left[\sum_k p(k)\exp(jk\omega/2)\right]\Phi\left(\frac{\omega}{2}\right) \\ &= P\left(\frac{\omega}{2}\right)\Phi\left(\frac{\omega}{2}\right)\end{aligned} \tag{10.7.6}$$

and similarly,

$$\Psi(\omega) = Q\left(\frac{\omega}{2}\right)\Phi\left(\frac{\omega}{2}\right) \tag{10.7.7}$$

where $P(\omega)$ and $Q(\omega)$ are the Fourier transform of the sequences of the low-pass and high-pass filters, as defined in (10.6.1) and (10.6.2). Both $P(\omega)$ and $Q(\omega)$are periodic functions of period 2π.

According to (10.7.6), the Fourier transform $\Phi(\omega)$ of the coarser resolution scaling function $\phi(t)$ is the product of the twice wider Fourier transforms $\Phi(\omega/2)$ of the finer resolution scaling function $\phi(2t)$ and that of the low-pass filter $P(\omega/2)$. Equation (10.7.6) is a recursion equation. The recursion can be repeated m times to yield $\Phi(\omega/2)$, $\Phi(\omega/4)$ … so on, that gives:

$$\Phi(\omega) = \prod_{i=1}^{m} P\left(\frac{\omega}{2^i}\right)\Phi\left(\frac{\omega}{2^m}\right) \tag{10.7.8}$$

When m approaches to infinity and $1/2^m$ tends to zero, we have the Fourier transform of the continuous scaling function expressed as:

$$\Phi(\omega) = \prod_{i=1}^{\infty} P\left(\frac{\omega}{2^i}\right) \tag{10.7.9}$$

provided that the scaling function $\phi(t)$ is normalized with respect to the $\boldsymbol{L}^1(\boldsymbol{R})$ as:

$$\int \phi(t)dt = \Phi(0) = 1$$

Similarly, we can replace the second term $\Phi(\omega/2)$ in the right-hand side of (10.7.7) with the infinite product derived in (10.7.9) and obtain:

$$\Psi(\omega) = Q\left(\frac{\omega}{2}\right)\prod_{i=2}^{\infty} P\left(\frac{\omega}{2^i}\right) \tag{10.7.10}$$

It can be proved that if for some $\varepsilon > 0$, the sequence of interscale coefficients, $p(n)$, satisfies:

$$\sum_n |p(n)||n|^{\varepsilon} < \infty$$

then the infinite product on the right-hand side of (10.7.9) converges pointwise and the convergence is uniform. That is, the low-pass filter $p(n)$ decays as fast as n^{ε}. This is a very mild condition, because in most practical cases, the low-pass filters, $p(n)$, are the finite impulse response (FIR) filters with only a limited number of $p(n) \neq 0$.

The two Equations (10.7.9) and (10.7.10) express relations between the Fourier transforms of the continuous scaling function and wavelet and the infinite product of the Fourier transforms of the low-pass and high-pass filters.

Filters Orthonormality

Using the Fourier domain two-scale relation (10.7.6) and the orthonormality condition (10.7.2), we can write:

$$\sum_n |\Phi(2\omega + 4n\pi)|^2 = |P(\omega)|^2 \sum_n |\Phi(\omega + 2n\pi)|^2 = |P(\omega)|^2$$

$$\sum_n |\Phi(2\omega + 2(2n+1)\pi)|^2 = |P(\omega+\pi)|^2 \sum_n |\Phi(\omega + (2n+1)\pi)|^2 = |P(\omega+\pi)|^2$$

which correspond to the summation of $\Phi(\omega)$ translated by $4n\pi$ and by $(2n+1)2\pi$, respectively. Adding these two equations and again applying the orthonormality condition (10.7.2) to the two summations of $\Phi(\omega)$ on the left-hand side of the preceding equations, we have:

$$|P(\omega)|^2 + |P(\omega+\pi)|^2 = 2 \tag{10.7.11}$$

This is the orthonormality condition for the square modulus of the low-pass filter $P(\omega)$ in the Fourier domain. Similarly, the orthonormality condition for the high-pass filter $\psi(\omega)$ in the Fourier domain is

$$\left|Q(\omega)\right|^2 + \left|Q(\omega+\pi)\right|^2 = 2 \tag{10.7.12}$$

Both (10.7.11) and (10.7.12) are identical to (10.6.13) introduced in Section 10.6.3.

Cross-Filter Orthogonality

The scaling functions and the wavelets must be mutually orthogonal within the same scale:

$$\int \phi(t-n')\psi(t-k)dt = 0$$

for all n', $k \in \boldsymbol{Z}$. In the Fourier domain the condition for the cross-filter orthogonality can be written as:

$$\int \Phi(\omega)\Psi^*(\omega)\exp(-jn\omega)d\omega = 0 \tag{10.7.13}$$

where $n = n' - k$ and $n \in \boldsymbol{Z}$. Using the Poisson summation formula (10.7.4):

$$\sum_n f(x+2n\pi) = \frac{1}{2\pi}\sum_n F(n)\exp(jnx)$$

and assuming that the product $\Phi(\omega)\psi^*(\omega)$ is regular and of finite support and let it be the $f(x)$ in the Poisson summation formula, and using the cross-filter orthogonality condition (10.7.13), we have the Fourier transform of $\Phi(\omega)\psi^*(\omega)$ equal to zero and:

$$\sum_n \Phi(\omega+2n\pi)\Psi^*(\omega+2n\pi) = 0 \tag{10.7.14}$$

We separate the translations of $4k\pi$ and of $(2k+1)2\pi$ of the product $\Phi(\omega)\psi^*(\omega)$ and rewrite (10.7.14) as:

$$\sum_n \Phi(2\omega+4n\pi)\Psi^*(2\omega+4n\pi) + \sum_n \Phi(2\omega+2(2n+1)\pi)\Psi^*(2\omega+2(2n+1)\pi) = 0$$

On substituting the Fourier domain two-scale relations (10.7.6) and (10.7.7) for $\Phi(\omega)$ and $\Psi^*(\omega)$ into the above expression and using the periodicity of period 2π of $P(\omega)$ and $Q(\omega)$, we have:

$$P(\omega)Q^*(\omega)\sum_n\left|\Phi(\omega+2n\pi)\right|^2 + P(\omega+\pi)Q^*(\omega+\pi)\sum_n\left|\Phi(\omega+(2n+1)\pi)\right|^2 = 0$$

Using the orthonormality condition for $\Phi(\omega)$ described in (10.7.2), we have:

$$P(\omega)Q^*(\omega) + P(\omega+\pi)Q^*(\omega+\pi) = 0$$
$$P^*(\omega)Q(\omega) + P^*(\omega+\pi)Q(\omega+\pi) = 0$$

This is the cross filter orthogonality condition on the low-pass and high-pass filters $P(\omega)$ and $Q(\omega)$ in the Fourier domain, which is identical to (10.6.14) introduced in Section 10.6.3.

Paraunitary Matrix

We observe the orthonormality conditions for the low-pass and high-pass filters and the cross-filter orthogonality in terms of the z-transform as:

$$\begin{aligned} P(z)P(z^{-1}) + P(-z)P(-z^{-1}) &= 2 \\ Q(z)Q(z^{-1}) + Q(-z)Q(-z^{-1}) &= 2 \\ P(z)Q(z^{-1}) + P(-z)Q(-z^{-1}) &= 0 \\ P(z^{-1})Q(z) + P(-z^{-1})Q(-z) &= 0 \end{aligned} \tag{10.7.15}$$

and choose the alternating flip filter bank as a solution for the cross-filter orthogonality as (10.6.15)

$$Q(z) = (-z)^{-(N-1)} P(-z^{-1}) \tag{10.7.16}$$

where N is an arbitrary even number. That leads to:

$$|Q(z)|^2 = |P(-z)|^2 \qquad \text{and} \qquad |Q(\omega)|^2 = |P(\omega+\pi)|^2 \tag{10.7.17}$$

The conjugate quadrature filters $|P(-z)|^2$ and $|Q(z)|^2$ are the mirror filters, as defined in (10.6.18).

The first two equations in (10.7.15) are

$$\begin{aligned} |P(z)|^2 + |P(-z)|^2 &= 2 \\ |Q(z)|^2 + |Q(-z)|^2 &= 2 \end{aligned} \tag{10.7.18}$$

From (10.7.17) and (10.7.18), we have:

$$\begin{aligned} |P(z)|^2 + |Q(z)|^2 = 2 \qquad \text{and} \qquad |P(\omega)|^2 + |Q(\omega)|^2 = 2 \\ |P(-z)|^2 + |Q(-z)|^2 = 2 \qquad \text{and} \qquad |P(\omega+\pi)|^2 + |Q(\omega+\pi)|^2 = 2 \end{aligned} \tag{10.7.19}$$

The filter pair $\{P(z), Q(z)\}$ are power complementary as defined in (10.6.24). The orthogonality conditions described in (10.7.15) and the power complementary properties described in (10.7.19) are equivalent to the requirement that the 2×2 modulation matrix defined in (10.6.8) should be paraunitary:

$$\begin{vmatrix} P(z^{-1}) & P(-z^{-1}) \\ Q(z^{-1}) & Q(-z^{-1}) \end{vmatrix} \begin{vmatrix} P(z) & Q(z) \\ P(-z) & Q(-z) \end{vmatrix} = 2 \begin{vmatrix} 1 & 0 \\ 0 & 1 \end{vmatrix} \tag{10.7.20}$$

The paraunitary properties are useful for designing the compactly supported orthonormal scaling function and the wavelet bases. All the properties for orthonormality, cross-filter orthonormality, alternating flip filters, conjugate quadrature mirror filters, complementary filters and the paraunitary filter banks, and relations (10.7.11) to (10.7.20) have been introduced and discussed in Section 10.6 from the perfect reconstruction property of the filter bank. However, the orthonormality of $P(\omega)$ and

$Q(\omega)$ and the cross-filter orthonormality are obtained here from the orthonormality of the scaling function and wavelet bases.

Example: Orthonormality of the Haar's Bases

Let us consider the orthonormality condition for the Haar's bases, as an example. We know that the Haar's bases are orthonormal at every scale. The Fourier transforms of the Haar scaling functions and wavelets are

$$\Phi(\omega) = e^{-j\omega/2}\frac{\sin(\omega/2)}{\omega/2}$$

$$\Psi(\omega) = e^{-j\omega/2}\frac{\sin^2(\omega/2)}{\omega/4}$$

We have for the scaling function $\Phi(\omega)|_{\omega=0} = 1$ and for the wavelet $\Psi(\omega)|_{\omega=0} = 0$. It can be verified that the orthonormality condition expressed as:

$$\sum_n \left|\Phi(\omega + 2n\pi)\right|^2 = 1$$

$$\sum_n \left|\Psi(\omega + 2n\pi)\right|^2 = 1$$

are satisfied.

The two-scale relations of the Haar scaling functions and the Haar wavelets obtained in Section 10.5.2. On substituting the interscale coefficients of the Haar's bases: $p(n) = 1/\sqrt{2}$ for $n = 0, 1$ and $p(n) = 0$ otherwise, $q(0) = 1/\sqrt{2}$, $q(1) = -1/\sqrt{2}$, and $q(n) = 0$ otherwise into the Fourier transform of $p(n)$ and $q(n)$, (10.6.1), we obtain the quadrature mirror filters of the Haar's bases as:

$$P(\omega) = 2^{-1/2}\cos\frac{\omega}{2}\exp(-j\omega/2)$$

$$Q(\omega) = j2^{-1/2}\sin\frac{\omega}{2}\exp(-j\omega/2)$$

It is easy to verify that the Haar's quadrature mirror filters satisfy all the orthonormality conditions because:

$$\left|P(\omega)\right|^2 + \left|P(\omega+\pi)\right|^2 = \frac{1}{2}\left[\cos^2\left(\frac{\omega}{2}\right) + \cos^2\left(\frac{\omega+\pi}{2}\right)\right] = 1$$

$$\left|Q(\omega)\right|^2 + \left|Q(\omega+\pi)\right|^2 = \frac{1}{2}\left[\sin^2\left(\frac{\omega}{2}\right) + \sin^2\left(\frac{\omega+\pi}{2}\right)\right] = 1$$

and

$$P(\omega)Q^*(\omega) + P(\omega+\pi)Q^*(\omega+\pi) = -j\frac{1}{2}\cos\frac{\omega}{2}\sin\frac{\omega}{2} - j\frac{1}{2}\cos\frac{\omega+\pi}{2}\sin\frac{\omega+\pi}{2} = 0$$

We have also that:

$$\left|P(\omega)\right|^2 + \left|Q(\omega)\right|^2 = 1$$

$$\left|P(-\omega)\right|^2 + \left|Q(-\omega)\right|^2 = 1$$

and that the matrix:

$$\begin{vmatrix} p(\omega) & Q(\omega) \\ P(\omega+\pi) & Q(\omega+\pi) \end{vmatrix}$$

are paraunitary.

10.7.3 Orthonormal Filters in Time Domain

Double-Shift Orthonormality

When the basic scaling function and the wavelet satisfy the orthonormality condition, their discrete translates with integer translation steps form two orthonormal bases, and those two bases are mutually orthogonal:

$$\langle \phi_{0,k}, \phi_{0,n} \rangle = \delta_{k,n}$$

$$\langle \psi_{0,k}, \psi_{0,n} \rangle = \delta_{k,n}$$

$$\langle \psi_{0,k}, \phi_{0,n} \rangle = 0$$

In Section 10.5.4 we obtained (10.5.20) and (10.5.21) from the two-scale relations:

$$\langle \phi_{1,k}, \phi_{0,n} \rangle = 2^{-1/2} p(n-2k)$$

$$\langle \psi_{1,k}, \phi_{0,n} \rangle = 2^{-1/2} q(n-2k)$$

Hence, at the resolution level $i = 1$ the inner products of two translated scaling functions and wavelets may be written in terms of $p(n)$ and $q(n)$ as:

$$\begin{aligned} \langle \phi_{1,k}, \phi_{1,k'} \rangle &= \sum_{n,m} p(n-2k) p(m-2k') \langle \phi_{0,n}, \phi_{0,m} \rangle \\ &= \sum_{n,m} p(n-2k) p(n-2k') = \delta_{k,k'} \\ \langle \psi_{1,k}, \psi_{1,k'} \rangle &= \sum_{n,m} q(n-2k) q(m-2k') \langle \phi_{0,n}, \phi_{0,m} \rangle \\ &= \sum_{n} q(n-2k) q(n-2k') = \delta_{k,k'} \\ \langle \psi_{1,k}, \phi_{1,k'} \rangle &= \sum_{n,m} q(n-2k) p(m-2k') \langle \phi_{0,n}, \phi_{0,m} \rangle \\ &= \sum_{n} q(n-2k) p(n-2k') = 0 \end{aligned}$$

The double-shift orthonormality and cross-filter orthonormality also have been obtained from the paraunitary matrix properties of the filter bank in Section 10.6.4.

Equal Contribution Constraint

The low-pass filter $p(n)$ in time domain should satisfy the equal contribution constraint, stipulating that all the node in one resolution level contribute the same total amount to the next level and that the sum of all the weights for a given node n is independent of n. Hence, the weighting function should satisfy:

$$\sum_n p(2n) = \sum_n p(2n+1)$$

In an example of multiresolution signal analysis shown in Figure 10.8 the odd number nodes and the even number nodes in the data sequence $c_{i-1}(n)$ have two different connections with the low-pass filter $p(n)$ because of the down-sampling by 2 of $c_i(k)$. The even nodes in $c_0(n)$ are connected to $c_1(n)$ with the weighting factors $p(-2)$, $p(0)$, and $p(2)$, the odd nodes are connected to $c_1(n)$ with the weighting factors $p(-1)$ and $p(1)$. When the preceding relation is satisfied, the sums of the weights are equal for odd and even nodes in $c_1(n)$.

From the orthonormality condition (10.7.2):

$$\sum_k \left|\Phi(\omega + 2k\pi)\right|^2 = 1$$

we find that if the scaling function is normalized such that its mean value is unity:

$$\int \phi(t)dt = 1 \qquad \text{and} \qquad \Phi(0) = 1$$

then at $\omega = 0$, we have $\Phi(2k\pi) = 0$ for $k = 1, 2, \ldots$. Therefore, we have $\sum_k \left|\Phi\left[2(2k+1)\pi\right]\right|^2 = 0$. Using the two-scale relation:

$$\Phi(2\omega) = P(\omega)\Phi(\omega)$$

at $\omega = (2k + 1)\pi$, we have:

$$\sum_k \left|P\left[(2k+1)\pi\right]\right|^2 \left|\Phi\left[(2k+1)\pi\right]\right|^2 = 0$$

Because $\Phi[(2k + 1)\pi] \neq 0$, we must have $P[(2n+1)\pi] = 0$ and equivalently for the low-pass filter in the time domain we have, according to the Fourier transform (10.6.1):

$$P(\pi) = \sum_k (-1)^k p(k) = 0$$

but

$$P(0) = \sum_k p(k) = 1$$

Addition and subtraction of the two preceding equations yield, respectively:

$$\sum_k p(2k) = 1 \qquad \text{and} \qquad \sum_k p(2k+1) = 1$$

This is the equal constraint condition for the multiresolution signal analysis filters.

10.7.4 Wavelet and Subband Filters

The discrete orthonormal wavelet transform low-pass and high-pass filters are simply the two-band paraunitary perfect reconstruction quadrature mirror filters developed in the subband coding theory. The novelties of the wavelet transform are

1. *Continuous function bases*: The wavelet transform is defined on the scaling function and wavelet bases, which are continuous function bases of continuous variables, so that the wavelet transform can serve as a mathematical transform tool to analog signal functions. The subband coding technique is based on the discrete filters and applied to discrete data.
2. *Zero-mean, high-pass filter*: Applying the wavelet admissible condition $\Psi(\omega)|_{\omega=0} = 0$ to the Fourier domain two-scale relation (10.7.10), it follows that:

$$Q(\omega)\Big|_{\omega=0} = 0 \tag{10.7.21}$$

   The high-pass filter $q(n)$ in the time domain must have a zero mean.
3. *Regularity of the scaling function and wavelet*: On substituting the zero mean property of the high-pass filter, $Q(\omega)|_{\omega=0} = 0$, into the quadrature mirror filter property (10.7.17), we have $P(\omega)|_{\omega=\pi} = 0$. The low-pass filter $P(\omega)$ must contain at least one term of $(1 + e^{-j\omega})$ or $(1 + z^{-1})$, which equals to zero at $\omega = \pi$ or $z = -1$. The regularity of the low-pass filter $P(\omega)$ ensures the iterations of the low-pass filter to converge, as will be discussed in Section 10.7.5.

10.7.5 Regularity

The regularity of the wavelets is an important property of the wavelet transform that results in the localization of the wavelet transform in both time and frequency domains. In Section 10.2.2 we discussed the regularity condition for the continuous wavelet transform. For the wavelet transform coefficients to decay as fast as $s^{n+1/2}$ with an increase of $(1/s)$, where s is the scale factor, the wavelet $\psi(t)$ must have the first $n+1$ moments of the order $0, 1, \ldots n$ equal to zero, and equivalently, the Fourier transform $\Psi(\omega)$ of the wavelets must have the first n derivatives of the order up to n equal to zero about zero frequency $\omega = 0$.

In this section we shall discuss the regularity condition on the orthonormal scaling functions and wavelets, and on the quadrature mirror filters $P(\omega)$ and $Q(\omega)$ in the multiresolution analysis framework. We shall discuss the regularity condition in a slightly different way from that in Section 10.2.2. The regularity conditions are applied for ensuring convergence of the reconstruction from the orthonormal wavelet decomposition. However, the regularity conditions obtained in both approaches are equivalent.

Smoothness Measure

The regularity is a measure of smoothness for scaling functions and wavelets. The regularity of the scaling function is determined by the decay of its Fourier transform, $\Phi(\omega)$, and is defined as the maximum value of r such that:

$$\left|\Phi(\omega)\right| \le \frac{c}{\left(1+|\omega|\right)^r}$$

for $\omega \in R$. Hence, the $|\Phi(\omega)|$ has exponential decay as ω^{-M}, where $M \le r$. This in turn implies that $\phi(t)$ is $(M-1)$-times continuously differentiable, and both $\phi(t)$ and $\psi(t)$ are smooth functions.

Convergence of Wavelet Reconstruction

The reconstruction from the wavelet series decomposition is described by (10.5.33):

$$c_0 = \sum_{i=1}^{M} (L_0)^{i-1} H_0 d_i + (L_0)^M c_M$$

where the synthesis filtering operators applied to a sequence $\alpha(k)$, L_0 and H_0, are defined as:

$$(L_0\alpha)(n) = \frac{1}{\sqrt{2}} \sum_k p(n-2k)\alpha(k)$$

$$(H_0\alpha)(n) = \frac{1}{\sqrt{2}} \sum_k q(n-2k)\alpha(k)$$

Note that in the reconstruction it is the low-pass filter L_0 that is iterated.

The problem of the convergence of the wavelet reconstruction may be formulated for a particular example where the original function to be decomposed is the scaling function itself. In this case the wavelet series coefficients must be $c_M = \delta_{0,n}$ and $d_0 = \cdots d_M = 0$, where the sequence $\delta_{0,n}$ has only one nonzero entry for $n = 0$. The reconstruction formula becomes:

$$c_0(n) = (L_0)^M c_M$$

Therefore, it is important to study the behavior of the iterated filtering operator $(L_0)^i c_M$ for large i,. Ideally we want $(L_0)^i c_M$ to converge to a reasonably regular function when i tends to infinity. However, when i approaches to infinity $(L_0)^i c_M$ can converge to a continuous function, or to a function with finite discontinuities, even to a fractal function. The sequence $(L_0)^i c_M$ may also not converge at all. The condition for the reconstruction to converge is the regularity of the scaling function.

With a graphic representation shown in Figure 10.15, we represent the sequence $c_M(n)$ at the resolution level $i = M$ by a rectangular function $\eta_0(t)$:

$$\eta_0(t) = \begin{cases} 1 & -1/2 \le t \le 1/2 \\ 0 & \text{otherwise} \end{cases}$$

Assume that the sequence $c_M(n)$ has the time clock rate of 1. At the next finer resolution level $i = M - 1$ the sequence $c_{M-1}(n)$is

$$C_{M-1}(n) = L_0 c_M(n) = \sum_k p(n-2k)\delta_{0,k} = p(n)$$

In fact, to compute $c_{M-1}(n)$we first increase the time clock rate such that $c_M(n)$ is with a time interval of length *1/2*. The $c_M(n)$ is then convolved with the discrete filter $p(n)$ that has also the time interval of *1/2*. The amplitude of $c_{M-1}(n)$is equal exactly to $p(n)$, as shown in Figure 10.14. We represent $c_{M-1}(n)$ by a piecewise constant function, $\eta_1(t)$, that is constant over the interval of *1/2*. It is easy to see that the $\eta_1(t)$ may be expressed as:

$$\eta_1(t) = \sum_n p(n)\eta_0(2t-n)$$

Continuing for computing $c_{M-2}(n) = (L_0)^2 c_M(n)$, we put a zero between each node of the sequence $c_{M-1}(n)$ and increase the time clock rate. Thus, at this resolution level both the data sequences $c(n)$ and the filter $p(n)$

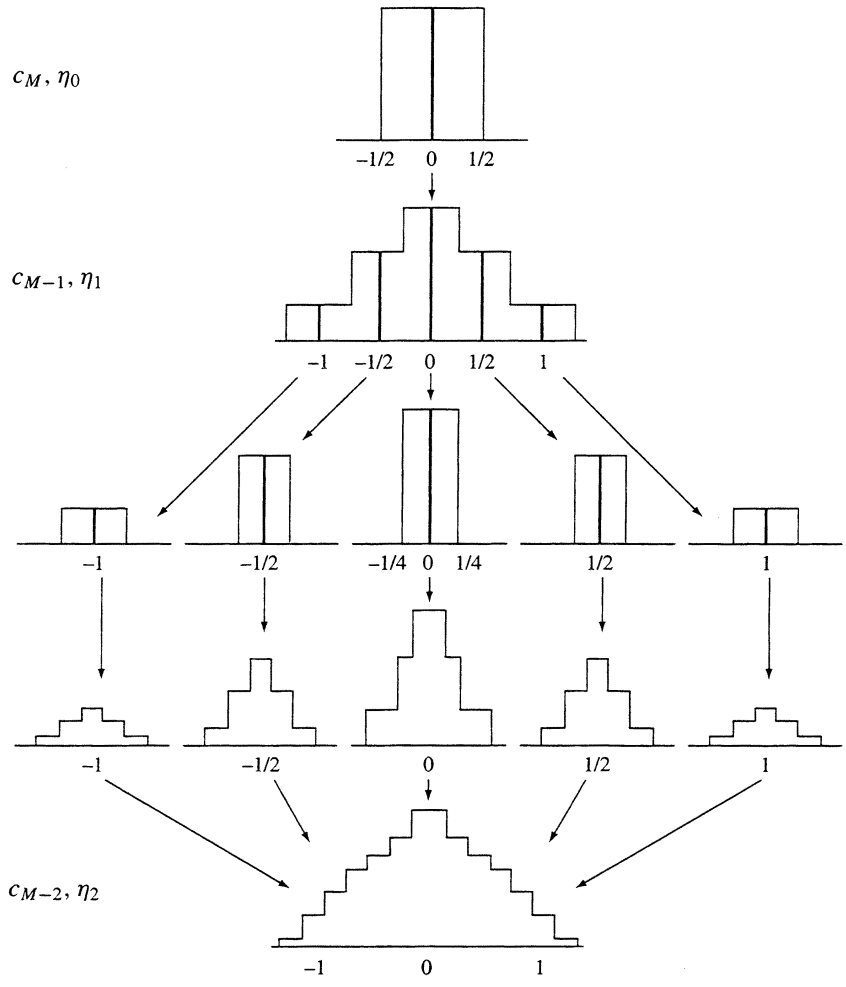

FIGURE 10.15 Reconstruction from $c_M(n) = 1$, for $n = 0$ and $c_M(n) = 0$ for $n = 0$ and the corresponding rectangle function $\eta_0(t)$. The time clock rate is equal to 1 for $c_M(n)$, 1/2 for $c_{M-1}(n)$ and 1/4 for $c_{M-2}(n)$. (From Daubechies, I., *Commun. on Pure and Appl. Math*, XLI, 909, 1988. With permission.)

have the time interval of *1/4*. Their convolution yields the sequence $c_{M-2}(n)$. We represent $c_{M-2}(n)$ by the piecewise constant function $\eta_2(t)$ of a step of length *1/4*, as shown in Figure 10.15. It is easy to verify that:

$$\eta_2(t) = \sum_n p(n)\eta_1(2t-n)$$

Similarly, $\eta_i(t) = (L_0)^i c_M(n)$ is a piecewise constant function with a step of length 2^{-i} and

$$\eta_i(t) = \sum_n p(n)\eta_{i-1}(2t-n)$$

When i approaches to infinity $(L_0)^i c_M$ can converge to η_∞ and

$$\lim_{i\to\infty} \eta_\infty(t) = \phi(t)$$

The condition that the scaling function, $\phi(t)$, is regular shall be discussed next.

Construction of Scaling Function

The above recursion process with the low-pass filter operator L_0 associated to the low-pass filter $p(n)$, is a reconstruction of the scaling function $\phi(t)$. Starting from the rectangular function η_0, the recursion gives the values of $\phi(t)$ of half-integers. Then, the recursion gives $\phi(t)$ at the quarter-integers, and ultimately, at all dyadic point $t = k/2^i$. Finer and finer detail of $\phi(t)$ is achieved by the recursion when the number of iterations i approaches to infinity. Therefore, the basic scaling function $\phi(t)$ is constructed from the discrete low-pass filter $p(n)$. This process is useful to compute the continuous scaling and wavelet functions, $\phi(t)$ and $\psi(t)$ from the discrete low-pass and high-pass filters, $p(n)$ and $q(n)$.

Regularity of Quadrature Mirror Filter

The regularity of the scaling function should not only ensure that the reconstructed scaling function $\eta_\infty(t)$ converges, but also ensure that (1) $\eta_\infty(t)$ is sufficiently regular or the Fourier transform of $\eta_\infty(t)$ has sufficient decay, and (2) $\eta_i(t)$ converges to $\eta_\infty(t)$ point-wise when i approaches to infinity. Daubechies[13] has proven that the above two conditions can be satisfied when the Fourier transform of the low-pass filter $p(n)$ satisfies:

$$P(\omega) = \left(\frac{1+e^{-j\omega}}{2}\right)^M F\left(e^{-j\omega}\right) \tag{10.7.22}$$

or, written in terms of the z-transform, as:

$$P(z^{-1}) = \left(\frac{1+z^{-1}}{2}\right)^M F(z^{-1})$$

where $M > 1$ and $F(z^{-1})$ is a polynomial in z^{-1}, or in $e^{-j\omega}$ with real coefficients and satisfies some conditions so that the infinite product:

$$\left|\prod_{k=0}^{\infty} F\left(z^{k/2}\right)\right| \le 2^{k(N-M-1)} \tag{10.7.23}$$

converges and is bounded. Because the low-pass filter $p(n)$ is a finite impulse response (FIR) filter, $p(n) \ldots 0$ only for $n = 0, 1, \ldots, N-1$, then its Fourier transform, $P(\omega)$, is a polynomial in $e^{-j\omega}$ or in z^{-1}, of degree $N-1$. Hence, $F(z^{-1})$ is a polynomial in z^{-1} of degree $N-1-M$ where N is the length of $p(n)$.

According to (10.7.22), the quadrature mirror filter $P(\omega)$ must have M zeros at $\omega = \pi$ or $z = -1$. We know that $P(\omega)$ must have at least one zero at $\omega = \pi$ because, according to the wavelet admissible condition for the high-pass filter (10.7.21):

$$Q(\omega)\big|_{\omega=0} = 0$$

and the quadrature mirror filter condition (10.7.17):

$$\left|P(\omega+\pi)\right|^2 = \left|Q(\omega)\right|^2$$

Hence,

$$P(\omega)\big|_{\omega=\pi} = 0$$

$P(\omega)$ must contain at least one term of $(1 + e^{-j\omega})$, the power M in (10.7.22) must be at least equal to one. However, the regularity condition (10.7.22) requires $P(\omega)$ to have more zeros with $M > 1$ to ensure convergence of the wavelet reconstruction.

Regularity of Scaling Function

Regularity condition (10.7.22) implies that:

$$\left|P\left(\omega\right)\right| = \left|\cos\frac{\omega}{2}\right|^{M} \left|F\left(e^{-j\omega}\right)\right|$$

On substituting the preceding relation into the infinite product form (10.7.9) of the Fourier transform $\Phi(\omega)$ of the scaling function, we obtain the regularity condition on $\Phi(\omega)$ as:

$$\left|\Phi\left(\omega\right)\right| = \prod_{i=1}^{\infty}\left|\cos\frac{\omega}{2^{i+1}}\right|^{M} \cdot \left|\prod_{i=1}^{\infty} F\left(e^{-j\omega/2^{i}}\right)\right| \tag{10.7.24}$$

but,

$$\cos\frac{\omega}{2} = \frac{\sin\omega}{2\sin\left(\omega/2\right)}$$

The first infinite product term in (10.7.24) is therefore:

$$\lim_{M\to\infty}\left|\prod_{i=1}^{M}\left|\frac{\sin\left(\omega/2^{i}\right)}{2\sin\left(\omega/2^{i+1}\right)}\right|^{M}\right| = \lim_{M\to\infty}\left|\frac{\sin\left(\omega/2^{i}\right)}{2^{M}\sin\left(\omega/2^{M+1}\right)}\right|^{M} = \left[\frac{\sin\left(\omega/2\right)}{\left(\omega/2\right)}\right]^{M}$$

and

$$\left|\Phi\left(\omega\right)\right| = \left|\frac{\sin\left(\omega/2\right)}{\omega/2}\right|^{M}\left|\prod_{i=1}^{\infty} F\left(e^{-j\omega/2^{i}}\right)\right| \tag{10.7.25}$$

The first term in the right-hand side of (10.7.25) contributes to the exponential decay of $\Phi(\omega)$ as ω^{-M}. The second term is bounded according to the condition (10.7.23).

The number M of zeros of the quadrature mirror filter $P(\omega)$ at $\omega = \pi$, or at $z = -1$ is a measure of flatness of $P(\omega)$ at $\omega = \pi$. From the regularity conditions (10.7.22) and (10.7.25), we see that the exponential decay of the scaling function $\Phi(\omega)$ and the flatness of the quadrature mirror filter $P(\omega)$ are equivalent. When the scaling function $\Phi(\omega)$ has the exponential decay as ω^{-M}, the quadrature mirror filter $P(\omega)$ has number M of zero at $\omega = \pi$. M is a measure of the regularity of the scaling function.

Smoothness in Time Domain

The regularity also implies the smoothness of the low-pass filter $p(n)$ in the time domain. We rewrite (10.7.22) as:

$$P\left(\omega\right) = \exp\left(-jM\omega/2\right)\left(\cos\frac{\omega}{2}\right)^{M} F\left(\omega\right)$$

Its *r*th derivative is

$$\frac{d^r P(\omega)}{d\omega^r} = \left(\cos\frac{\omega}{2}\right)^{M-r} g_r(\omega) \tag{10.7.26}$$

where $[\cos(\omega/2)]^{M-r}$ is the minimum power of $\cos(\omega/2)$ that the *r*th derivative contains and $g_r(\omega)$ is the residual terms of the derivative. The term $[\cos(\omega/2)]^{M-r}$ makes the *r*th derivative of $P(\omega)$ equal to zero at $\omega = \pi$ for $r = 0, 1, \ldots, M-1$. On the other hand, because $P(\omega)$ is the Fourier transform of $p(n)$, we have

$$\frac{d^r P(\omega)}{d\omega^r} = \sum_n (-jn)^r p(n) \exp(-jn\omega)$$

Then,

$$\left.\frac{d^r P(\omega)}{d\omega^r}\right|_{\omega=\pi} = (-j)^r \sum_n n^r (-1)^n p(n) = 0 \tag{10.7.27}$$

for $r = 0, 1, \ldots, M-1$. Hence, the low-pass filter $p(n)$ is a smooth filter. Substituting the alternating flip filter expression:

$$Q(z) = (-z)^{-(N-1)} P(-z^{-1})$$

where N is an even number, into the regularity condition (10.7.22) we have:

$$Q(z) = \left(\frac{1-z}{2}\right)^M z^{-N} F(-z^{-1})$$

or in terms of the Fourier transform frequency ω as:

$$Q(\omega) = \left(\sin\frac{\omega}{2}\right)^M g_r(\omega)$$

where $g_r(\omega)$ is the residual terms. The $[\sin(\omega/2)]^M$ term ensures that $Q(\omega)$ has the vanishing derivatives at $\omega = 0$

$$\left.\frac{d^r Q(\omega)}{d\omega^r}\right|_{\omega=0} = 0$$

Because $Q(\omega)$ is the Fourier transform of $q(n)$, the *r*th derivative of $Q(\omega)$ is equal to zero at $\omega = 0$ for $r = 0, 1, \ldots, M-1$ is equivalent to:

$$\sum_n r^n q(n) = 0 \tag{10.7.28}$$

The high-pass filter $q(n)$ has a vanishing moment of order, *r*.

Both the low-pass filter $p(n)$ and high-pass filter $q(n)$ are finite impulse response (FIR) filters: $p(n) \neq 0$ only for $n = 0, 1, \ldots, N-1$ and N is the length of $p(n)$. The compactness of $p(n)$ and $q(n)$, described by $(N-1)$ is in contrast with the regularity of $P(\omega)$ and $Q(\omega)$ and of the scaling and wavelet functions, described by M because, according the regularity condition (10.7.22), $M < N - 1$. There is a tradeoff between the compactness of the filters and the regularity of the scaling function and wavelet. We will discuss this issue in Section 10.8.3.

10.8 Some Orthonormal Wavelet Bases

In this section we summarize some orthonormal wavelet bases. In general, the orthonormal wavelet bases generated in the multiresolution analysis framework are associated to the orthonormal scaling function bases. Different orthonormal scaling function and wavelet bases are designed to satisfy the orthonormality condition and the regularity condition in slightly different ways.

More filter banks and wavelet filter coefficients may be founded in MATLAB Wavelet Toolbox and WaveLab (http://playfair.stanford.edu/~wavelab), and in many other computer software programs.

10.8.1 B-Spline Bases

One of the basic methods for constructing the orthonormal wavelet families involves the B-spline functions, which are familiar in the approximation theory for interpolating a given sequence of data points. In this subsection we give a brief description of the multiresolution analysis with the B-spline scaling function and wavelet bases, and the related low-pass and high-pass filters.

B-Spline

The B-spline of degree n is generated by repeated $(n+1)$-fold convolutions[14] of the rectangular function :

$$\beta^0(t) = \begin{cases} 1 & \text{for } 0 \le t < 1 \\ 0 & \text{otherwise} \end{cases} \tag{10.8.1}$$

where n is an arbitrary positive integer. The nth degree B-spline is then:

$$\begin{aligned} \beta^n(t) &= \left(\beta^{n-1} * \beta^0\right)(t) \\ &= \int_{-\infty}^{\infty} \beta^{n-1}(t-x)\beta^0(x)dx = \int_0^1 \beta^{n-1}(t-x)dx \end{aligned} \tag{10.8.2}$$

Equation (10.8.2) is recursive. Because of the repeated convolutions, the nth degree B-spline has a support of size $(0,n+1)$ in time. This support increases with the degree, n. The B-spline is a bell-shaped and symmetric function with respect to the center of its support $t = 1/2$. There is also the central B-spline which is defined such that it is symmetric with respect to the origin.

The B-spline of zero degree, $\beta^0(t)$, has been used as the Haar scaling function. It is not even differentiable. The B-spline of first degree is the linear spline, which is a triangle function, called the hat function. Its first derivative is not continuous. The B-spline of second degree is the quadratic spline. It has continuous first derivatives. The B-spline of degree 3 is the cubic spline. It has the first and second continuous derivatives. The higher order B-splines with the degree $n > 1$, are smooth, bell–shaped functions and have continuous derivatives of orders up to $n-1$.

According to the definition, the Fourier transform of the B-spline of degree n is

$$B^n(\omega) = \left(\frac{1-e^{-j\omega}}{j\omega}\right)^{n+1} = e^{-j(n+1)\omega/2}\left(\frac{\sin(\omega/2)}{\omega/2}\right)^{n+1} \tag{10.8.3}$$

Its modulus, $|B^n(\omega)|$ has the exponential decay as $1/\omega^{n+1}$. When n increases, the B-spline becomes more regular but its support becomes less compact. There is then the typical trade-off between the regularity and the compactness of the B-splines.

Spline Interpolation

The polynomial splines are linear combinations of the translated B-splines. The polynomial splines $f^n(t)$ can be used to interpolate a given sequence of data point $\{s(k)\}$:

$$f^n(t) = \sum_k c(k)\beta^n(t-k)$$

When the polynomial coefficients equal to the signal data $c(k) = s(k)$, $f^n(t)$ is a cardinal spline interpolator, that has piecewise polynomial segments of n-degree. Hence, the B-spline of degree n is the interpolation function. When $n = 0$, the sequence of points $\{s(k)\}$ with equal intervals is interpolated by $\beta^0(t)$ which is a staircase function, as that shown in the case of the Haar scaling function approximation. When $n = 1$, the sequence of points are connected by the straight line segment in each interval $[k, k+1]$. When $n > 2$, the data points is interpolated by a function that is, in each interval, a polynomial in degree, n.

Spline Scaling Function

The B-spline itself can be used as the scaling function. The scaling function can be dilated and translated to form the spline scaling function bases at different resolution levels. However, the B-spline of degree n has a support of $(0, n+1)$. Their integer translates do not necessarily form an orthonormal basis within a resolution level.

When the B-spline of degree $m–1$ is used as the scaling function $\Phi(\omega) = B^{m-1}(\omega)$, the corresponding low-pass filter $P(\omega)$ can be derived in the following. From the two-scale relation (10.7.6)

$$\Phi(2\omega) = P(\omega)\Phi(\omega)$$

and (10.8.3) we have

$$\left(\frac{1-e^{-2j\omega}}{2j\omega}\right)^m = P(\omega)\left(\frac{1-e^{-j\omega}}{j\omega}\right)^m \quad \text{and} \quad P(\omega) = \left(\frac{1+e^{-j\omega}}{2}\right)^m = \left(\frac{1+z^{-1}}{2}\right)^m \tag{10.8.4}$$

The coefficients of the corresponding low-pass filter, $p(k)$, in the time domain can be obtained from (10.8.4) by the inverse z-transform.

Example

When the cubic spline is the scaling function in the multiresolution analysis, the corresponding low-pass filter:

$$P(z) = \left[\left(1+z^{-1}\right)/2\right]^4 = \left(1+4z^{-1}+6z^{-2}+4z^{-3}+z^{-4}\right)/16$$

Hence, the low-pass filter in time is $p(k) = [1, 4, 6, 4, 1]$.

10.8.2 Lemarie and Battle Wavelet Bases

The Lemarie and Battle wavelet bases are a family of orthonormal scaling functions and wavelets that are associated to the B-spline, with an additional condition that the Lemarie and Battle polynomial scaling functions and wavelets are orthonormal within the given resolution level. The orthonormality is obtained by imposing the orthonormality constraints on the B-spline scaling functions and wavelets.

Nonorthonormal Spline Bases

When the spline of degree is *m–1*, $\beta^{m-1}(\omega)$ is used as the scaling function. The orthonormality condition is not satisfied, because from (10.8.3) we have:

$$\sum_k \left|B^{m-1}(\omega+2\pi k)\right|^2 = \sum_k \left(\frac{\sin[(\omega/2)+\pi k]}{((\omega/2)+\pi k)}\right)^{2m} = \sin^{2m}(\omega/2)\sum\nolimits_{2m}\left(\frac{\omega}{2}\right) \tag{10.8.5}$$

where with $x = \omega/2$ we define:

$$\sum\nolimits_{2m}(x) \equiv \sum_k \left(\frac{1}{x+\pi k}\right)^{2m}$$

From the complex analysis we have:

$$\cot x = \lim_{n\to\infty}\sum_{k=-n}^{n}\frac{1}{x+nk}$$

We can differentiate this identity *2m–1* times to obtain:

$$\sum\nolimits_{2m}(x) = \sum_k \frac{1}{(x+\pi k)^{2m}} = -\frac{1}{(2m-1)!}\frac{d^{2m-1}}{dx^{2m-1}}\cot x \tag{10.8.6}$$

Substituting (10.8.6) into (10.8.5), we obtain:

$$\sum_k \left|\beta^{m-1}(\omega+2\pi k)\right|^2 = \frac{-\sin^{2m}(x)}{(2m-1)!}\frac{d^{2m-1}}{dx^{2m-1}}\cot x \tag{10.8.7}$$

where $x = \omega/2$. Hence, for the zero-degree spline $m = 1$, we have:

$$\sum_k \left|\beta^0(\omega+2\pi k)\right|^2 = 1$$

The Haar scaling function is orthonormal. However, for the spline with $m = 2$, we have:

$$\sum_k \left|\beta^1(\omega+2\pi k)\right|^2 = \frac{1}{3}+\frac{2}{3}\cos^2\left(\frac{\omega}{2}\right)$$

which is between 1/3 and 1. The linear spline scaling function basis is not orthonormal. In general, the higher degree spline scaling function bases are not orthogonal.

Lemarie–Battle Basis

The Lemarie and Battle's multiresolution basis[15] is built from the B-spline. Lemarie has found a scaling function that is associated to the *(m–1)*th degree splines and its integer translates form an orthonormal basis within the same resolution level. The Lemarie–Battle scaling function is given by its Fourier transform as:

$$\Phi(\omega)=\frac{1}{\omega^m}\left(\sum_k\left(\frac{1}{(\omega+2\pi k)^{2m}}\right)\right)^{-1/2}=\frac{1}{\omega^m\sqrt{\sum_{2m}(\omega)}} \tag{10.8.8}$$

It is easy to verify that the orthonormality condition:

$$\sum_k\left|\Phi(\omega+2\pi k)\right|^2=1$$

is satisfied. The Lemarie–Battle scaling function $\Phi(\omega)$ defined in (10.8.8) can be computed using (10.8.6).

Quadrature Mirror Filters

The low-pass quadrature mirror filter $P(\omega)$ can be obtained from the two-scale relation in the Fourier domain, described in (10.7.6)

$$\Phi(2\omega)=P(\omega)\Phi(\omega)$$

According to (10.8.8), we obtain:

$$P(\omega)=\sqrt{\frac{\sum_{2m}(\omega)}{2^{2m}\sum_{2m}(2\omega)}} \tag{10.8.9}$$

The Fourier transform of the corresponding orthonormal wavelet can be derived also from the two-scale relation:

$$\Psi(\omega)=Q\left(\frac{\omega}{2}\right)\Phi\left(\frac{\omega}{2}\right)$$

where the conjugate quadrature mirror filter $Q(\omega)$ satisfying the orthonormal condition is obtained from the alternating flip property as described in (10.6.16)

$$Q(z)=(-z)^{-(N-1)}P(-z^{-1})$$

$$Q(\omega)=e^{-j(N-1)(\omega+\pi)}P^*(\omega+\pi)$$

where N is an even number. Hence,

$$\Psi(\omega)=e^{-j(N-1)(\omega+\pi)/2}P^*\left(\frac{\omega+\pi}{2}\right)\Phi\left(\frac{\omega}{2}\right) \tag{10.8.10}$$

Example

The Lemarie and Battle scaling function basis from the cubic spline with $m–1 = 3$ can be obtained from (10.8.8) and (10.8.6) as[25]

TABLE 10.1 Low-Pass Filter p(k) of the Lemarie–Battle Wavelet Basis Associated with the Cubic B-Spline

k	*p(k)*	*q(k)*	*k*	*p(k)*	*q(k)*
0	0.542	–0.189	6	0.012	0.005
1	0.307	0.099	7	–0.013	0.054
2	–0.035	0.312	8	0.006	0.027
3	–0.078	0.099	9	0.006	0.018
4	0.023	–0.189	10	–0.003	0.017
5	–0.030	–0.161	11	–0.002	0.000

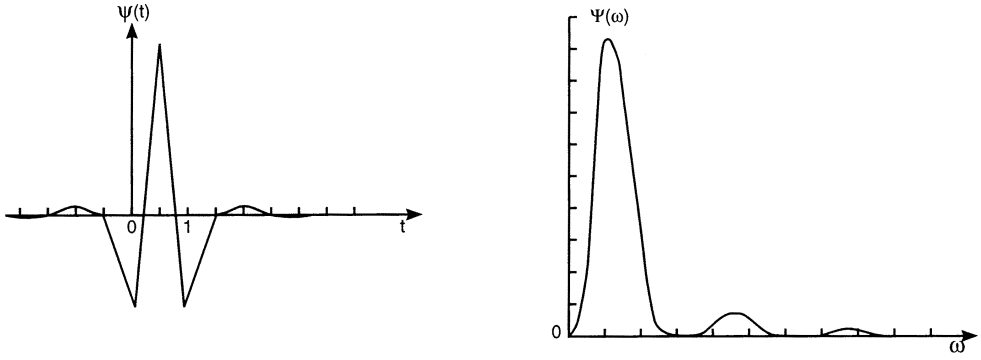

FIGURE 10.16 Lemarie–Battle wavelet and its Fourier transform associated with the second order B-spline. (From Sheng, Y. et al. *Opt. Eng.*, 31, 1840, 1992. With permission.)

$$\Phi(\omega)=\omega^{-4}\left[\sum(\omega+2\pi k)^{-8}\right]^{-1/2}=8\omega^{-4}\left(\frac{1}{315}\frac{d^7}{d\omega^7}\cot\frac{\omega}{2}\right)^{-1/2}$$

$$=\frac{16\sqrt{315\sin^4(\omega/2)}}{\omega^{-4}\sqrt{315\cos^6(\omega/2)+515\cos^4(\omega/2)\sin^2(\omega/2)+231\cos^2(\omega/2)\sin^4(\omega/2)+17\sin^6(\omega/2)}}$$

From the expression for $\sum_{2m}(\omega)$, the Fourier transforms Φ(ω) and Ψ(ω) of the scaling function and wavelet and the quadrature mirror filters, $P(\omega)$ and $Q(\omega)$, can be calculated. Table 10.1 gives the first 12 coefficients of the discrete low-pass filter *p(n)* that are the impulse response of $P(\omega)$ useful for the wavelet series decomposition. The coefficients of the high-pass filter *q(n)* obtained from the low-pass filter *p(n)* with (10.8.10) are also given.

Figure 10.16 shows the Lemarie–Battle wavelet ψ*(t)* and its Fourier transform Ψ(ω), which is given by (10.8.10). The wavelet is associated to the linear spline of degree $m = 1$. Hence, the wavelet consists of the straight line segments between the discrete nodes. When m increases, the Lemarie–Battle scaling function and wavelet associated to high order B-splines becomes smoother. The Lemarie–Battle wavelet is symmetrical to $t = 1/2$ and has no compact support. The wavelet ψ*(t)* decays slowly with time, t.

10.8.3 Daubechies Basis

The Daubechies wavelet basis[13] is a family of orthonormal, compactly supported scaling and wavelet functions that have the maximum regularity and the maximum flatness at ω = 0 and ω = π for a given length of the support of the quadrature mirror filters. The Daubechies basis is not given in closed

form. The decomposition and the reconstruction are implemented by iterating the discrete low-pass and high-pass filters $p(n)$ and $q(n)$.

Maximum Flatness Filter

The Daubechies scaling and wavelet functions are built based on the consideration for the regularity condition, (10.7.22), and the orthonormality, (10.7.11), on the quadrature mirror filter $P(\omega)$ in the Fourier domain, expressed as:

$$P(\omega) = \left(\frac{1+e^{-j\omega}}{2}\right)^M F\left(e^{-j\omega}\right) \tag{10.7.22}$$

and

$$\left|P(\omega)\right|^2 + \left|P(\omega+\pi)\right|^2 = 1 \tag{10.7.11}$$

The square modulus of the low-pass filter $|P(\omega)|^2$ is half-band. The length N of the discrete low-pass filters $p(n)$ is to be chosen first. The discrete high-pass filters, $q(n)$, has the same length of N. The low-pass filter $p(n)$ of a compact support of length N is the finite impulse response (FIR) filter or called the N-tap filter, $p \neq 0$ only for $n = 0, 1, \ldots, N-1$. Its Fourier transform, $P(\omega)$, is a polynomial in $e^{-j\omega}$ of degree $N-1$, according to the definition (10.6.1):

$$P(\omega) = \sum_{k=0}^{N-1} p(k)\exp(-jk\omega)$$

In the regularity condition (10.7.22), $M > 1$ is the regularity, and $F(e^{-j\omega})$ is a polynomial in $e^{-j\omega}$ with real coefficients. Since $P(\omega)$ is a polynomial in $e^{-j\omega}$ of degree N-1, the polynomial $F(e^{-j\omega})$ in $e^{-j\omega}$ is of degree $N - 1 - M$. The quadrature mirror filter $P(\omega)$ and its impulse response $p(n)$ is determined by the choice of the polynomial $F(e^{-j\omega})$.

We consider the square modulus relation for $|P(\omega)|^2$, which is from (10.7.22):

$$\left|P(\omega)\right|^2 = \left(\cos^2\frac{\omega}{2}\right)^M \left|F\left(e^{-j\omega}\right)\right|^2 \tag{10.8.11}$$

where $|P(\omega)|^2$ should be a polynomial in $\cos^2(\omega/2)$ and $\sin^2(\omega/2)$ of degree $N-1$. Because the polynomial $F(e^{-j\omega})$ has real-valued coefficients, $F^*(e^{-j\omega}) = F(e^{j\omega})$ and $|F(e^{-j\omega})|^2$ is a symmetric polynomial and can be rewritten as a polynomial in $\cos\omega$ or, equivalently, as a polynomial in $\sin^2(\omega/2)$, rewritten as $G[\sin^2(\omega/2)]$:

$$\left|F\left(e^{-j\omega}\right)\right|^2 = G\left(\sin^2\frac{\omega}{2}\right)$$

which is of degree

$$L = N - 1 - M \tag{10.8.12}$$

Introducing a variable $y = \cos^2(\omega/2)$, (10.8.11) can be written as:

$$\begin{aligned} \left|P(\omega)\right|^2 &= (y)^M G(1-y) \\ \left|P(\omega+\pi)\right|^2 &= (1-y)^M G(y) = 1 \end{aligned} \tag{10.8.13}$$

Combining these regularity conditions with the orthonormality condition, we obtain:

$$y^M G(1-y)+(1-y)^M G(y)=1$$

This equation can be solved for $G(y)$, which is a polynomial in y, of minimum degree $M–1$. Daubechies chose the minimum degree for $G(y)$ as $L = M - 1$. Compared with (10.8.12), we have:

$$M = N/2$$

Hence, the term $(\cos^2(\omega/2))^M$ has the maximum value of M. The regularity M of the Daubechies scaling function is then the maximum, and increases linearly with the width of their support, i.e., with the length, N, of the discrete filters $p(n)$ and $q(n)$, because $M = N/2$.

In (10.8.13) the term $[\cos(\omega/2)]^M$ ensures $|P(\omega)|$ to have M zeros at $\omega = \pi$, and to have M vanishing derivatives at $\omega = 0$. The term $G(\sin^2(\omega/2))$ ensures $|P(\omega + \pi)|$ to have $L = (M–1)$ zeros at $\omega = 0$, and to have $M–1$ vanishing derivatives at $\omega = \pi$. This corresponds to the unique maximally flat magnitude response of the frequency responses of the Daubechies low-pass and high-pass filters. Daubechies solved for $P(\omega)$ from $|P(\omega)|^2$ by spectral factorization.

Daubechies Filters in Time Domain

The values of the coefficients $p_M(n)$ for the cases $M = 2, 3, \ldots, 10$ are listed in Table 10.2, where the filter length $N = 2M$. For the most compact support at $M = 2$ and $N = 4$, the discrete low-pass filter is given as:

$$\begin{aligned} p(0) &= \frac{1}{4}\left(1+\sqrt{3}\right)\ \sqrt{2} = 0.483 \\ p(1) &= \frac{1}{4}\left(3+\sqrt{3}\right)\ \sqrt{2} = 0.836 \\ p(2) &= \frac{1}{4}\left(3-\sqrt{3}\right)/\sqrt{2} = 0.224 \\ p(3) &= \frac{1}{4}\left(1-\sqrt{3}\right)\ \sqrt{2} = -0.13 \end{aligned} \qquad (10.8.14)$$

The discrete high-pass filter, $q(n)$, can be obtained from $p(n)$ by the alternating flip relation:

$$q(n)=(-1)^n p(N-1-n)$$

where N is an even number and $n = 0, 1, 2, \ldots, N$.

It is easy to verify that the translates of $p(n)$ and $q(n)$ with double integer steps are orthonormal, respectively. Figures 10.17a and 10.17b show the Daubechies scaling function and wavelet with compact support $M = 2$ and $N = 4$ and their Fourier transforms. The scaling function is generated from the quadrature mirror filter, $p(n)$, given with the method of reconstruction discussed in Section 10.5.5. Those functions have the most compact support, but are neither smooth nor regular. When the length of the filters, $p(n)$ and $q(n)$, increase the Daubechies scaling functions and wavelets become more smooth and regular at the cost of larger number of nonzero coefficients of $p(n)$ and $q(n)$, this results in large support widths for the scaling functions and wavelets.

Another important feature of Figure 10.17 is the lack of any symmetry or antisymmetry axis for the Daubechies scaling function and wavelet. Daubechies has shown that it is impossible to obtain an orthonormal and compactly supported wavelet that is either symmetric or antisymmetric around any axis, except for the trivial Haar wavelets.

TABLE 10.2 The Low-Pass Filter of the Daubechies Wavelet Bases with the Support of the Filter $N = 2M$ and $M = 2, 3, \ldots, 10$

	n	$P_M(n)$		n	$P_M(n)$
$M = 2$	0	.482962913145	$M = 8$	0	.054415842243
	1	.836516303738		1	.312871590914
	2	.224143868042		2	.675630736297
	3	−.129409522551		3	.585354683654
$M = 3$	0	.332670552950		4	−.015829105256
	1	.806891509311		5	−.284015542962
	2	.459877502118		6	.000472484574
	3	−.135011020010		7	.128747426620
	4	−.085441273882		8	−.017369301002
	5	.035226291882		9	−.044088253931
$M = 4$	0	.230377813309		10	.013981027917
	1	.714846570553		11	.008746094047
	2	.630880767930		12	−.004870352993
	3	−.027983769417		13	−.000391740373
	4	−.187034811719		14	.000675449406
	5	.030841381836		15	−.000117476784
	6	.032883011667	$M = 9$	0	.038077947364
	7	−.010597401785		1	.243834674613
$M = 5$	0	.160102397974		2	.604823123690
	1	.603829269797		3	.657288078051
	2	.724308528438		4	.133197385825
	3	.138428145901		5	−.293273783279
	4	−.242294887066		6	−.096840783223
	5	−.032244869585		7	.148540749338
	6	.077571493840		8	.030725681479
	7	−.006241490213		9	−.067632829061
	8	−.012580751999		10	.000250947115
	9	.003335725285		11	.022361662124
$M = 6$	0	.111540743350		12	−.004723204758
	1	.494623890398		13	−.004281503682
	2	.751133908021		14	.001847646883
	3	.315250351709		15	.000230385764
	4	−.226264693965		16	−.000251963189
	5	−.129766867567		17	.000039347320
	6	.097501605587	$M = 10$	0	.026670057901
	7	.027522865530		1	.188176800078
	8	−.031582039318		2	.527201188932
	9	.000553842201		3	.688459039454
	10	.004777257511		4	.281172343661
	11	−.001077301085		5	−.249846424327
$M = 7$	0	.007852054085		6	−.195946274377
	1	.396539319482		7	.127369340336
	2	.729132090846		8	.093057364604
	3	.469782287405		9	−.071394147166
	4	−.143906003929		10	−.029457536822
	5	−.224036184994		11	.033212674059
	6	.071309219267		12	.003606553567
	7	.080612609151		13	−.010733175483
	8	−.038029936935		14	.001395351747
	9	−.016574541631		15	.001992405295
	10	.012550998556		16	−.000685856695
	11	.000429577973		17	−.000116466855
	12	−.001801640704		18	.000093588670
	13	.000353713800		19	−.000013264203

Source: Dauchies, I., *Commun. on Pure and Appl. Math.*, XLI, 909, 1988. With permission.

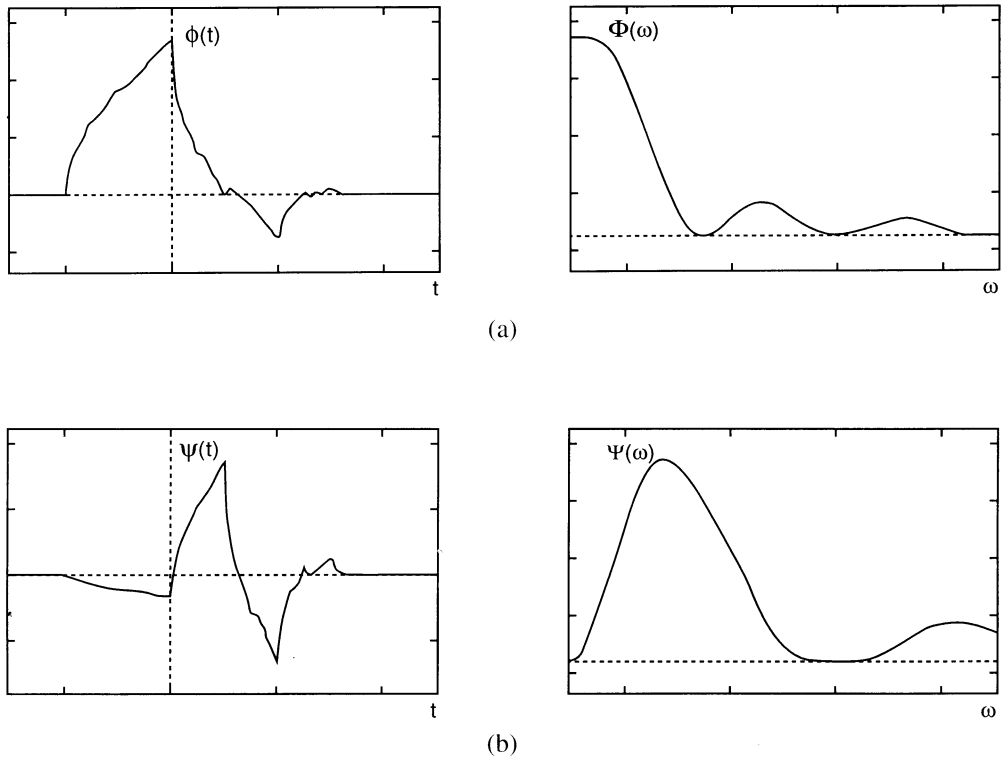

FIGURE 10.17 Daubechies scaling function (a) and wavelet (b) and their Fourier transforms with the compact support $N = 4$. (From Daubechies, I., *Commun. on Pure and Appl. Math.*, XLI, 909, 1988. With permission.)

10.9 Fast Wavelet Transform

The wavelet transform is not ready for explicit calculus. The wavelet transform has analytical solutions as given in Section 10.2.4 for only a few simple functions. For most functions the wavelet transforms must be computed in the digital computer. In the multiresolution analysis framework, the orthonormal wavelet transform is implemented by iterating the quadrature mirror filters in the tree algorithm. In the computer both the function to be transformed and the iterated quadrature mirror filters are discrete. The orthonormal wavelet series decomposition and reconstruction are essentially discrete. The wavelet tree algorithm permits the fast wavelet transform. One of the main reasons for the recent success of the wavelet transform is the existence of this fast wavelet transform algorithm which only requires a number $O(L)$ of the operations where L is the size of the initial data.

The discrete wavelet decomposition and reconstruction algorithms are discussed in Sections 10.5.4 and 10.5.5. In this section we implement the algorithm by matrix operations and introduce the discrete wavelet matrix and discuss the number of operations, the time bandwidth product of the wavelet transform output.

10.9.1 Wavelet Matrices

The discrete orthonormal wavelet transform is a linear operation. Given a vector of data that has a length of an integer power of two, the wavelet decomposition and reconstruction are numerically computed by recurring two conjugate quadrature mirror filters, $p(n)$ and $q(n)$, that are the finite impulse response (FIR) filters compactly supported with a finite number, N, of nonzero coefficients. The degree of the Laurent polynomial of the transfer function of the filters is $N - 1$. The wavelet decomposition and

reconstruction are computed with recursive applications of the wavelet filter bank in the tree algorithm. In the following we show an example of the wavelet decomposition and reconstruction with the Daubechies wavelets of $N = 4$, called the DAUB4, in the matrix formalization.

Let $f(n)$ be the vector of initial data, we generate a wavelet transform matrix[17] with the translated discrete filters as:

$$\begin{pmatrix} c(1) \\ d(1) \\ c(2) \\ d(2) \\ \cdot \\ \cdot \\ \cdot \\ \cdot \\ \cdot \\ \cdot \end{pmatrix} = \begin{pmatrix} p(0) & p(1) & p(2) & p(3) & \cdot & \cdot & \cdot & \cdot & \cdot & \cdot & \cdot & \cdot \\ p(3) & -p(2) & p(1) & -p(0) & \cdot & \cdot & \cdot & \cdot & \cdot & \cdot & \cdot & \cdot \\ \cdot & \cdot & p(0) & p(1) & p(2) & p(3) & \cdot & \cdot & \cdot & \cdot & \cdot & \cdot \\ \cdot & \cdot & p(3) & -p(2) & p(1) & -p(0) & \cdot & \cdot & \cdot & \cdot & \cdot & \cdot \\ \cdot & \cdot & \cdot & \cdot & \cdot & \cdot & \cdot & \cdot & \cdot & \cdot & \cdot & \cdot \\ \cdot & \cdot & \cdot & \cdot & \cdot & \cdot & \cdot & \cdot & \cdot & \cdot & \cdot & \cdot \\ \cdot & \cdot & \cdot & \cdot & \cdot & \cdot & \cdot & \cdot & p(0) & p(1) & p(2) & p(3) \\ \cdot & \cdot & \cdot & \cdot & \cdot & \cdot & \cdot & \cdot & p(3) & -p(2) & p(1) & -p(0) \\ p(2) & p(3) & \cdot & \cdot & \cdot & \cdot & \cdot & \cdot & \cdot & \cdot & p(0) & p(1) \\ p(1) & -p(0) & \cdot & \cdot & \cdot & \cdot & \cdot & \cdot & \cdot & \cdot & p(3) & -p(2) \end{pmatrix} \begin{pmatrix} f(1) \\ f(2) \\ f(3) \\ f(4) \\ \cdot \\ \cdot \\ \cdot \\ \cdot \\ \cdot \\ f(N) \end{pmatrix} \quad (10.9.1)$$

In the wavelet transform matrix the odd rows are the low-pass filters $p(n)$. The low-pass filter, $p(n)$, in the third row is translated by two with respect to that in the first row and so on. The even rows are the high-pass filters, $q(n)$, that are also translates by two from the second row to the fourth row, and so on. The wavelet transform matrix acts on a column vector of data, $f(n)$, resulting in two related correlations between the data vector, $f(n)$, and the filters, $p(n)$ and $q(n)$, that are the discrete approximation, $c(n)$, and the discrete wavelet coefficients, $d(n)$, respectively.

It is easy to verify that the low-pass filter, $p(n)$, is a smoothing filter as described in (10.7.27). With the coefficients of the Daubechies' bases given in (10.8.14), we have:

$$P(0)^2 + P(1)^2 + P(2)^2 + P(3)^2 = 1$$

The high-pass filter, $q(n)$, is obtained from the low-pass filter, $p(n)$, from the cross filter orthogonality (10.6.16)

$$q(n) = (-1)^n p(N-1-n)$$

Let $N = 4$ and $n = 0, 1, 2, 3$, we have $q(0) = p(3)$, $q(1) = -p(2)$, $q(2) = p(1)$, and $q(4) = -p(0)$. The high-pass filter, $q(n)$, has the property that:

$$p(3) - p(2) + p(1) - p(0) = 0$$

corresponding to (10.7.21), $Q(0) = 0$, obtained from the orthonormality condition, and

$$0p(3) - 1p(2) + 2p(1) - 3p(0) = 0$$

corresponding to (10.7.28) obtained for the regularity of the wavelets.

It is easy to see that in the wavelet transform matrix the orthonormality between the double integer translates, $p(n)$, and that of $q(n)$ and the cross filter orthogonality between $p(n)$ and $q(n)$ are ensured because

$$p(2)p(0)+p(3)p(1)=0$$

It is also possible to reconstruct the original data, *f(n)* of length L, from the approximation sequence, *c(n)*, and the wavelet coefficients, *d(n)*, both sequences are of the length of *L/2*. From the preceding equations we see that the wavelet transform matrix in (10.9.1) is orthonormal, so that its inverse is just the transposed matrix:

$$\begin{pmatrix}
p(0) & p(3) & \cdot & \cdot & \cdot & \cdot & \cdot & \cdot & \cdot & \cdot & p(2) & p(1) \\
p(1) & -p(2) & \cdot & \cdot & \cdot & \cdot & \cdot & \cdot & \cdot & \cdot & p(3) & -p(0) \\
p(2) & p(1) & p(0) & p(3) & \cdot & \cdot & \cdot & \cdot & \cdot & \cdot & \cdot & \cdot \\
p(3) & -p(0) & p(1) & -p(2) & \cdot & \cdot & \cdot & \cdot & \cdot & \cdot & \cdot & \cdot \\
\cdot & \cdot & \cdot & \cdot & \cdot & \cdot & \cdot & \cdot & \cdot & \cdot & \cdot & \cdot \\
\cdot & \cdot & \cdot & \cdot & \cdot & \cdot & \cdot & \cdot & \cdot & \cdot & \cdot & \cdot \\
\cdot & \cdot & \cdot & \cdot & \cdot & \cdot & p(2) & p(1) & p(0) & p(3) & \cdot & \cdot \\
\cdot & \cdot & \cdot & \cdot & \cdot & \cdot & p(3) & -p(0) & p(1) & -p(2) & \cdot & \cdot \\
\cdot & \cdot & \cdot & \cdot & \cdot & \cdot & \cdot & \cdot & p(2) & p(1) & p(0) & p(3) \\
\cdot & \cdot & \cdot & \cdot & \cdot & \cdot & \cdot & \cdot & p(3) & -p(0) & p(1) & -p(2)
\end{pmatrix} \tag{10.9.2}$$

The discrete wavelet decomposition is computed by applying the wavelet transform matrix with the operation (10.9.1) hierarchically with the down-sampling by a factor of two after each iteration. The down-sampling by two is implemented by a permutation of the output vector in the left-hand side of (10.9.1) as shown in the following diagram with $N = 16$.

$$\begin{pmatrix} f(1) \\ f(2) \\ f(3) \\ f(4) \\ f(5) \\ f(6) \\ f(7) \\ f(8) \\ f(9) \\ f(10) \\ f(11) \\ f(12) \\ f(13) \\ f(14) \\ f(15) \\ f(16) \end{pmatrix}
\xrightarrow{(10.9.1)}
\begin{pmatrix} c(1) \\ d(1) \\ c(2) \\ d(2) \\ c(3) \\ d(3) \\ c(4) \\ d(4) \\ c(5) \\ d(5) \\ c(6) \\ d(6) \\ c(7) \\ d(7) \\ c(8) \\ d(8) \end{pmatrix}
\xrightarrow{permute}
\begin{pmatrix} c(1) \\ c(2) \\ c(3) \\ c(4) \\ c(5) \\ c(6) \\ c(7) \\ c(8) \\ d(1) \\ d(2) \\ d(3) \\ d(4) \\ d(5) \\ d(6) \\ d(7) \\ d(8) \end{pmatrix}
\xrightarrow{(10.9.1)}
\begin{pmatrix} C(1) \\ D(1) \\ C(2) \\ D(2) \\ C(3) \\ D(3) \\ C(4) \\ D(4) \\ d(1) \\ d(2) \\ d(3) \\ d(4) \\ d(5) \\ d(6) \\ d(7) \\ d(8) \end{pmatrix}
\xrightarrow{permute}
\begin{pmatrix} C(1) \\ C(2) \\ C(3) \\ C(4) \\ D(1) \\ D(2) \\ D(3) \\ D(4) \\ d(1) \\ d(2) \\ d(3) \\ d(4) \\ d(5) \\ d(6) \\ d(7) \\ d(8) \end{pmatrix}
\xrightarrow{\cdots\cdots}
\begin{pmatrix} C'(1) \\ C'(2) \\ D'(1) \\ D'(2) \\ D(1) \\ D(2) \\ D(3) \\ D(4) \\ d(1) \\ d(2) \\ d(3) \\ d(4) \\ d(5) \\ d(6) \\ d(7) \\ d(8) \end{pmatrix} \tag{10.9.3}$$

If the length of the data vector $N > 16$ there were be more stages of applying (10.9.3) and permuting.

The final output vector will always be a vector with two approximation coefficients, *C′(1)* and *C′(2)* at the lowest resolution, and a hierarchy of the wavelet coefficients, *D′(1)* and *D′(2)* for the lowest

resolution, *D(1) – D(4)* for higher resolution, and *d(1)* to *d(8)* for still higher resolution, etc. Notice that once the wavelet coefficients *d's* are generated, they simply propagate through to all subsequent stages without further computation.

The discrete wavelet reconstruction can be computed by simple reversed procedure, starting with the lowest resolution level in the hierarchy and working from right to left with the diagram (10.9.3). The inverse wavelet transform matrix (10.9.2), is used instead of (10.9.1).

The above wavelet transform matrix method shows a clear figure of the discrete wavelet decomposition and reconstruction. The wavelet transform can also be computed with other methods iterating the discrete filters in the tree algorithms without using the wavelet transform matrix.

10.9.2 Number of Operations

We consider now the number of operations required for the discrete orthonormal wavelet transform of a vector of data. Let L be the length of the data vector and N the length of the finite impulse response (FIR) filters, $p(n)$ and $q(n)$. The wavelet transform is a local operation, usually $N << L$, and at the highest frequency band, the first stage of decomposition requires $2NL$ multiplies and adds. In the tree algorithm at the next coarser frequency band, the length of the vector of the discrete approximation, $c(n)$, is reduced to $N/2$. Therefore, the next stage of decomposition requires $2(NL/2)$ multiplies and adds. The total number of operations of the orthonormal wavelet decomposition is then

$$2\left(NL+\frac{NL}{2}+\frac{NL}{4}+\cdots\right)=2NL\left(1+\frac{1}{2}+\frac{1}{4}+\ldots.\right)\approx 4NL$$

The orthonormal wavelet transform requires only an $O(L)$ computation. This is even faster than the Fast Fourier Transform (FFT) for the Fourier transform requires $O(L\log_2 L)$ multipliers and additions, due to its global nature.

10.9.3 Time Bandwidth Product

The wavelet transform is a mapping of a function of time, in one-dimensional case, to the two-dimensional time-scale joint representation. At first glance the time bandwidth product of the wavelet transform output would be squared of that of the signal. In the multiresolution analysis framework, however, the size of the data vector is reduced by a factor of two in moving from one frequency band to the next coarser resolution frequency band. The time bandwidth product is also reduced by a factor of two. If the original data vector $c_0(n)$ has L samples, in the tree algorithm for the wavelet decomposition shown in Figure 10.11, the first-stage wavelet coefficients outputs, $d_1(n)$, has $L/2$ samples that of the second stage has $L/4$ samples, etc. Let the length of the data vector, $L = 2^K$, the total time-bandwidth product of the wavelet decomposition including all the wavelet coefficients, $d_i(n)$ with $i = 1, 2, \ldots. K–1$ and the lowest resolution approximation $c_{k-1}(n)$ is equal to:

$$L\left(\frac{1}{2}+\frac{1}{4}+\ldots.\right)\approx L$$

10.10 Applications of the Wavelet Transform

In this section we present some popular applications of the wavelet transform for multiresolution transient signal analysis and detection, image edge detection and compression with some simple examples.

10.10.1 Multiresolution Signal Analysis

In this subsection we show an example of multiresolution analysis for a simple transient signal. Transient signals in the power system are nonstationary time-varying voltage and current that can occur as a result of changes in the electrical configuration and in industrial and residential loads, and of a variety of disturbances on transmission lines, including capacitor switching, lightning strikes and short-circuits. The waveform data of the transient signals are captured by digital transient recorders. Analysis and classification of the power system disturbance can help to provide more stability and efficiency in power delivery by switching transmission lines to supply additional current or switching capacitor banks to balance inductive loads and help to prevent system failures.

The power system transient signals contain a range of frequencies from a few hertz to impulse components with microsecond rise times. The normal 60 Hz sinusoidal voltage and current waveforms are interrupted or superimposed with impulses, oscillations, and reflected waves. An experienced power engineer can visually analyze the waveform data in order to determine the type of system disturbance. However, the Fourier analysis with its global operation nature is not as appropriate for the transient signals as the time-scale joint representation provided by the wavelet transform.

Multiresolution Wavelet Decomposition of Transient Signal

The wavelet transform provides a decomposition of power system transient signals into meaningful components in multiple frequency bands, and the digital wavelet transform is computationally efficient.[18] Figure 10.1 in Section 10.1 shows the wavelet components in the multiple frequency bands. At the top is the input voltage transient signal. There is a disturbance of a capacitor bank switching on a three-phase transmission line. Below the first line are the wavelet components as a function of the scale and time shift. The scales of the discrete wavelets increase by a factor of two successively from SCALE 1 to SCALE 64, corresponding to the dyadic frequency bands. The vertical axis in each discrete scale is the normalized magnitude of the signal component in voltage. The three impulses in high frequency band SCALE 1 correspond to the successive closing of each phase of the three-phase capacitor bank. SCALE 2 and SCALE 4 are the bands of system response frequencies. SCALE 4 contains the most energy from the resonant frequency caused by the addition of a capacitor bank to a primarily inductive circuit. The times of occurrence of all those components can be determined on the time axis. SCALE 64 contains the basic signal of continuous 60 Hz.

The wavelet analysis decomposes the power system transient into the meaningful components, whose modulus maxima then can be used for further classification. The nonorthogonal multiresolution analysis wavelets with finite impulse response (FIR) quadratic spline wavelet filters were used in this example of application.

Shift Invariance

One problem in this application and many other applications with the dyadic wavelet transform is the lack of shift invariance. The dyadic wavelet transform is not shift invariant. In the wavelet decomposition the analysis low-pass and high-pass filters are double shifted by two as described by (10.5.27). If the input signal is shifted by one sampling interval distance, the output of the dyadic wavelet transform is not simply shifted by the same distance, but the values of the wavelet coefficients would be changed dramatically. This aliasing error is caused by the down-sampled factor of two in the multiresolution signal analysis and is discussed in Section 10.6.2. This is a disadvantage of the dyadic wavelet transform, because many applications such as real-time signal analysis and pattern recognition require shift invariant wavelet transform. In the above example of application, the orthonormal quadrature mirror filters have been found sensitive to translations of the input. Hence, nonorthonormal quadratic spline wavelets have been used.

10.10.2 Signal Detection

The detection of weak signals embedded in a stronger stationary stochastic process, such as the detection of radar and sonar signals in zero-mean Gaussian white noise, is a well-studied problem. If the shape of the expected signal is known, the correlation and the matched filter provide optimum solution in terms of the signal-to-noise ratio in the output correlation.

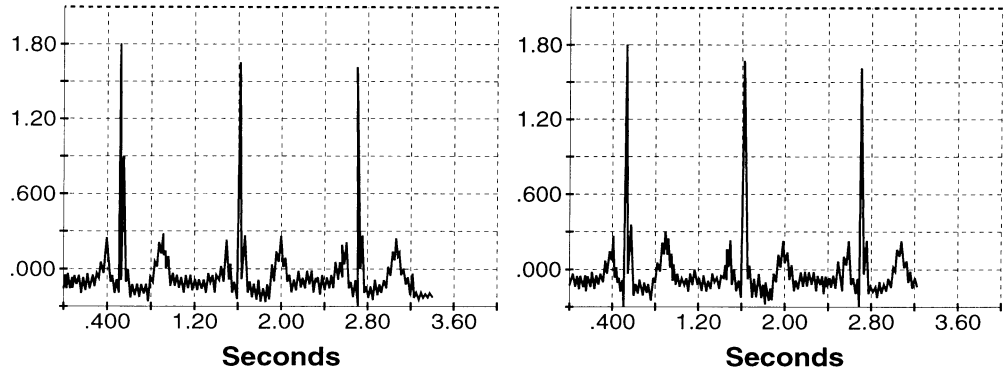

FIGURE 10.18 (Left) Normal electrocardiogram, (right) electrocardiogram with VLP abnormality. (From Combes, J. M. et al., *Wavelets*, 2nd ed. Springer-Verlag, Berlin, 1990. With permission.)

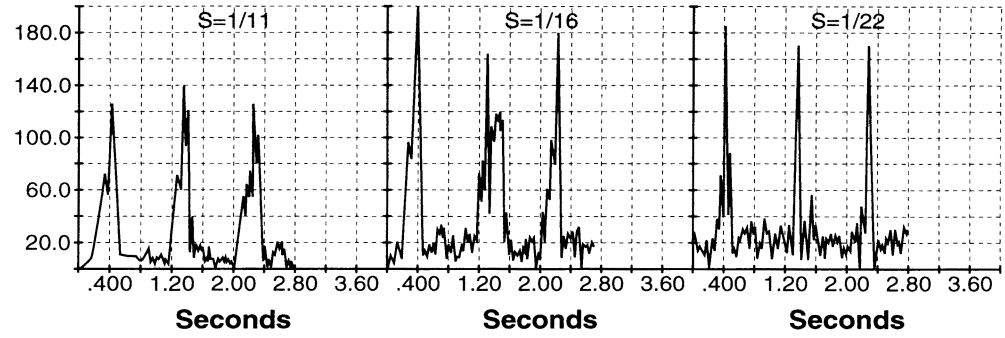

FIGURE 10.19 Wavelet transform of the abnormal electrocardiogram for scale factor $s = 11, 16, 22$. The bulge to the right of the second QRS peak for $s = 1/16$ indicates the presence of the VLP. (From Combes, J. M. et al., *Wavelets*, 2nd ed. Springer-Verlag, Berlin, 1990. With permission.)

In the detection of speech or biomedical signals, the exact shape of the signal is unknown. The Fourier spectrum analysis could be effective for those applications, only when the expected signal has spectral features that clearly distinguishes it from the noise. The effectiveness of the Fourier spectrum analysis is generally proportional to the ratio of the signal to noise energy. For short-time, low-energy transients, the change in the Fourier spectrum is not easily detected. Such transient signals can be detected by the wavelet transform. An example of an electrocardiogram signal detection follows.[19]

Figure 10.18 shows the clinical electrocardiogram with normal QRS peaks and an abnormality called ventricular late potentials (VLP) right after the second QRS peak. The amplitude of the VLP signal is about 5% of the QRS peaks. Its duration was about 0.1 second, or a little less than 10% of the pulse period. The VLPs are weak signals, swamped by noise, and they occur somewhat randomly.

Figure 10.19 shows the magnitude of continuous wavelet transform with the cos-Gaussian wavelets of scale $s = 1/11,\ 1/16$ and $1/22$. The peak after the second QRS spike observed for $s = 1/16$ is very noticeable and gives a clear indication of the presence of the VLP.

10.10.3 Image Edge Detection

Edges and boundaries, representing shapes of objects, intersections between surfaces and between textures, are among the most important features of images, useful for image segmentation and pattern recognition. An edge in image is a set of locally connected pixels which are characterized by sharp intensity variation in their neighborhood in one direction and smooth intensity variation in another perpendicular direction. Edges are local features of an image.

The wavelet transform is a local operation. The wavelet transform of a constant is equal to zero and the wavelet transform of a polynomial function of degree, n, is also equal to zero if the Fourier transform of the wavelet has the zero of order $n + 1$ about the frequency $\omega = 0$, as described in Section 10.2.4. Hence, the wavelet transform is useful for detecting singularities of functions and edges of images.

Edge Detectors

The edge detectors first smooth an image at various scales and then detect sharp variation from the first- or second-order derivative of the smoothed images. The extrema of the first-order derivative correspond to the zero crossing of the second-order derivative and to the inflection points of the image.

A simple example of edge detector is the first- or second-order derivative of the Gaussian function $g(x,y)$. The Gaussian function $g_s(x,y)$ is scaled by a factor, s. The first- and second-order derivative, i.e., the gradient and the Laplacian, of $g_s(x,y)$ are the Gaussian wavelets satisfying the wavelet admissible condition, as described in Section 10.2.5.

By definition, the wavelet transform of an image $f(x,y)$, is a correlation between $f(x,y)$ and the scaled wavelets. We derive that:

$$W_f(s;x,y) = f * (s\nabla g_s) = s\nabla(f * g_s)(x,y)$$

where * denotes the correlation with the first-order derivative Gaussian wavelet and that:

$$W_f(x,y) = f * (s^2\nabla^2 g_s) = s^2\nabla^2(f * g_s)(x,y)$$

with the second-order derivative Gaussian wavelet, which is the Mexican hat wavelet. The wavelet transform is then the gradient or the Laplacian of the image smoothed by the Gaussian function $g_s(x,y)$ at the scale s.

The local maxima of the wavelet transform with the first-derivative of a Gaussian wavelet can be extracted as edges. This is the Canny edge detector. The zero-crossing of the wavelet transform with the Mexican hat wavelet corresponds to the inflection points of the smoothed image, $f * g_s(x,y)$, which can be extracted as edges. This is the zero-crossing Laplacian edge detector.

Two-Dimensional Wavelet Transform

The wavelet transform can be easily extended to a two-dimensional (2-D) case for image processing applications. The wavelet transform of a two-dimensional image $f(x,y)$ is

$$W_f(s_x,s_y;u,v) = \frac{1}{\sqrt{s_x s_y}} \iint f(x,y)\psi\left(\frac{x-u}{s_x};\frac{y-v}{s_y}\right)dx\,dy$$

which is a four-dimensional function. It is reduced to a set of two-dimension functions of (u, v) with different scales, when the scale factors $s_x = s_y = s$. When $\psi(x,y) = \psi(r)$ with $r = (x^2 + y^2)^{1/2}$, the wavelets are isotropic and have no selectivity for spatial orientation. Otherwise, the wavelet can have particular orientation. The wavelet can also be a combination of the two-dimensional wavelets with different particular orientations, so that the two-dimensional wavelet transform has orientation selectivity.

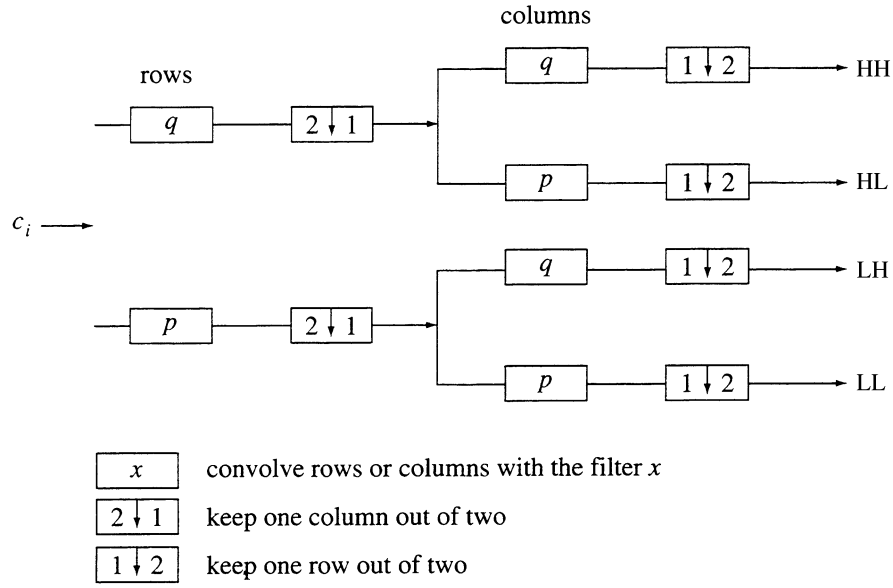

FIGURE 10.20 Schematic two-dimensional wavelet decomposition with quadrature mirror low-pass and high-pass filters $p(n)$ and $q(n)$.

At each resolution the pair of the 1-D low-pass and high-pass filters are first applied to each row of the image that results in a horizontally approximation image and a horizontal detail image. Then the pair of the 1-D filters are applied to each column of the two horizontally filtered images. The down-sampling by two is applied after each filtering. The two-step filtering and down-sampling result in four subband images: (LL) for the low-pass image filtered both horizontally and vertically, (HH) for the high-pass image filtered both horizontally and vertically, (LH) for the low-pass image filtered in a horizontal direction and the high-pass image filtered in a vertical direction, and (HL) for high-pass image filtered in a vertical direction and high-pass image filtered in a horizontal direction, as shown in Figure 10.20.[16]

All the four images have the half size of the input image. We put the detail images (LH), (HL), and (HH) in three respective quadrants as shown in Figure 10.21. The image (LL) is the approximation image in both horizontal and vertical directions and is downsampled in both directions. Then, we apply the whole process of two-step filtering and down-sampling again to the image (LL) in this lower resolution level. The iteration can continue many times until, for instance, the image (LL) has only a size of 2×2. Figure 10.21 show a disposition of the detail images (LH), (HL), and (HH) at three resolution levels (1, 2, 3) and the approximation image (LL) at the fourth low resolution level (4). If the original image has L^2 pixels at the resolution $i = 0$, then each image (LH), (HL), and (HH) at resolution level i has $(L/2^i)^2$ pixels $(i > 0)$ The total number of pixels of the orthonormal wavelet representation is therefore still equal to L^2, as shown in Figure 10.21. The dyadic wavelet transform does not increase the volume of data. This is owing to the orthonormality of the discrete wavelet decomposition.

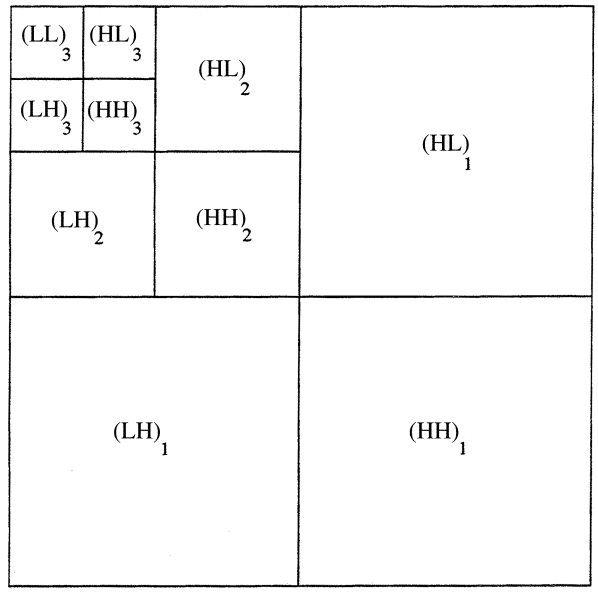

FIGURE 10.21 Presentation of the two-dimensional wavelet decomposition. The detail images d_i^n and the approximation c_i are defined by Equations (10.9.5) and (10.9.7).

Multiscale Edges

The wavelet transform of a two-dimensional image for edge detection is performed at a set of dyadic scales, generating a set of detail images. Similarly to the reconstruction process described in Section 10.5.5, the detail images from the wavelet decomposition can be used to reconstruct the original image.

If the wavelet is the first-order derivative of the Gaussian smoothing function and we retain the modulus maxima of the wavelet components, then we obtain the edge images that correspond to the maximum variation of the smoothed image at a scale *s*. The multiscale edge information provided by the wavelet transform can also be used to analyze the regularity of the image function by observing the propagation of the modulus maxima from one scale to next. A similar approach is used to reduce the noise in the image, since the noise has different regularity than that of the image and image edges.

10.10.4 Image Compression

Image compression is to use fewer bits to represent the image information for different purposes, such as image storage, image transmission, and feature extraction. The general idea behind it is to remove the redundancy in an image to find a more compact representation.

A popular method of image compression for removing the spatial redundancy is so-called transform coding, which represents the image in the transformation basis such that the transformation coefficients are decorrelated. We see in Section 10.5.4 that the multiresolution wavelet decomposition is projections onto subspaces spanned by scaling function basis and the wavelet basis. The projections on the scaling function basis yield approximations of the signal and the projections on the wavelet basis yield the differences between the approximations at two adjacent resolution levels. Therefore, the wavelet detail images are decorrelated and can be used for image compression. Indeed, the detail images obtained from the wavelet transform consist of edges in the image. There is only few correlations among the values on pixels in the edge images.

One example of image compression applications is the compression of gray-scale fingerprint images using the wavelet transform.[20] The fingerprint images are captured as 500 pixels per inch and 256 gray levels. The wavelet subband decomposition is accomplished by the tree algorithm described by Figure 10.20. The dominant ridge frequency in fingerprint images is in roughly $\omega = \pi/8$ up to $\omega = \pi/4$

bands. Because the wavelet decomposition removes the correlation among image pixels, only the wavelet coefficients with large magnitudes are retained. The wavelet decomposition uses pairs of symmetric biorthogonal wavelet filters with 7 and 9 taps.

Most wavelet transform coefficients are equal or close to zero in the regions of smooth image intensity variation. After a thresholding on the wavelet coefficients, the retained coefficients are subsequently coded according to a scalar quantizer and are mapped to a set of 254 symbols for Huffman encoding using the classical image coding technique. The thresholding and the Huffman coding can achieve a high compression ratio.

The analysis of low-pass and high-pass filters, the quantization rule, and the Huffman code table are included with the compressed images, so that a decoder can reconstruct approximations of the original images by performing the inverse wavelet transform. After compression at 20:1, the reconstructed images conserve the ridge features. Ridge endings or bifurcations contain definitive information useful for determination.

References

1. D. Gabor, Theory of communication, *J. Inst. Elec. Eng.*, 93, 429-457, 1946.
2. E. Wigner, On the quantum correction for thermodynamic equilibrium, *Phys. Rev.* 40, 749-759, 1932.
3. A. W. Rihaczek, *Principles of High Resolution Radar*, McGraw-Hill, New York, 1969.
4. C. Gasquet and P. Witomski, *Analyse de Fourier et Applications*, Chap. XII, Masson, Paris, 1990.
5. A. Harr, Ph.D. dissertation, Appendix, 1910.
6. R.K. Martinet, J. Morlet, and A. Grossmann, Analysis of sound patterns through wavelet transforms, *Int. J. Patt. Recogn. Artific. Intell.* 1, 2, 273-302, 1987.
7. D. Marr and E. Hildreth, Theory of edge detection, *Proc. R. Soc. Lond.* B 207, 187-217, 1980.
8. I. Daubechies, The wavelet transform: time-frequency localization and signal analysis, *IEEE Trans. Inf. Theory*, 36, 5, 961-1005, 1990.
9. S. G. Mallat, Multifrequency channel decompositions of images and wavelet models, *Trans. IEEE Acous. Speech Sig. Proc.* ASSP-37, 12, 2091-2110, 1989.
10. P. J. Burt and E. H. Adelson, The Laplacian pyramid as a compact image code, *IEEE Trans. Comm.*, 31, 4, 532-540, 1983.
11. A. N. Akansu and R. A. Haddad, *Multiresolution Signal Decomposition*, Academic Press, Boston, 1992.
12. G. Strang, Wavelets and dilation equations: a brief introduction, *SIAM Rev.*, 31, 4, 614-627, 1989.
13. I. Daubechies, Orthonormal bases of compactly supported wavelets, *Comm. Pure Appl. Math.* XLI, 909-996, 1988.
14. C. K. Chui, Ed., *Wavelets: A Tutorial Theory and Applications*, vol. 2, Academic Press, Boston, 1992.
15. P. G. Lemarie and Y. Meyer, Ondelettes et bases Hibertiennes, *Revista Matematica Iberoamericana*, 1Y2, 2, 1986.
16. S. Mallat, A theory for multiresolution signal decomposition: the wavelet representation, *IEEE Trans. Pattern Anl. Machine Intell.*, PAMI-31, 674-693, 1989.
17. W. H. Press et. al., *Numerical Recipes*, 2nd ed., Chap. 13, Cambridge, London, 1992.
18. D. C. Robertson, O. I. Camps, and J. Mayer, Wavelets and power system transients: feature detection and classification, *Proc. SPIE*, 2242, 474-487, 1994.
19. J. M. Combes, A. Grosmann, and Ph. Tchamitchian, Eds., *Wavelets*, 2nd ed., Springer-Verlag, Berlin, 1990.
20. T. Hopper, Compression of gray-scale fingerprint images, *Proc. SPIE*, 2242, 180-187, 1994.
21. Y. Sheng, D. Roberge, and H. Szu, Optical wavelet transform, *Opt. Eng.*, 31, 1840-1845, 1992.
22. H. Szu, Y. Sheng, and J. Chen, The wavelet transform as a bank of matched filters, *Appl. Optics*, 31, 17, 3267-3277, 1992.

23. M. O. Freeman, Wavelet signal representations with important advantages, *Opt. Photonics News*, 8-14, August 1995.
24. G. Strang and T. Hguyen, *Wavelets and Filter Banks*, Wellesley, Cambridge, U.K., 1996.
25. R. L. Allen et al., Laplacian and orthogonal wavelet pyramid decomposition in coarse-to-fine registration, *IEEE Trans. Signal Proc.* 41, 12, 3.536-3540, 1993.